A THESIS

ON

SOME STUDIES ON UNDERWATER IMAGE ENHANCEMENT

BY

RAJNI SETHI

(2K14/PHD/IT/07)

UNDER THE SUPERVISION OF

PROF. S. INDU

PROFESSOR AND DEAN (STUDENT WELFARE)

(DEPARTMENT OF ELECTRONICS AND COMMUNICATION ENGINEERING)

SUBMITTED IN PARTIAL FULFILLMENT OF THE REQUIREMENTS OF THE DEGREE OF

DOCTOR OF PHILOSOPHY

TO THE

DELHI TECHNOLOGICAL UNIVERSITY, DELHI, INDIA

2019

A THESIS

ON

SOME STUDIES ON UNDERWATER IMAGE ENHANCEMENT

BY

RAJNI SETHI

(2K14/PHD/IT/07)

UNDER THE SUPERVISION OF

PROF. S. INDU

PROFESSOR AND DEAN (STUDENT WELFARE)

(DEPARTMENT OF ELECTRONICS AND COMMUNICATION ENGINEERING)

SUBMITTED IN PARTIAL FULFILLMENT OF THE REQUIREMENTS OF THE DEGREE OF

DOCTOR OF PHILOSOPHY

TO THE

DELHI TECHNOLOGICAL UNIVERSITY, DELHI, INDIA

2019

Declaration

I hereby declare that the work which is being presented in the thesis entitled **Some Studies on Underwater Image Enhancement** in partial fulfillment of the requirements for the award of the degree of Doctor of Philosophy and submitted in the department of Information Technology of Delhi Technological University, Delhi is an authentic record of my own work carried out during the period from 2014 to 2019 under the supervision of Prof S.Indu, Professor, Department of Electronics and Communication Engineering, Delhi Technological University, Delhi, India. The content of this thesis has not been submitted either in part or whole to any other university or institute for the award of any degree or diploma.

Rajni Sethi

Certificate

This is to certify that the thesis titled **Some Studies on Underwater Image Enhancement** being submitted by Rajni Sethi to the Department of Information Technology, Delhi Technological University, Delhi, for the award of the degree of Doctor of Philosophy, is a record of bonfide research work carried out by her under my guidance and supervision. In my opinion, the thesis has reached the standards fulfilling the requirements of the regulations relating to the degree.

The results contained in this thesis have not been submitted to any other university or institute for the award of any degree or diploma.

Prof. S. Indu
Professor and Dean (Student Welfare)
Department of Electronic and Comm. Engg.
Delhi Technological University
Delhi- 110042

Acknowledgments

Through hard work, perseverance and a faith in God, you can live your dreams.

- - - Ben Carson

By the grace of God, I marked an end to this hard yet a great learning experience of PhD, which will stay with me for my whole life. There are many people and pillars of strength who supported me in this seems to be never ending journey. I can not start this thesis without thanking them.

First of all, I would like to thank my supervisor, **Prof. S. Indu**, for her continuous guidance, support, encouragement and highly positive attitude. I have learned a lot from her and these learning will guide me throughout my life. She always channelized my efforts towards my goals. Whenever I stumbled upon a pit in terms of paper rejections, she was there to lift me up with a supporting hand and smiling face to take me to heights. She let me do my work at my own pace and all the research work which I have done is because of the trust she have in me that I will do it. I can not explain in words how much I owe to her for the unending support and guidance.

I am also thankful to all the faculty and staff of Information Technology, Computer Science and Electronics and Communication Engineering Department of Delhi Technological University for their help and support for completing my work.

I would like to extend deep gratitude:

To my friends Isha Singh, Anshu Khurana and Dr. Shraddha Chaudhary for keeping my morale up, for stabilizing my mood swings and giving me positive reviews.

To my two sweet mothers, Mrs. Neelam Gumber who always wanted me to be a doctor and my mother in law, Mrs. Sunita Rani for always being there as pillar of strength and support

to manage my personal and professional life.
To my two fathers, Mr. Surinder Gumber for his warm wishes for my life and my father in law, Mr. Ravi Sethi for always trusting and counseling me during this journey.
To my brother Sachin, sister-in-law Shikha and brother-in-law Rajat for cheering me and motivating me.
I feel myself very lucky to have a great family who have supported me throughout the journey of my research work.
Last but not the least, without whom I could not imagine being enrolled in PhD, my husband Mr. Rohit Sethi, for his unwavering encouragement, undeterred faith in me and being the biggest pillar of strength who supported me all the way till the end. A special thanks to my son Rohan Sethi for bearing my absence and always loving me. It would not have been possible to complete my research work without their love, encouragement and support.

New Delhi
Nov 2019

RAJNI SETHI

Abstract

Oceans covers 70% of the earth and are required to be explored for various scientific studies like setting up underwater pipelines, knowing the ecological balance by taking population census of various aquatic species etc. To get such information, capturing images is safe and effective solution, but underwater imagery suffers from poor contrast, bluish green color cast, hazy appearance, blurring and noise due to inherent property of water.
Enhancement of underwater images is a challenging task as images are captured in different media having varying salinity, turbidity, green matter etc. and captured at varying depth. Thus, there is a need of an adaptive method which works for all type of underwater images. This thesis provides an effective solution to pre-process the underwater images to make them suitable for scientific studies. Under the umbrella of pre-processing, sub-problems like color correction, contrast correction , haze removal have been addressed irrespective of the underwater media and depth at which the images have been captured. The contributions presented in this thesis are outlined below:

- We propose an adaptive method for enhancement of underwater images by using fuzzy rules to find the color cast. Since the color correction depends upon the media, some parameters required for controlling the degree of color correction are found using Multi-Objective optimization (MOPSO). Performance measures which are optimized using MOPSO act as proper guiding mechanisms so that the resultant images have few or no artifacts. Various non-reference based performance measures like entropy, histogram spread, UICM have been used to analyze the results.

- We propose a local enhancement solution which tackles the artifacts caused by artificial lighting. It performs color and contrast correction in a localized manner. The two versions are then fused using wavelet based fusion with the help of effective weight maps which chooses the required features from the two versions.

- We proposed a complete solution which addresses the three major issues of underwater images i.e. color cast, poor contrast, haze. Using basic image enhancement and restoration based methods, the proposed method handles the mentioned issues for the images captured at different depths and in media with varying salinity, turbidity.

Contents

List of Figures

List of Tables

List of Algorithms

Chapter 1

Introduction

1.1 Need for underwater studies and associated challenges

A major portion of the Earth is covered by water and life in these water bodies forms a significant part of the ecosystem. Therefore, the study of the aquatic environment is gaining a lot of attention as underwater imagery not only unravels the mystery beneath water but also provides information required for underwater scientific studies by establishing ocean observing systems (OOS) [9], such as understanding marine ecology [10], assisting aquatic robots [11], understanding underwater geology [12] and fish species recognition [13] and also for lots of offshore facilities like drinking water reservoirs [14], underwater cable framework installations [15] etc. These underwater studies and facilities are usually inspected visually by divers manually. This strategy has disadvantages which are very evident: it is hazardous, expensive, time-consuming and yet often does not provide a complete evaluation.

The solution to avoid these issues is (1) using sonar sensors or (2) using cameras to capture the underwater imagery. Although sonar sensors have features advantageous for the underwater medium but there was a major disadvantage: the enormous amount of data in shape and reflectance of objects, the visual impression, as well as the chance of direct visual evaluation by the specialist is wasted as data is not obvious. On the other hand, camera-based imaging modalities for underwater applications have many other prospective uses: seaweed

assessment, ocean floor surveying, shipwreck hunt, oil and natural gas discovery etc. Design of camera systems has to be robust enough to deal with waves, turbulence of water and also it has to be waterproof to avoid damage to its sensors. Such design issues have been taken care of with modern technology. But using the camera for underwater apps includes several technology-related difficulties such as camera system design, suitable lighting specifications and computer vision improvement methods. Flash light is used for compensating for the light absorbed by water medium. But such measure leads to artifacts in the images like uneven illumination, bubble effect etc [16]. Thus, The most suitable solution to this is pre-processing the captured images with certain image processing algorithms to get a clear picture of the underwater scenery. Next section discusses how underwater images are formed and the issues associated with underwater images which need to be addressed while processing them.

1.2 Underwater Camera based Imaging and associated issues

Underwater images are of very poor quality with greenish blue appearance. The color quality of underwater images are distorted due to the inherent physical property of water [17] as depicted in Fig. 1.1. The different constituent wavelengths of light are selectively absorbed in the decreasing order of wavelengths [18] owing to the absorption property of water. It means that colors like red, orange etc. which have higher wavelengths disappear with depth as the light enters the water as compared to colors like blue, green etc. which have lower wavelengths. Apart from the color constancy issue in underwater images, another major issue is low visibility due to scattering property of water. Most of the light incident on surface of water is reflected back and rest enters the water [19]. Thus, owing to poor visibility, underwater images have bad contrast. Thus, the two main problems of underwater images is color cast and bad contrast.

Color Cast: Depending upon the surrounding like presence of corals, plants etc., color cast can be blue, green or greenish blue. Thus, there is need of finding the actual color cast of

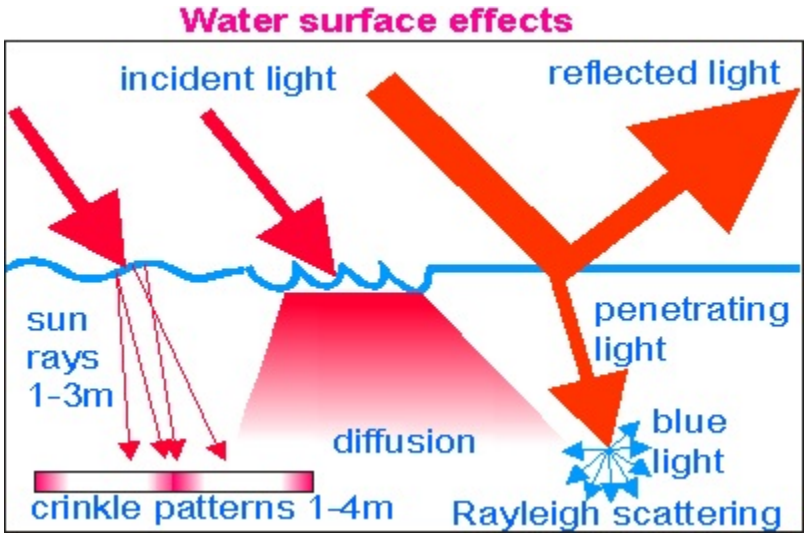

(a) Penetration of light inside water

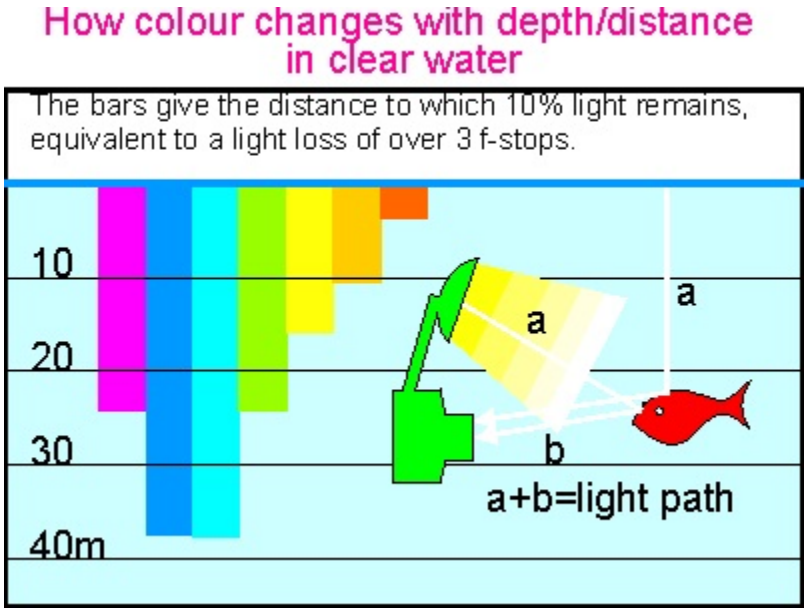

(b) Absorption of wavelength inside water

Figure 1.1: Effect of water medium on light [1]

an underwater image instead of assuming it so as to pre-process the image effectively.

Poor Contrast: Due to reflection of light rays from the water surface, very few light rays penetrate into water. Moreover, the salinity and turbidity of the aquatic medium also affects the propagation of light deep into the water, thereby leading to darkness in captured images. Fig. 1.1 shows the effect of water surface on light and wavelength absorption pattern in water. The above-mentioned two factors altogether affect the information content of the image.

Thus owing to these problems in underwater images, we need to apply image processing techniques to acquire a clear underwater image.

Image processing techniques can be classified mainly into two categories: image enhancement and image restoration. Image enhancement based techniques are relatively simple to understand and apply. It works on pixel intensity values in order to achieve a pleasant and enhanced picture. On the other hand, image restoration methods employ the knowledge of the image formation model to restore the original scene from the captured scene.

Image formation process is different for an ideal transmission medium and underwater medium due to various factors affecting underwater. As we know, the ideal transmission medium has little or no effect on light and light is mainly affected by characteristics of the objects in focus and capturing device like angle of shooting, lens aperture. On the other hand, Underwater transmission medium affects the light by absorption and scattering of wavelengths. Also, factors like depth of the scene to be captured, salinity level of water, turbidity level of water and time of capturing the underwater image (during the onset of sun or during sunset etc.) have a drastic impact on the formation of image. Basic theory for underwater image formation was laid by McGlamery in 1980 [20] and Jaffe [21] extended the theory for artificial lighting in underwater environment. According to Jaffe-McGlamery theory, total irradiance at any point in image is composed of E_d, E_f and E_b. E_d is the direct constituent of light that the object reflected, E_f is the forward scatter constituent of light which the object reflected but scattered at small angles by water and manage to enter the camera and E_b is backward scatter constituent of incident light which did not come in contact with the object. Direct constituent of light at any coordinate (i,j) of image is given by Eq. 1.1

$$E_d(i,j) = J(i,j)e^{-\eta.d(i,j)} \tag{1.1}$$

where J(i,j) is the original radiance of the image scene, d(i,j) is the distance of image plane from the camera and η is the attenuation coefficient.
Since forward scatter component is result of scattering of reflected light or direct component, thus it can be computed by convolution of direct component with point spread function. Back scatter component of light mainly leads to color and contrast loss. Thus, avoiding the forward scatter, the total radiance at a point (i,j) in an image is given in Eq. 1.2.

$$\begin{aligned} I(i,j) &= E_d(i,j) + E_b(i,j) \\ &= J(i,j)e^{-\eta.d(i,j)} + B(i,j).(1 - e^{-\eta.d(i,j)}) \end{aligned} \tag{1.2}$$

where, I(i,j) is perceived radiance at point (i,j), B(i,j) is back scatter color vector and $e^{-\eta.d(i,j)}$ is transmission map
Since the underwater medium can be different e.g. saline, turbid, dense due to aquatic flora and fauna etc., determining the attenuation coefficient is difficult. Thus, the aim of image restoration techniques is to find J(i,j) from I(i,j). Thus, Eq. 1.2 of underwater image formation is similar to the equation of light propagation with additional factors affecting the attenuation coefficient (scattering and absorption).

1.3 Problem Definition

Lots of efforts are going in enhancing the underwater images to acquire information for underwater scientific studies. The main objective of this thesis is enhancement of underwater images for various scientific applications. Following are the problems addressed in this thesis:

- Underwater images, as mentioned earlier, have color cast issue. But the method for handling this color cast is very naive as it is assumed to be green or blue depending upon the underwater region in which it is captured. For example, if the image is captured in a medium where algae content of water is high, there will be greenish color cast and if the image is captured in deeper water then there will be blue cast.

Most of the techniques remove color distortion of underwater images assuming that there is blue color cast in the images. But color cast depends upon the depth of the water.

- Since artificial light is required for underwater images which lead to uneven illumination and artifacts in the image. This issue of the uneven light illumination is disregarded by the vast majority of the researchers. Since artificial lighting is a mandatory requirement to capture images underwater as there is very less illumination beneath the water specially at deeper levels. But with this aid comes a problem i.e. only the objects in focus are clear but still the imagery is not that clear for study. So when we process such an image, this lead to artifacts like false colors in image.

- Lastly, There are multiple problems associated with underwater images along with color cast and poor contrast, like haze, noise etc. There is not much effort has been made to integrate color correction and noise removal both of the underwater images. Scattering effect of water has been removed to a great extent, but the absorption effect of water is not being handled well by the researchers.

1.4 Scope and Objectives of the thesis

Underwater imagery is required in diverse fields of scientific and technological applications specifically in civil and military related applications. Machine vision plays a key role for multiple uses such as monitoring of pipelines and telephone wires, mine detection, coral reefs, surveying of rare underwater species, fossils, etc. Some of them are listed below:

- **Underwater Inspection** Underwater inspections are often carried out for oil contamination and servicing of underwater pipelines and structures. Ship's hull inspection is component of the maintenance activities. Ships entering ports serve as carriers for radioactive materials such as nukes. Autonomous rover vehicles have replaced divers for the maintenance activities. Navy requires seabed exploration for mine detection and activities by enemies underwater in which computer vision plays an important role.

- **Marine Oceanography**: Underwater imaging applications include studying aquatic species behavior and habitat mapping like monitoring shark activities [22], marine geological activities like state of seabed and corals [23] etc.

- **River Sediment Analyis**: Geologists are nowadays paying attention towards a new area using underwater imaging i.e. to analyze grain size in sediments found in riverbed. It is a time and money intensive task required for sediment analysis. Quick and easy way for the grain size change and its tracking over time is nowadays done using image processing techniques which employ analysis of microscopic digital images.

Information about underwater scenario is required for various reasons and challenges associated with getting the information at real time have been discussed in section 1.1. Following are the objectives of the thesis:

- For every underwater image, we need to study the image first, or we should have the prior information about the medium and the depth of water in which image is captured before processing it. Thus, we need an adaptive enhancement method which requires no information about the underwater medium to process it and should remove the color cast which is there in the image.

- Artificial light is required to capture the underwater imagery but there are associated issues like false colors etc. which are introduced on pre-processing of the images. Thus, there is need to consider the uneven illumination during processing so that artifacts are not there.

- All the problems associated with underwater images should be removed altogether and also for different types of medium in terms of salinity, turbidity, green matter concentration etc. Thus, there is need to handle all these problems altogether for different underwater media so that the image is suitable for scientific studies.

1.5 Contribution and Thesis Layout

The different problems and issues as mentioned in section 1.2 motivates us to provide solution to them in this thesis. There are solutions provided to all the sub-problems referred in section 1.3. This thesis provides an effective solution to solve the lighting, color, noise issues of the underwater images captured in different media (different salinity, turbidity, depth etc.) so as to make them suitable for various underwater scientific studies. Following are the main contributions of the work done in this thesis:

- Fuzzy rules are developed to find the color cast in underwater images. Gray world algorithm has been modified to remove the linearity in color correction to adapt with the underwater medium.

- The color cast and contrast of underwater images vary according to the type of water in which it is captured. Hence, adaptive algorithms are developed which work for every type of underwater image irrespective of the depth, region in which it is captured.

- Appropriate weight maps have been designed to extract information from the images which further aid in enhancement of underwater images. Main aspect of underwater images is the identification of various objects in the scene for which local entropy and gradient information act as good measures.

- An algorithm is developed to remove three major problems (color cast, poor contrast and haze) of underwater images. To utilize the information from underwater images, it should be free from color cast, bad contrast and hazy appearance.

Finally, the thesis is organized in the following layout:

- **Chapter 1: Introduction**
  Chapter 1 presents the underwater imaging model along with the different issues associated with underwater images. Contributions and thesis layout is also discussed.

- **Chapter 2: Literature Review**
  Chapter 2 describes the existing image processing techniques. A brief study of image enhancement and image restoration based techniques available for underwater images has been done.

- **Chapter 3: Optimal Underwater Image Enhancement**
  Chapter 3 presents an optimal fuzzy gray world based approach 'CIEUI' for underwater image enhancement. All the basic concepts employed in CIEUI have been explained. Chapter is concluded with results and comparative analysis with the related work.

- **Chapter 4: Fuzzified Color and Contrast Correction of Underwater Images**
  Chapter 4 presents a local enhancement based algorithm 'FCCC' using the extension of previous fuzzy gray world algorithm for handling the artifacts caused by artificial lighting. FCCC is explained followed by results and comparison with the existing methods in the literature.

- **Chapter 5: Fusion of Underwater Image Enhancement and Restoration**
  This chapter explains FUIER, a technique based on fusion of image enhancement and restoration to handle major issues like color, contrast and haze of the underwater images. Finally, the analysis of results of FUIER is done with various state-of-the-art techniques.

- **Chapter 6: Conclusion and Future Works**
  Lastly in Chapter 6, results of the proposed work has been discussed and summarized. Future scope of the work has also been discussed in the later section.

Chapter 2

Literature Review

Underwater images are inherent requirement for underwater applications dealing with studies like inspecting state of flora and fauna inside water, effect of climatic changes on the their population sensus etc. Advanced expensive cameras help in getting underwater images but the quality of images still need to be improved. Researchers are working in these field for last one decade using various image processing techniques. These underwater image processing methods belong to one of the following classes: image restoration (model based) or image enhancement (subjective criteria based). However, these broad classes can be further categorized into different classes depending on their way of addressing the problems of underwater images. Fig. 2.1 represents the classification of underwater image processing methods.

2.1 Underwater Image Enhancement Methods

Underwater image enhancement can work either by modifying the pixel distribution so as to change the overall contrast or color of the image. Thus, underwater images can be enhanced by changing their contrast or color or both at the same time.

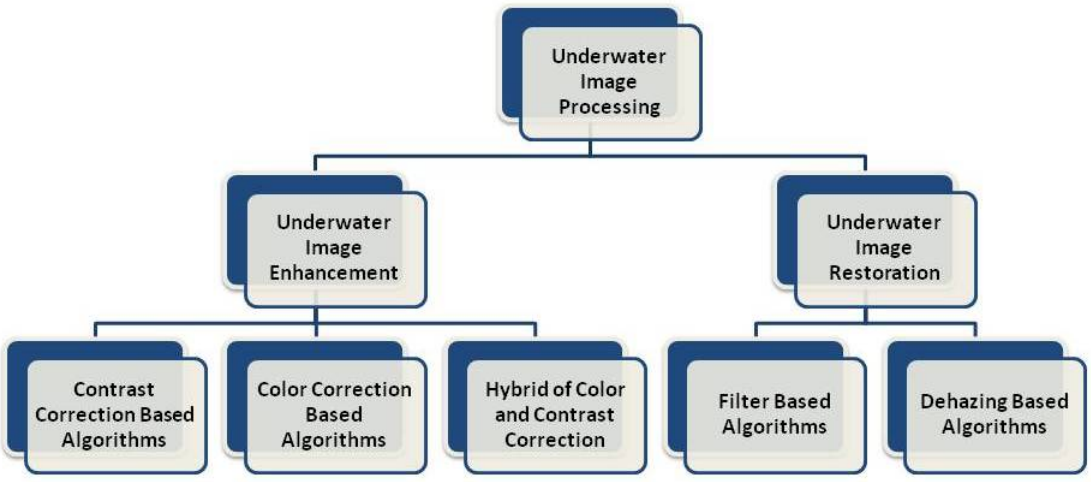

Figure 2.1: Classification of Underwater Image Processing Methods

2.1.1 Contrast Correction based Algorithms

One class of underwater image enhancement methods is contrast correction based algorithms which tackle the problem of poor contrast in underwater images. One of the popular and traditional method for contrast enhancement is histogram equalization (HE) [24]. But HE does not give the desired results as underwater images have non-uniform contrast and color distortion which can not be rectified by HE. Adaptive HE [25] can address the problem of non-uniform contrast in underwater images but again color distortion problem is unaddressed. Some researchers employed histogram stretching for underwater image enhancement e.g. Integrated Colour Model (ICM) [26] used contrast stretching of RGB and HSI model to achieve enhanced image. [27] employed CLAHE (Contrast Limited Adaptive HE) of RGB and HSI model and formed the enhanced image by taking the euclidean norm of contrast stretched RGB and HSI images. Ghani *et al.* [28] applied contrast correction on different color models and integrated their results to improve the overall quality of the image. [29] proposed an adaptive fuzzy based contrast correction method for underwater images captured in turbid media. [30] applied CLAHE on HSV and YIQ color space to improve the contrast and fused their result to get the final image. This fusion improves the

color quality but this method is slow and results are also not visually appealing. [31] also employed histogram equalization of RGB channels to improve the contrast of underwater images. Mathur *et al.* [32] fused the results of CLAHE and guided filters to get an enhanced image but results still had poor contrast.
Since poor contrast is not the only issue of underwater images. Thus, only contrast correction does not yield desirable results. Color correction, on the other hand, sometimes improve the contrast of the images also by changing the color distribution of the pixels in the three color channels. Next subsection provides insight into color correction based underwater image enhancement.

2.1.2 Color Correction based Algorithms

Another class of underwater image enhancement methods focuses on color correction of underwater images to remove the problem of color cast. The fundamentals of color correction include gray world assumption [33], white balance [34] and retinex theory [35]. These theories form the basis for the methods for underwater image color correction. [36] used gray world based assumption and white balance in $l\alpha\beta$ space for color correction of underwater images. [37] modified Automatic Color Equalization (ACE) [38], which is based on white balance theory so that modified ACE can be applied on underwater videos. Although stated automatic, the method requires tuning of parameters, thus making it less usable for underwater images. [39] employed empirical mode decomposition (EMD) and used genetic algorithm to adjust the weights for the layers of EMD to enhance the underwater images but contrast is not improved to a good extent. [40] used retinex theory along with some optimization strategy for underwater image enhancement and this method can also be applied on different types of color degraded images. [2] proposed RAHIM (Recursive Adaptive Histogram Modification) which processed histograms column-wise to enhance underwater images. This method produced enhanced images with good information content but contrast is poor. Hou *et al.* [41] applied filtering to saturation and intensity values and not changing the hue component. Results are appealing but contrast is not good and haze is present in the images. [42] restored the colors of the image by applying rayleigh distribution based stretching on YCbCr color model.

Both color and contrast related issues need to be eliminated from underwater images to achieve desired results. Hence, most of the work in literature are hybrid of color and contrast correction algorithms.

2.1.3 Hybrid of Color and Contrast Correction

Another class is hybrid of contrast and color correction algorithms which solves the contrast and color related problem in underwater images. Unsupervised Color correction Method (UCM) [43] used gray world assumption theory for color correction, followed by contrast stretching for enhanced image. The above-mentioned method sometime generates over-enhanced and under-enhanced regions in the output image. To overcome these drawbacks, Ghani *et al.* [44] proposed a technique which combined the modified ICM [26] and UCM [43] to produce better results. This technique produces visually appealing results but create halos and artifacts for low-lit images. Ghani *et al.* [45] applied contrast correction using modified von kries hypothesis [46] followed by color correction applied on HSV model to enhance the underwater images. But the resultant images of this technique still have drawbacks like poor contrast, blue green illumination and partial enhancement. [3] performed underwater image enhancement by blending CLAHE and percentile methodologies but the color quality of the images is poor. Ancuti *et al.* [47] proposed a fusion of two versions (color corrected and contrast corrected) of input image using four different weight maps derived from those versions. In [48], Ancuti *et al.* extended [47] by modifying the contrast correction method and reducing the number of weight maps. Both the techniques employ multi-scale Laplacian pyramid decomposition based fusion and give good results but a little haze is still present in the output. Zhang *et al.* [49] proposed an underwater image enhancement method which first restores the image and then fuses the two versions of the restored image using multi-scale fusion but the results are not better than those obtained by Ancuti *et al.* [48]. Wong *et al.* [50] combined color and contrast correction using adaptive gray world and histogram equalization to remove color cast and improve contrast of underwater images. But the color quality of images were not good. [51] modified gray world assumption and improved the color correction method and applied PSO on contrast correction method so as to control the artifacts in the resultant image. Results have im-

proved color but with hazy appearance which reduces the overall quality of image.
Hybrid of color and contrast correction based algorithms handle both color and contrast related problems of underwater images, thereby producing better results than other underwater image enhancement classes mentioned above. But there is lack of guidance mechanism during contrast stretching and most of the techniques assume color cast as blue only for every underwater image. Artificial lighting is also not been taken care by most of the techniques which leads to over-enhanced and under-enhanced regions in the output image. Being computationally less intensive and fast, underwater image enhancement methods have an edge over restoration methods as they handle two major problems of underwater images effectively and do not need for any other prior information about the image.

2.2 Underwater Image Restoration Methods

Underwater image restoration works on some image formation model or noise model to restore the image. Nowadays, underwater image dehazing model is gaining popularity for processing of underwater images.

2.2.1 Noise model or Image model based methods

One class under underwater image restoration techniques makes use of different filters to remove problem of noise in underwater images. In [52], pre-processing step using various filters has been proposed to enhance the image quality by removing noise. Lu *et al.* [53] used trigonometric filter for enhancement of underwater images. Sheng *et al.* [54] employed multi-wavelet transform and median filter for underwater image enhancement. [55] employed modified Multi-Scale Retinex (MSR) [56] which employs bilateral and trilateral filters instead of gaussian for underwater image enhancement. Nnolim [57] proposed partial differential equations for optimizing entropy and gradient based image processing algorithms.
Researchers are also working to find the parameters of image formation model using different soft computing techniques to restore the image. A PSO based technique is proposed for underwater images by Abunaser *et al.* [58] but it requires repeated execution of PSO

to tune the parameters for image enhancement. Some researchers are also focusing on training convolutional neural network (CNN) with image restoration techniques to dehaze underwater images [59], [7]. Another deep neural network based study for underwater image enhancement [60] has trained the CNN for finding the parameters of image formation model using synthetic underwater images. Trained neural networks give good results. However, it requires a lot of time to exhaustively train the neural networks with every type of underwater image to get effective results.
This class of underwater image restoration methods considers noise as the only problem in underwater images and give satisfactory results for some images. Thus, to address all the problems of underwater images, an extensive filter design is necessary which is a computationally expensive and difficult approach.

2.2.2 Dehazing Model Based Methods

One more category of algorithms for underwater image restoration considers blurriness and color cast in underwater image analogous to haze in outdoor images and apply dehazing based techniques [61] for underwater image enhancement. Another reason for applying these techniques is the similarity between the equations of image formation in underwater medium and atmospheric medium. These techniques require estimation of transmission map and waterlight (airlight for atmospheric images) by making use of dark channel prior (DCP) [62] or its variant to get an enhanced image. Chao *et al.* [63], Carlevaris-Bianco *et al.* [64] used dark channel prior to clarify the blurred underwater images but failed to color correct the images. [65] also employed dark channel prior for image deblurring and then followed it with a color correction method. Chaing *et al.* [66] proposed a dark channel prior based algorithm which further removes artifacts caused by artificial light. [67] developed a dark channel prior based algorithm in which estimation of dark channel is done using image blurriness model. [68] modified the dark channel prior to bright channel prior to enhance the underwater images. [69] formulated the problem around red channel restoration as red color attenuates the most in underwater environment. [70] proposed an algorithm which used minimum information loss principle for image dehazing and followed it with a contrast enhancement algorithm for further enhancement of image. Peng

et al [71] proposed a method for estimating the depth of the image formation model based on image blurriness and light absorption pattern. [72] proposed new adaptive attenuation prior for image restoration which delivered good results but still there is need for accurate assumption of attenuation coefficients. [73] used an optimized version of DCP which estimates the ambient color and helped in object detection in water medium but it does not give accurate results in turbid medium. [74] dehazed the underwater image using a approach which applies edge preserving smoothing at different level along with dehazing. Results are convincing but some images have spurious color which indicates that parameter tuning is required. In [75], a new method to estimate transmission map using inverse red channel attenuation prior for dehazing model. Lu *et al.* [76] proposed a method based on dark channel prior and Multi-Scale Cycle Generative Adversarial Network (MCycle GAN) for underwater image restoration. But both methods can not handle non-uniform illumination due to artificial lighting. These dark channel prior based methods give good results but require high computation. Results are highly dependent on correct estimation of transmission map so these methods works only for some underwater images.

To summarize, image restoration based techniques give good result for few images, for which the parameters have been estimated correctly. These techniques are computationally intensive and requires either parameter estimation for existing models or formation of new model or priors for different types of underwater images. Moreover, efficacy of such models is best only for the media for which their parameters have been tuned.

Chapter 3

Optimal Underwater image enhancement

3.1 Introduction

An effective solution to the problems in underwater images, should correct the color distortion and improve the contrast of the images. The various image processing algorithms pre-process an underwater image by using either enhancement or restoration based algorithms. Image enhancement based methods have been the obvious choice owing to their inexpensive and simple nature. As we know, image enhancement algorithms try to tweak the histograms of the image to improve its color and contrast, it may lead to overstretching of the histogram since there is no way to guide to which extent the stretching should be done. Moreover the underwater medium can also vary, i.e., salinity, turbidity, organic matter of the medium can also affect the image quality [77]. As the extent of color and contrast correction varies for different media, there is need of a method which can handle both color and contrast problem in different underwater media.

In this chapter, a method called 'Contrast and Information Enhancement for Underwater Images' (CIEUI) has been formulated for this purpose. CIEUI employs Multi-objective Particle Swarm Optimization (MOPSO) [78] to perform color, contrast correction and in-

formation enhancement simultaneously. The parameters of CIEUI decide the degree of color correction for different media which are tuned by MOPSO. Objective functions of MOPSO are chosen to act as guiding mechanism to ensure color, contrast correction and information enhancement respectively without introducing artifacts caused by overstretching of histogram.

3.2 Problem Formulation

Underwater images are distorted in terms of color and contrast quality due to the nature of underwater media. Depending upon the media constituents (algae matter, coral population, flora and fauna, depth etc.), color cast can be different and so is the contrast. Hence, one can not presume the color cast to be just blue always. We need to have a solution which identifies the color cast and then depending on the color cast and contrast, stretches the histogram accordingly. Hence, CIEUI has been formulated which first identifies the color cast using fuzzy rules and then the color correction is done in accordance with some factors which are found using Multi-objective Particle Swarm Optimization (MOPSO).
CIEUI is a multi-objective adaptive color correction and information enhancement technique for underwater images which has been framed using the fuzzy gray world technique [8]. CIEUI employs MOPSO to ensure that desired results are produced without artifacts like false colors, light image, halos etc. Performance measures namely 'Histogram Spread (HS)' and 'Entropy' are chosen as objective functions of MOPSO to produce an output image with enhanced contrast and information content. Color cast detection and correction is performed using fuzzy gray world algorithm which requires non-linearity factors dependent on the type of media. These factors act as guiding mechanism to control the overstretching of the histogram. MOPSO identifies these factors with the help of appropriate performance measures. CIEUI delivers results with enhanced information and contrast as compared to other algorithms for underwater images. Basic concepts used in CIEUI are explained in further sections in detail.

3.3 Fuzzy Gray World Algorithm

Fuzzy Gray world Algorithm is the combination of fuzzy logic [79] and gray world assumption [33] for removing the color cast of underwater images. Most of the research in the field of underwater image enhancement assumes that there is blue color cast in underwater images as lower wavelengths are absorbed as light enters deep in water. However, use of artificial light while capturing photographs, can lead to a change in this pattern as artificial light compensates for the loss of energy of the red wavelength of light on penetrating water. The problem of color cast identification can be addressed by fuzzy logic effectively because the decision about color cast in the image is fuzzy in nature. Ambiguous concepts like 'reddish green color' or 'bluish appearance', etc. can be effectively handled using fuzzy sets [79]. Fig. 3.1 shows the image of a scuba diver (without artificial light) and a fish (captured using artificial light) with their histograms. The fish image fails the above assumption as the blue color histogram is not skewed towards higher intensities. The fuzzy gray world algorithm does not consider the assumption that blue color is always concentrated towards higher intensities as the underwater images can be captured in different types of media having varying salinity, turbidity, organic concentration etc. which can affect the color cast pattern. Color cast in underwater images can not be clearly categorized as blue or green, sometimes it is a combination of blue and green, sometimes there may not be any color cast if artificial light is employed or sometimes due to the surroundings like corals, algae etc., there can be greenish color cast. Thus, there is need to find the color cast for a given image. Fuzzy gray world algorithm finds the actual color cast and performs color correction instead of assuming color cast as blue like other conventional histogram based techniques.

Consider the RGB image I_{ij} where i and j represent the pixel coordinate $I_{ij} = (R_{ij}, G_{ij}, B_{ij})$ with $R_{ij}, G_{ij}, B_{ij} \in [0, 255]$. The first step is to calculate of the mean intensities of the red, green and blue channels of the given Image I. Means are denoted by $\bar{R}, \bar{G}$ and $\bar{B}$ respectively and are calculated by using Eq. 3.1.

$$\bar{R} = \frac{1}{mn}\sum_{j=1}^{n}\sum_{i=1}^{m} R_{ij} \quad \bar{G} = \frac{1}{mn}\sum_{j=1}^{n}\sum_{i=1}^{m} G_{ij} \quad \bar{B} = \frac{1}{mn}\sum_{j=1}^{n}\sum_{i=1}^{m} B_{ij} \tag{3.1}$$

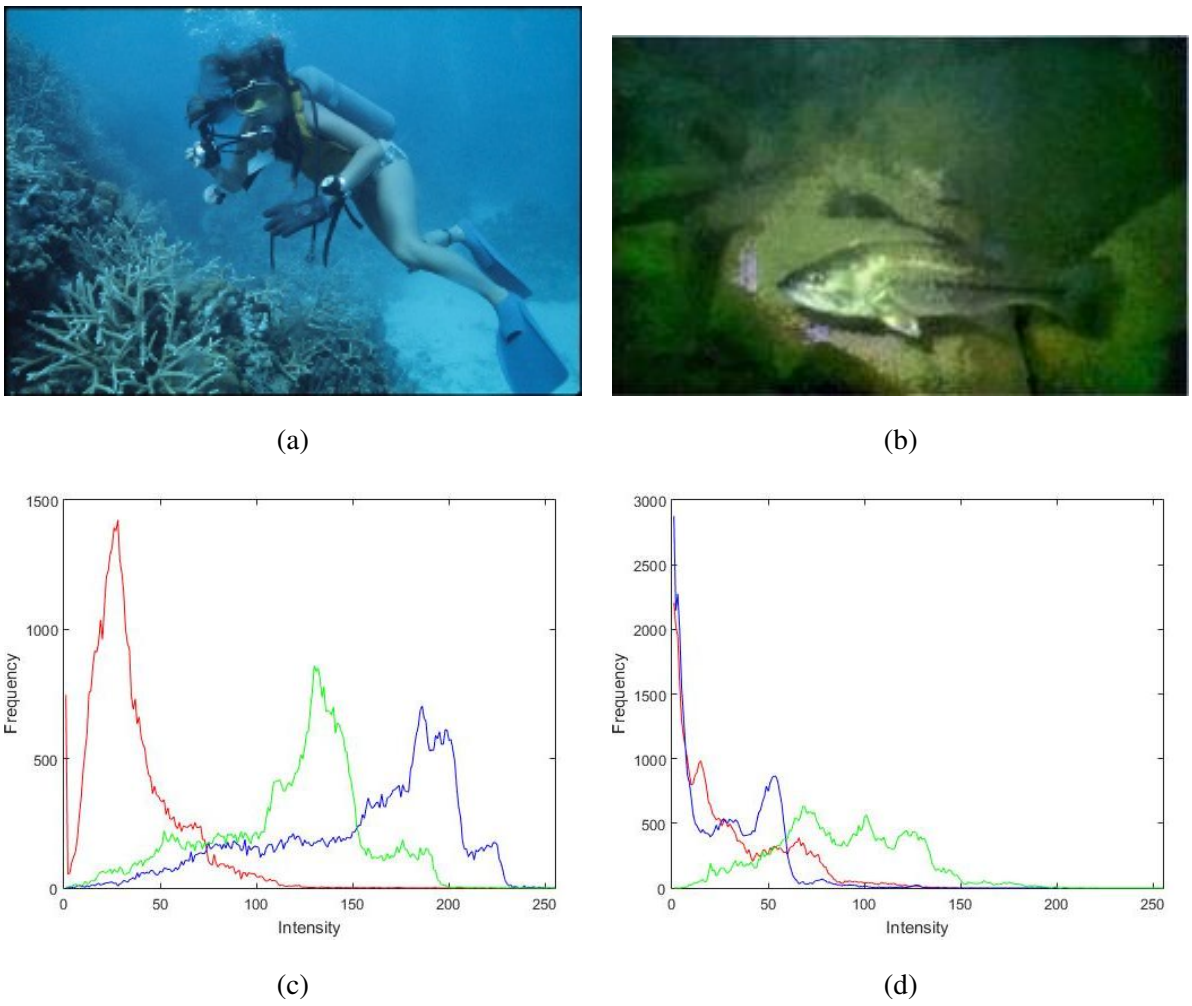

Figure 3.1: (a) Scuba Diver (b) Fish (c) Histogram of Scuba Diver image (d) Histogram of Fish image

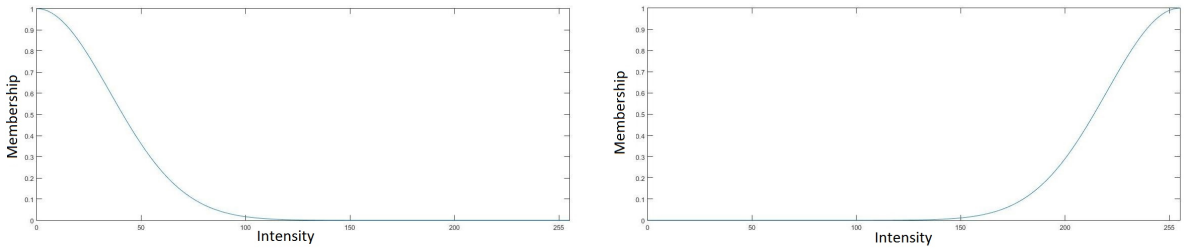

(a) LOW Fuzzy Set (b) HIGH Fuzzy Set

Figure 3.2: Gaussian Membership function for fuzzy sets (a) Low (b) High

The second step is to fuzzify the individual color channels. There are two fuzzy sets named 'LOW' and 'HIGH' which indicate the extent to which an intensity value is low and high respectively. These fuzzy sets use the gaussian membership function given by Eq. 3.2 and curves for the fuzzy sets are shown in Fig. 3.2.

$$\mu(x) = \exp\left(\frac{-(x-c)^2}{2(\sigma^2)}\right) \tag{3.2}$$

The parameter 'c' is the center of the gaussian curve at which membership function will have value '1'. The parameter σ is the standard deviation of the gaussian curve and defines the width of the curve. The membership functions for the two fuzzy sets, namely LOW and HIGH are stated in Eq. 3.3.

$$\mu_{LOW}(x) = \exp\left(\frac{-x^2}{2(35^2)}\right) \quad \mu_{HIGH}(x) = \exp\left(\frac{-(x-255)^2}{2(35^2)}\right) \tag{3.3}$$

$\mu_{LOW}(x)$ and $\mu_{HIGH}(x)$ are membership values for intensity value x in the fuzzy sets LOW and HIGH respectively. Thus, the center of the curve is chosen as '0' for 'LOW' fuzzy set because intensity 0 is the lowest possible intensity value and should have membership value as 1 for LOW. Similarly, the center of the curve for the HIGH fuzzy set is chosen as 255 which is the highest possible intensity value. Value of σ for the fuzzy sets should be such that the Gaussian curve follows the following conditions:-

(i) At 0, Membership value in the LOW fuzzy set should be 1 and start decreasing gradually with increasing intensity values. For intensities above 128, membership value should

Table 3.1: Fuzzy Rules and Base Channel

	If			**Then**	
Rule Number	**R(i,j)**	**G(i,j)**	**B(i,j)**	**Cast**	**Base**
1	High	Low	Low	Red	$\bar{R}$
2	Low	High	Low	Green	$\bar{G}$
3	Low	Low	High	Blue	$\bar{B}$
4	High	High	Low	Red and Green	$(\bar{R}+\bar{G})/2$
5	Low	High	High	Green and Blue	$(\bar{B}+\bar{G})/2$
6	High	Low	High	Red and Blue	$(\bar{R}+\bar{B})/2$

become '0' as these intensities are no longer low.
(ii) At 255, Membership value in the HIGH fuzzy set should be 1 and start decreasing gradually with decreasing intensity values. For intensities below 128, membership value should become '0' as these intensities are no longer high.
These conditions should be followed by every image. Value of σ is found experimentally as '35' as it is fulfilling the above-mentioned criteria. Membership of each pixel in the individual channel is found by using Eq. 3.3 and the pixel will belong to the fuzzy set with a high membership value.
Table 3.1 states six fuzzy rules and base for color correction. These rules are applied to every pixel in the three channels and the rule which is followed by the maximum number of pixels decides the color cast of the image. Color cast gives the base for subsequent color correction. Base is a matrix of size same as that of the image. It helps in computing the scale factors for each pixel in the three color channels. The next step is to find scale factors by using base decided from Table 3.1 and means calculated from Eq. 3.1. Scale factors $\alpha_r, \alpha_g \; and \; \alpha_b$ are calculated using Eq. 3.4.

$$\alpha_r = \frac{Base}{\bar{R}} \quad \alpha_g = \frac{Base}{\bar{G}} \quad \alpha_b = \frac{Base}{\bar{B}} \tag{3.4}$$

The final step is to perform color correction by using Eq. 3.5. Color correction gives corrected values for red, green and blue color channels denoted by $\hat{R}$, $\hat{G}$ and $\hat{B}$ respectively. λ_r, λ_g and λ_b are non-linearity factors for red, green and blue color channels respectively. These factors control the degree of color correction of each color channel. Since underwater images can be captured at different depth, in different salinity and turbidity levels of water, etc., the degree of color correction cannot be same for every image. This degree is tuned using Multi-objective Particle Swarm Optimization (MOPSO).

$$\hat{R} = (\alpha_r)^{\lambda_r} R \quad \hat{G} = (\alpha_g)^{\lambda_g} G \quad \hat{B} = (\alpha_b)^{\lambda_b} B \tag{3.5}$$

Values of these non-linearity factors $\lambda_r, \lambda_g \; and \; \lambda_b$ are computed by using MOPSO algorithm which optimizes performance measures namely histogram spread [80] and entropy [81] explained in the next section.

3.4 Performance Measures

Since underwater images have diminished color, contrast and bad illumination, performance measures chosen should ensure that color, contrast and information should improve. Two metrics chosen as performance measures are namely Histogram Spread (HS) [80] and Entropy [81]. HS [80] is a quantitative measure for assessing the overall contrast of an image. It quantifies the uniformity of histogram over the entire intensity range and should be close to 0.5 if the histogram is uniformly spread. Since for a good contrast image, the histogram should be uniformly spread across the whole intensity range, HS gives an index for measuring the uniformity of the histogram. Entropy ensures that the image has good information content and it should not decrease after enhancement.

3.5 Multi-Objective Particle Swarm Optimization for Contrast and Information Enhancement

There are a lot of meta-heuristic techniques proposed in the literature for multi-objective problems, e.g., non-dominated sorting genetic algorithm [82], Pareto-archived evolution

strategy [83] etc. These techniques are nature-inspired and evolutionary in nature. Another technique which is an advancement over these extensively used techniques is an optimization algorithm called Particle Swarm Optimization (PSO) [84]. PSO is gaining popularity due to its simplicity. The concept of population and a measure of performance used in PSO is analogous to population and the fitness value used in evolutionary algorithms. All the calculations performed in PSO are similar to crossover operator. However, there is an added advantage of solutions being scattered over a hyperspace, which is not available in traditional evolutionary algorithms. Another advantage of PSO over evolutionary algorithm is that it learns from the past experience. Thus, PSO has been choice for multi-objective problem which provides better convergence rate as well. Let us understand MOPSO in the next subsection.

3.5.1 Multi-Objective Particle Swarm Optimization

Let us understand multi-objective optimization first.

Definition 3.5.1. Multi-objective Optimization: Given n objective functions $f_1 : \chi \rightarrow R, ..., f_n : \chi \rightarrow R$ which map a decision space χ into R, a multi-objective optimization problem (MOP) is given by the following problem statement:
minimize $f_1(x), ..., f_n(x), x \in \chi$

Remark. Usually, we say $n > 1$ when we talk about multi-objective optimization problems. But, by convention, problems with large n are called many-objective optimization problems [85], [86] and not multi-objective optimization problems.

Hence, MOPSO [87] is a multi-objective problem in which we use PSO for the optimization of objective functions. Multi-Objective optimization for evolutionary algorithms like PSO [88], handles multi-objective optimization problems using the following principle:

1. Find the non-dominated solutions (found using PSO) which form the Pareto-optimal front.

2. Choose the best solution from the Pareto front using some extra information.

MOPSO is very similar to PSO as information about global and personal best locations is shared within flock in both the algorithms. However, PSO is slightly modified to handle multiple objectives in such a way that it discovers a set of solutions called 'Pareto Front' rather than a single global best solution. A pareto front (repository) is a set of all the non-dominated solutions found at each iteration. PSO and Pareto Front are explained in the next subsections.

3.5.1.1 Particle Swarm Optimization

PSO mimics the flocking behavior of animals who work in a group like birds, insects, bees etc. These group of animals (swarm) start looking for a piece of food. None of them know the exact location of the food. In PSO, each single solution is a particle in the search space. A fitness function which is to be optimized is associated with each particle. These particles have some position and move with a velocity in a random search space. The particle maintains two best solutions (1) best value of itself at which it has the best value of fitness function (pbest) and (2) the best value (particle) for the whole swarm (gbest). Both these values guide all the particles in the swarm. The particle updates its velocity and positions using pbest and gbest with following Eq. 3.6 and Eq. 3.7.

$$v_i = \omega * v_i + c1 * (pbest_i - present_i) + c2 * (gbest_i - present_i) \tag{3.6}$$

$$present_i = present_i + v_i \tag{3.7}$$

where v_i is velocity of particle i and $present_i$ is the current position of particle and $gbest_i$ is the global best particle. ω represents the interia weight. c1, c2 are personal and global learning coefficients respectively.

3.5.1.2 Pareto Front

While working with multiple fitness functions, there can not be a single solution which optimizes all the fitness function together. Thus, in multi-objective scenario, we deal with

contradictory objectives and the final solution should make a settlement between them. We can have a set of solutions in which any of the fitness function can have its best value. Thus, we need to find a set of solutions in which all the objective functions are improving and not even a single objective is worsening. Such a set of solutions is called pareto front. All the solutions in a pareto front are equally good if we don't have any other subjective criteria to distinguish between them. Some extra information is required to find the single best solution among these set of solutions.
In single objective optimization, best solution can be easily determined but for multi-objective optimization, we use the principle of dominance. One solution is said to dominate the other if at least one of the objective value is better than the other dominated solution and rest of the solutions should be either same or better than the dominated solution. All non-dominated solutions form Pareto front, which finally are the candidate solutions for finding one best solution. The domination between two solutions is based on mathematical concept called partial ordering and defined as follows:

Definition 3.5.2. A solution x is said to dominate other solution y, if it satisfies the following two conditions.

1. solution x is better than y in terms of objective function values.

2. solution x is strictly better than y in terms of at least one objective function.

MOPSO is based on PSO by using its position and velocity updation equations and generate a Pareto front to find the optimal solution as depicted in the flowchart in Fig. 3.3. From the flowchart, it is clear that MOPSO algorithm starts with the initialization of particles in the swarm with random values and various other parameters whose values are stated in Table 3.2. After initialization, the first step is to find the value of performance measures for the initial population in order to find the global and personal best solutions. Thus, HS and entropy is calculated for each particle of the swarm. Then, the non-dominated solutions from the swarm are found using the Pareto-optimality definitions [78] and stored in a repository. In each iteration, the global best solution is found out and velocities and position of particles are updated for the swarm just like PSO. Particles are then evaluated based on the performance measures and the personal best is found out. The repository

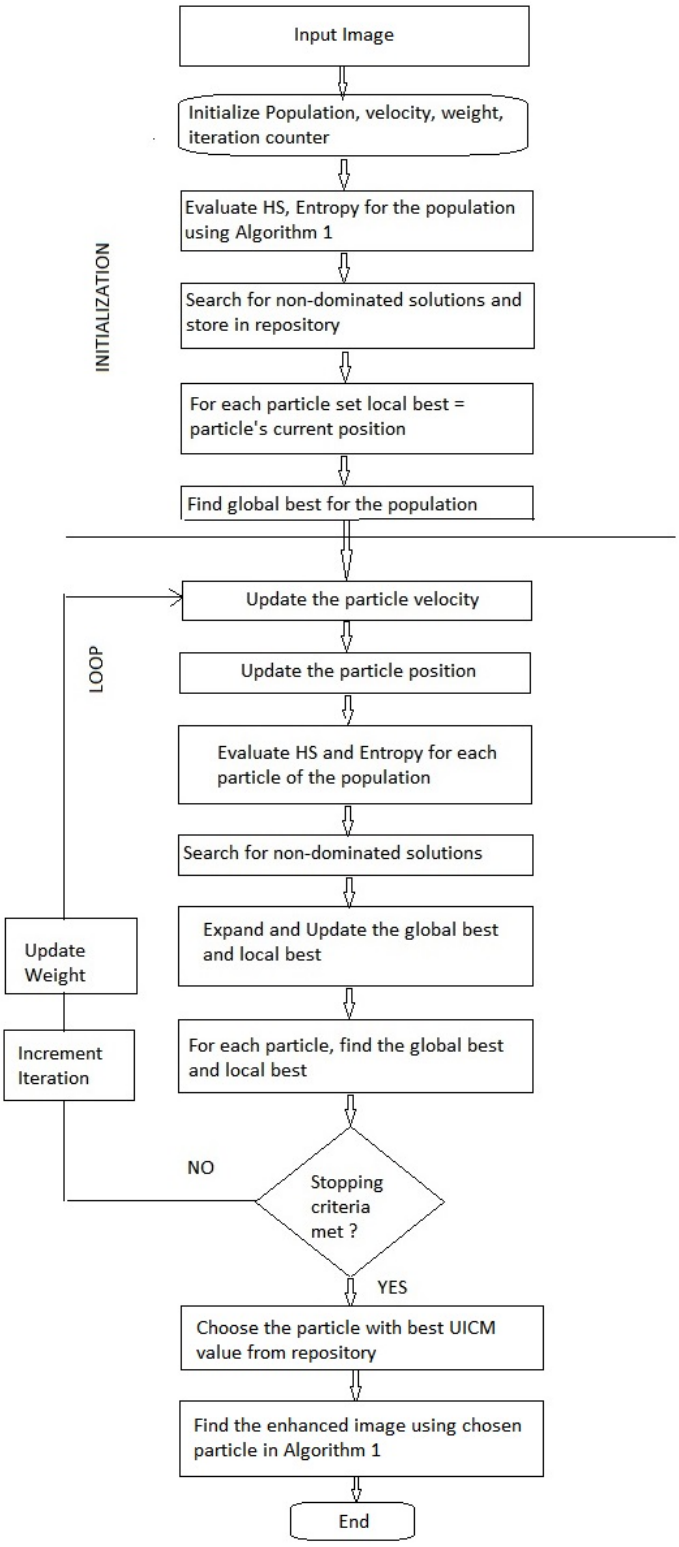

Figure 3.3: Working of MOPSO

is updated with global bests. After the end of iterations, the repository or Pareto-front is generated with the global best solutions from which one solution is chosen and an enhanced image is produced using the Algorithm 1.

Algorithm 1: Fuzzy Gray World Based Color Correction

Input: RGB Image I, $\lambda_r, \lambda_g, \lambda_b$
Output: HS, Entropy
Result: ColorCorrectedImage

Separate R,G,B channels of Image;
$[m, n] \leftarrow$ size of Each channel;
Compute Channel means using Eq. 3.1;
Initialize $Rulecount[6]$ to zero **for** $i \leftarrow 1$ **to** m **do**
    for $j \leftarrow 1$ **to** n **do**
        find $\mu_{LOW}(R(i,j))$ and $\mu_{HIGH}(R(i,j))$ using Eq. 3.3;
        find $\mu_{LOW}(G(i,j))$ and $\mu_{HIGH}(G(i,j))$ using Eq. 3.3;
        find $\mu_{LOW}(B(i,j))$ and $\mu_{HIGH}(B(i,j))$ using Eq. 3.3;
        Find the Fuzzy Membership of pixel in each channel using Mamdani Operator;
        `// Mamdani Operator assign the pixel to the fuzzy set which has higher membership value`
        $k \leftarrow$ fuzzy rule followed by the pixel in Table 3.1 .;
        `// value of` $k \in [1, 6]$
        $Rulecount[k] \leftarrow Rulecount[k] + 1$;
    end
end
$[max, DominatingRuleNo] = Maximum(RuleCount)$;
Find the base from Table 3.1 corresponding to $DominatingRuleNo$;
Compute $\hat{R}, \hat{G}, \hat{B}$ using Eq. 3.5 $ColorCorrectedImage = [\hat{R}, \hat{G}, \hat{B}]$;
Compute HS and Entropy of $ColorCorrectedImage$.

To achieve accelerated convergence and to reduce computational complexity, The number of iterations and swarm size are kept in a moderate range. Inertia weight is the con-

trol parameter for swarm velocity [89] and is given moderate value so that convergence does not become too fast without the exploration of a good range of positions. Personal learning coefficient is given lesser weight as compared to global learning coefficient so that position should be dependent more on global best positions than local best positions. Initial values of parameters have been taken by referring to state-of-the-art techniques [90] [87] and then updated after repeated executions for faster convergence and reduced time complexity. The detailed steps of MOPSO are shown in Algorithm 2.

Algorithm 2: CIEUI

Input: RGB Image
Output: Repository of Non-Dominated values of $\lambda_r, \lambda_g, \lambda_b$
Result: Enhanced Image

```
Initialize the MOPSO paramters ;
EVALUATE the value of HS and Entropy of each particle of the swarm using
  Algorithm 1. ;
Repository = SELECT the non-dominated solutions from the Swarm. ;
for t ← 1 to MaxIterations do
    for i ← 1 to size of swarm do
        SELECT the gbest ;
        UPDATE the velocity ;
        UPDATE the Position ;
        EVALUATE the Particle again by computing HS and Entropy using
          Algorithm 1. ;
        UPDATE the pbest;
    end
    UPDATE the repository with gbests;
    Report Results in the repository;
end
Choose the particle from repository with best UICM Value;
Output the Enhanced Image using Algorithm 1 for the chosen particle ;
```

Table 3.2: MOPSO Parameters

Parameter	**Value**
Number of Iterations	30
Size of Swarm	75
Size of Repository	20
Interia Weight	0.5
Personal Learning Coefficient	1.5
Global Learning Coefficient	2.5

(a) Divers

(b) Seal Fish

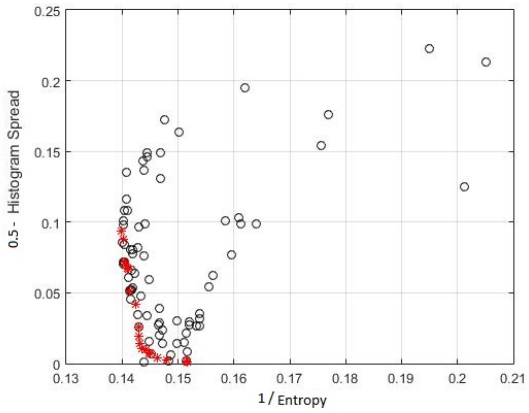

(c) PF of Divers

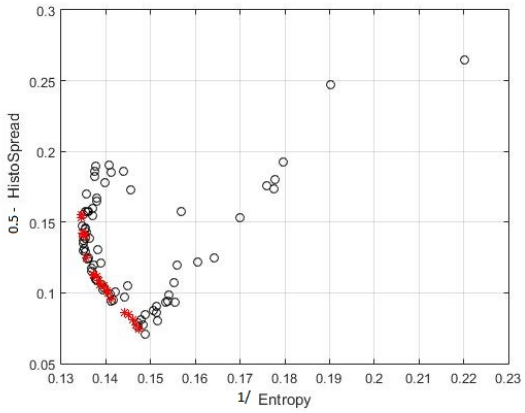

(d) PF of Seal Fish

Figure 3.4: Images and Their Pareto Fronts (PFs)

Thus, CIEUI aims to find the optimal value of the non-linearity factors $\lambda_r, \lambda_g \; and \; \lambda_b$ while optimizing the values of HS and entropy such that the HS value is close to 0.5 and the entropy value of the enhanced image is greater than or equal to the original image. MOPSO will provide a Pareto front which is a set of non-dominated solutions which are chosen as optimal if entropy can be improved without sacrificing histogram spread and vice-versa. Pareto fronts for a few images are shown in Fig. 3.4. Red dots in the plots are members of the Pareto front.

As discussed earlier, to find one solution from Pareto front, we need an extra information which is performance metric named 'UICM' (Underwater Image Colorfulness measure) [91]. It has been considered to choose from the set of candidate solutions as it tries to choose one solution which is having good information content (entropy), contrast (HS) and color quality (UICM). The solution with the best UICM value will be chosen as the optimal values of non-linearity factors required for computing the enhanced image.

3.6 Results and Comparative Analysis

Underwater images neither have any database with ground truth values nor any universally accepted quantitative measure for evaluating the extent of image enhancement. Thus, assessing the performance of underwater image enhancement methods is very challenging. Only non-reference based performance measures can be employed to judge the quality of image.
Recently, a few underwater image databases have been developed namely TURBID dataset [92] and WHOI color correction dataset [93]. The pictures of TURBID dataset are generated by experimentation for simulation of images in the turbid water body and WHOI (Woods Hole Oceanographic Institution) color correction dataset has original images along with reference images generated by the color correction method developed by scientists of WHOI. Thus, a comparison can be done with the results given on the WHOI website [93] using reference based performance measures like PSNR (Peak Signal to Noise Ratio) and MSE (Mean Squared Error) but these reference based performance measures cannot be used for quantitative evaluation of other underwater images.

Table 3.3: Average values of Entropy, HS and UICM for 200 Underwater Images

Technique	**Entropy**	**Histogram Spread**	**UICM**
Original	6.05	0.2531	3.0431
Gray World	6.89	0.3238	5.8244
UCM	7.18	**0.3771**	6.9969
Kwok *et al.* Method	6.06	0.2327	3.8461
Sethi *et al.* Method	6.89	0.3615	6.2657
CIEUI	**7.52**	0.3589	**7.1539**

CIEUI has been tested for 200 real underwater images taken from different underwater collections [94] and articles related to underwater image processing available on the internet for exhaustive comparison. The following methods have been used in our experiments: gray world technique [95], UCM [96], Kwok *et al.* [81] technique and Sethi *et al.* [8] technique. To demonstrate the efficacy of CIEUI, output and histograms of a few underwater images using the above-mentioned techniques are shown in Fig. 3.5 - 3.14. These underwater images are chosen as they are captured at different depths and in different water bodies.

For quantitative analysis of the above-mentioned techniques, the values of performance measures mentioned in section 3.5 which are 'Entropy', 'Histogram Spread' and 'UICM' are shown in Table 3.3 and Table 3.4. Entropy measures the information content of the image. Histogram Spread quantifies the contrast of the image. UICM measures the colorfulness of the image. The average of the above-mentioned performance metrics for 200 underwater images for the compared techniques are shown in Table 3.3. The values of these performance measures for different images are listed in Table 3.4 to compare CIEUI with the above-mentioned techniques. The bold values in each column of Table 3.4 represent the best value of the respective performance measure for particular image. Comparison of results shows that CIEUI is better than state-of-the-art algorithms in terms of entropy and

Table 3.4: Comparison of Various Techniques

Image	**Technique**	**Qualitative Analysis**		
		Entropy	**Histogram Spread**	**UICM**
Drum	Original	5.65	0.4005	2.9495
	Gray World	7.10	0.2822	4.9339
	UCM	7.45	0.5577	9.5244
	Kwok *et al.* Method	6.34	0.3163	3.0975
	Sethi *et al.* Method	6.85	0.5488	5.1326
	CIEUI	**7.78**	**0.4586**	**9.7180**
Divers	Original	5.44	0.2817	4.7572
	Gray World	6.97	0.4241	4.2785
	UCM	6.59	0.5563	4.7077
	Kwok *et al.* Method	5.74	0.2417	4.9282
	Sethi *et al.* Method	6.77	**0.5097**	6.2125
	CIEUI	**7.37**	0.4078	**11.3503**
Fish	Original	6.01	0.2553	1.3890
	Gray World	5.91	0.2639	2.0289
	UCM	**7.41**	0.4333	5.8051
	Kwok *et al.* Method	7.02	0.2939	1.4890
	Sethi *et al.* Method	**7.41**	0.4446	7.0389
	CIEUI	7.32	**0.4706**	**11.4956**
Seal Fish	Original	6.46	0.3081	1.2937
	Gray World	6.86	**0.4148**	**5.1796**
	UCM	7.19	0.4003	4.6775
	Kwok *et al.* Method	6.47	0.3120	1.7709
	Sethi *et al.* Method	6.95	0.3962	4.8969
	CIEUI	**7.63**	0.3506	2.7785
Scuba Diver	Original	6.25	0.1992	1.3890
	Gray World	7.58	0.3154	2.0289
	UCM	7.53	0.2550	5.8051
	Kwok *et al.* Method	6.36	0.1804	1.4891
	Sethi *et al.* Method	7.52	0.2901	7.0389
	CIEUI	**7.59**	**0.3351**	**11.4856**

UICM.

From the qualitative and quantitative analysis of results of the techniques to be compared, the following points can be inferred. Original underwater images have a washed out appearance with very less information content (low entropy values). Gray world technique [95] and UCM [96] try to bring color information in the image by manipulating the histograms of individual RGB channel but these techniques sometimes overstretch the histogram leading to false colors in image. From the Table 3.4, it can be concluded that the gray world technique [95] and UCM [96] produce images with improved entropy (information), histogram spread (contrast) and UICM (color). But, it can be seen in the visual results of gray world and UCM techniques that red color dominates the image.

Qualitative and quantitative analysis of Kwok *et al.* [81] method proves that it improves entropy (information content) to some extent but the contrast of the images is very poor. Histogram spread values of some of its output images are sometimes lower than the original images. Thus, It does not work well for underwater images but it claims to work for poor contrast images.

The Sethi *et al.* [8] technique improves entropy (information content), histogram spread (contrast) and UICM (color), but introduces false colors in the image just like UCM and gray world technique. Entropy of its output images is not increased as much as its histogram spread and UICM values. Reason for such results is that it concentrates only on contrast and color improvement which leads to introduction of false colors in the image.

Results of CIEUI technique have improved contrast and information content as compared to other techniques. In the fish image, it is introducing false colors which is due to presence of artificial light. From Table 3.3, CIEUI shows better overall performance than others in terms of improving entropy and UICM values. However, it lags behind UCM and Sethi *et al.* technique in terms of improving histogram spread as it computes an optimal value of histogram spread and entropy for producing an image with good contrast and information content. It delivers good results for every type of underwater image. For example, drum image is captured on the seabed which is very deep, divers image is at a moderate depth and moreover images are taken in different water bodies having different salinity and turbidity.

From the histograms of the test underwater images produced by the above-mentioned techniques and CIEUI, the following points can be inferred.

(a) Original (b) [95]

(c) [96] (d) [81]

(e) [8] (f) CIEUI

Figure 3.5: Results of Scuba Diver Image using different methods

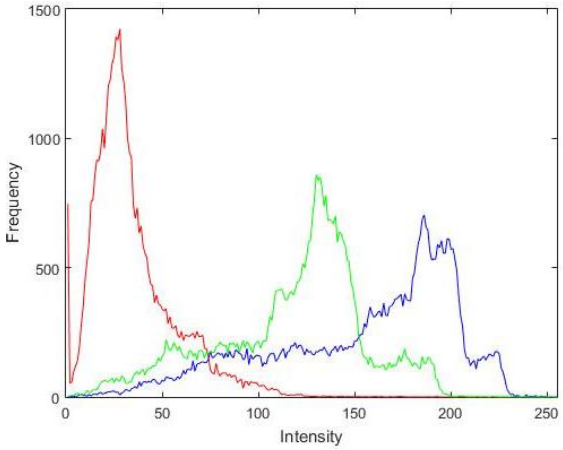

(a) Original Histogram

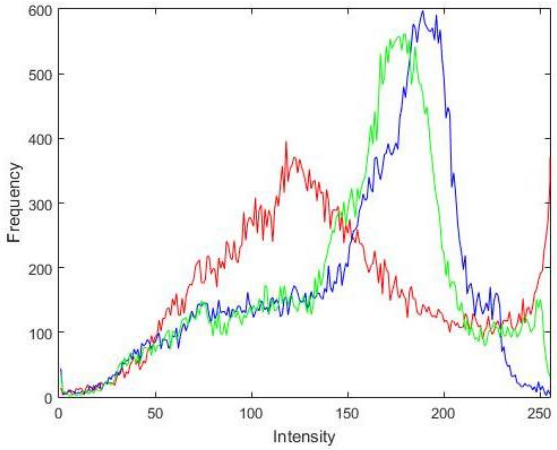

(b) [95]

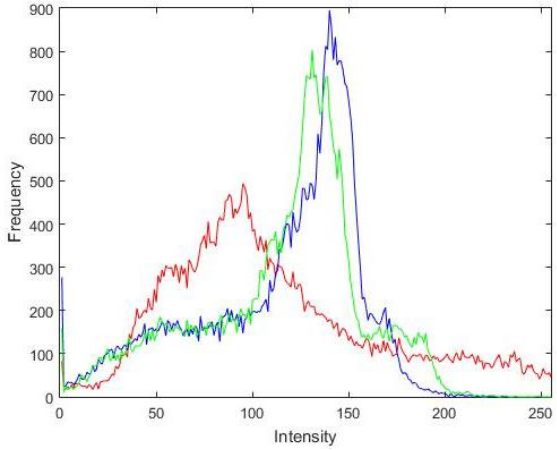

(c) [96]

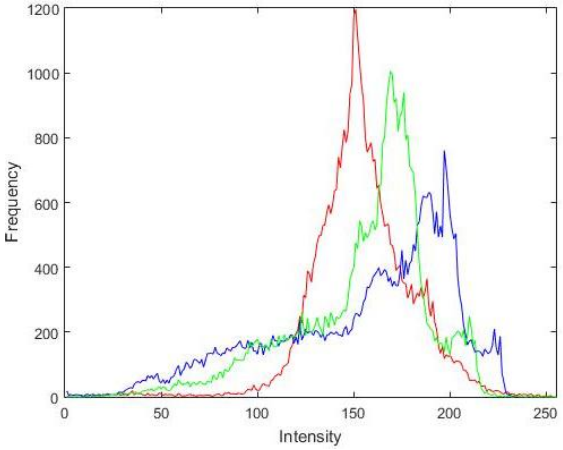

(d) [81]

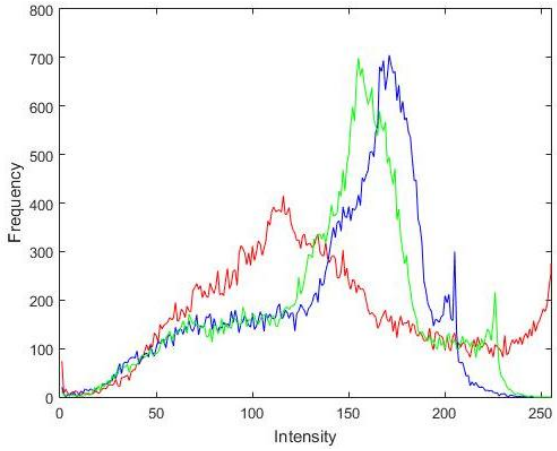

(e) [8]

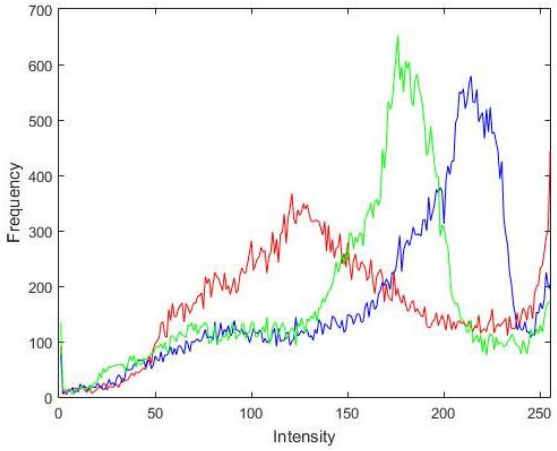

(f) CIEUI

Figure 3.6: Histograms of Scuba Diver Image for results obtained using different methods

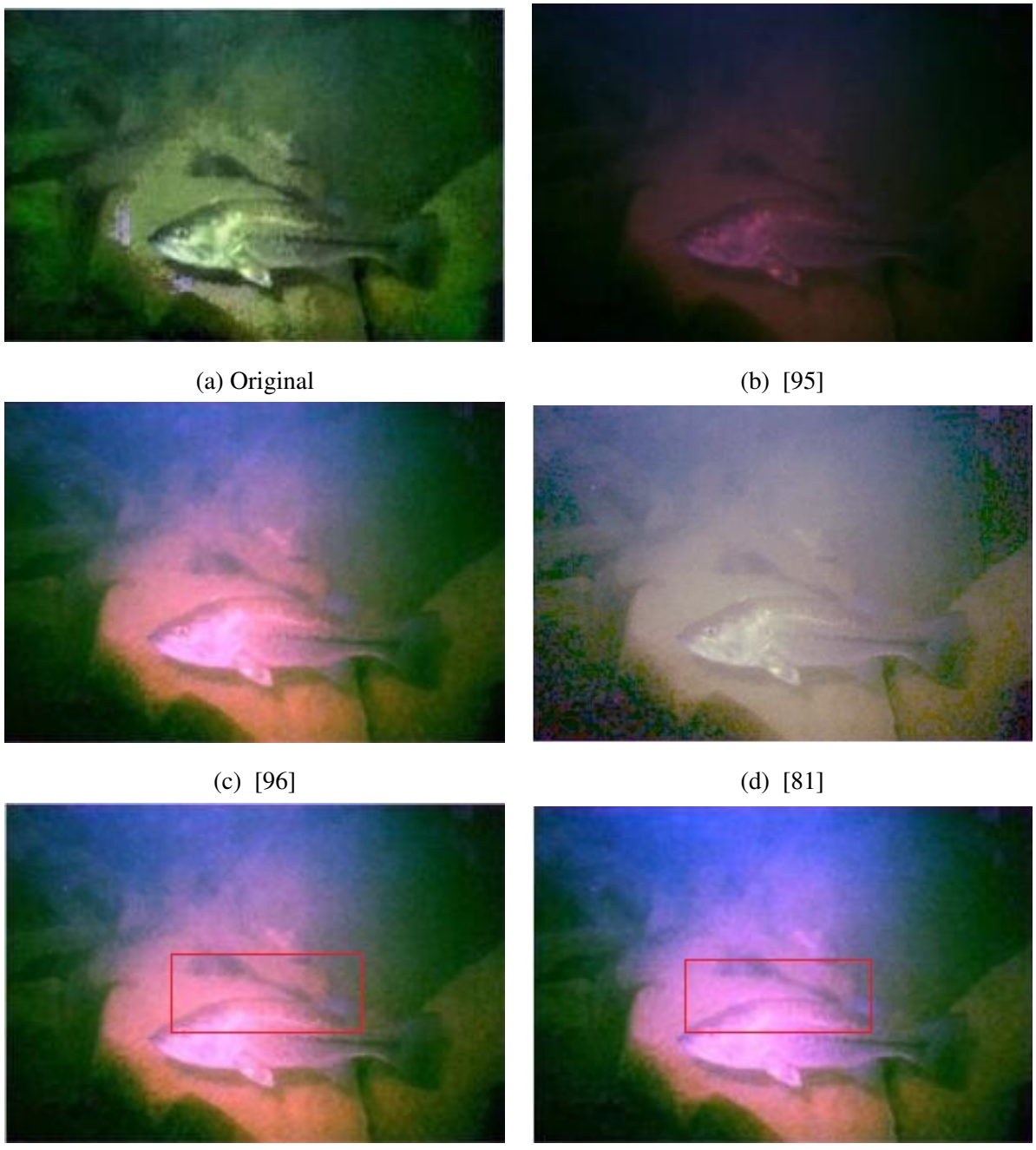

(a) Original (b) [95]

(c) [96] (d) [81]

(e) [8] (f) CIEUI

Figure 3.7: Results of Fish Image using different methods

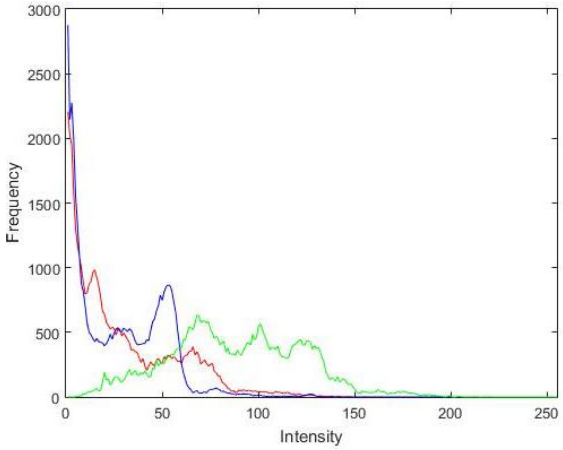

(a) Original Histogram

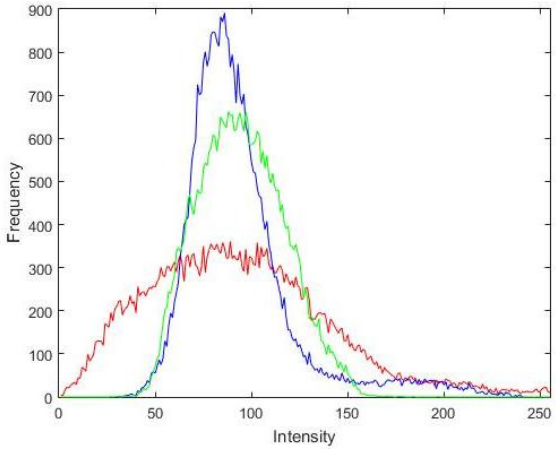

(b) [95]

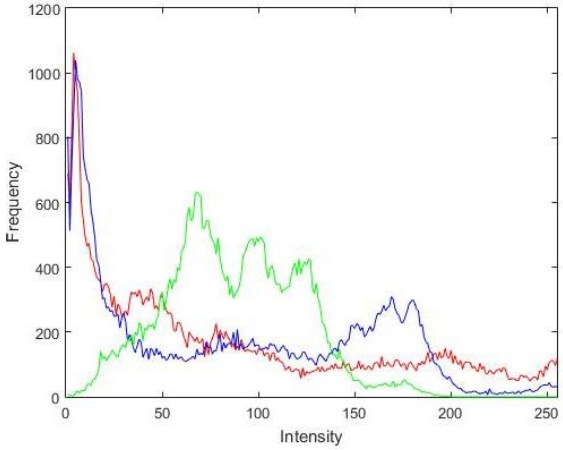

(c) [96]

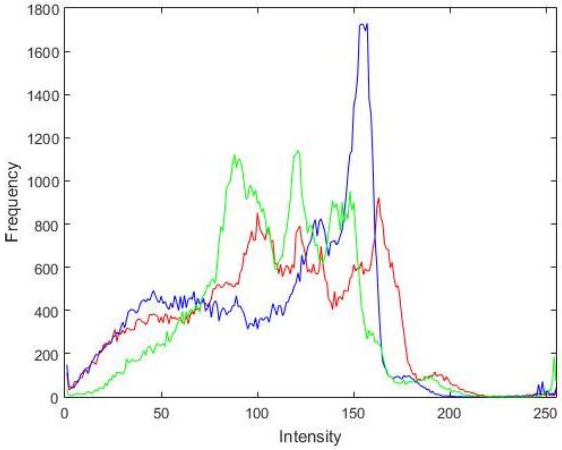

(d) [81]

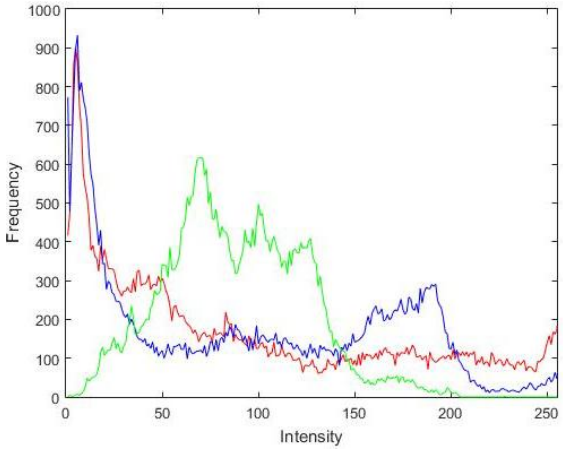

(e) [8]

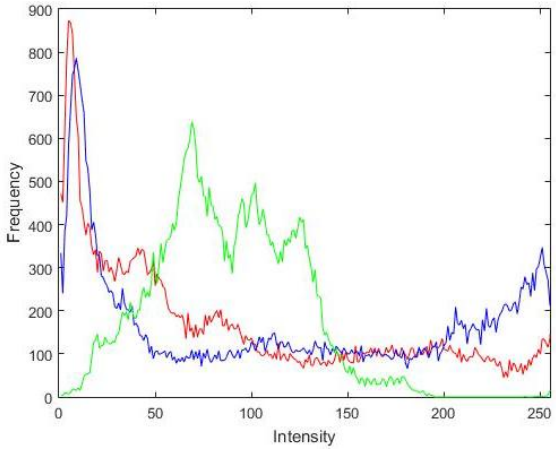

(f) CIEUI

Figure 3.8: Histograms of Fish Image for results obtained using different methods

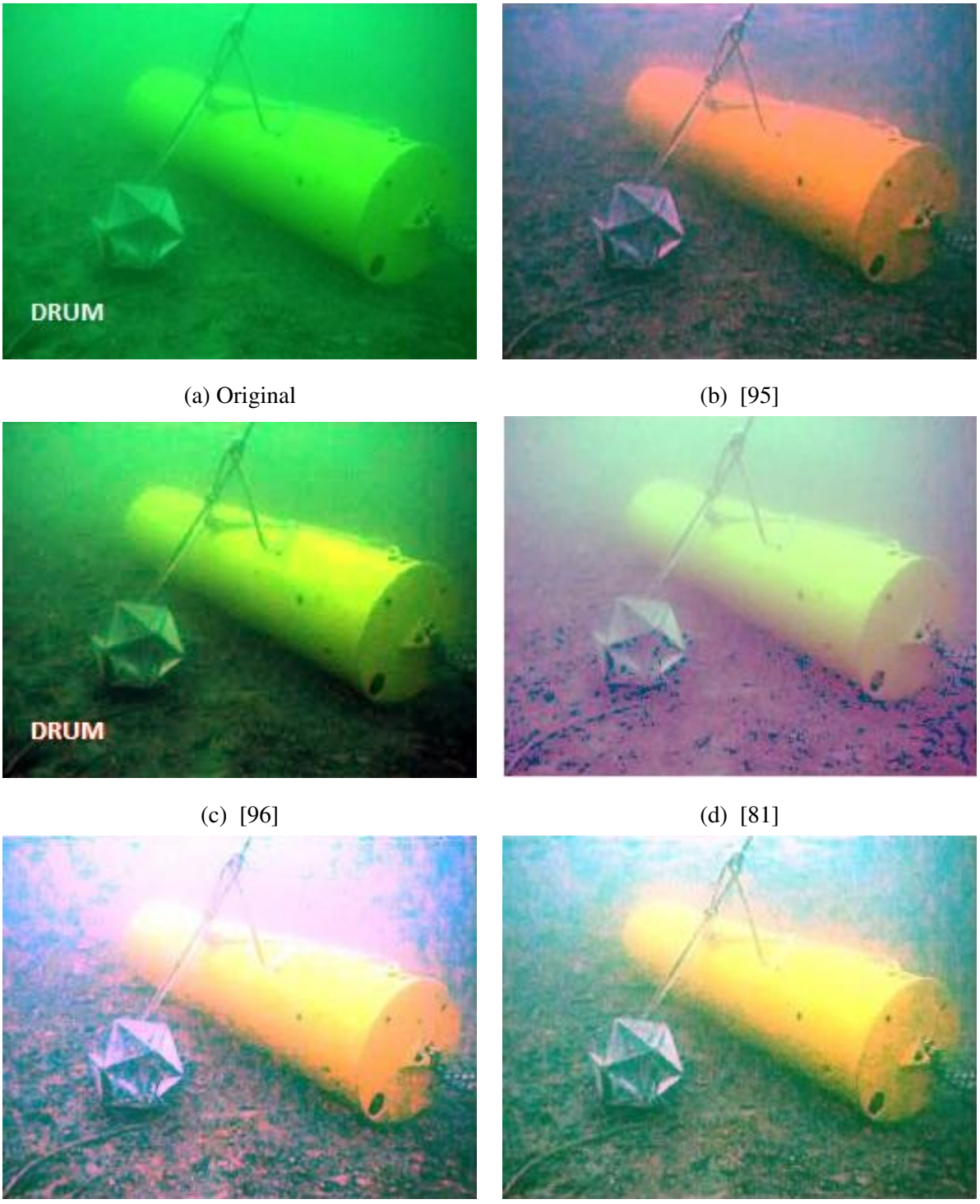

(a) Original (b) [95]

(c) [96] (d) [81]

(e) [8] (f) CIEUI

Figure 3.9: Results of Drum Image using different methods

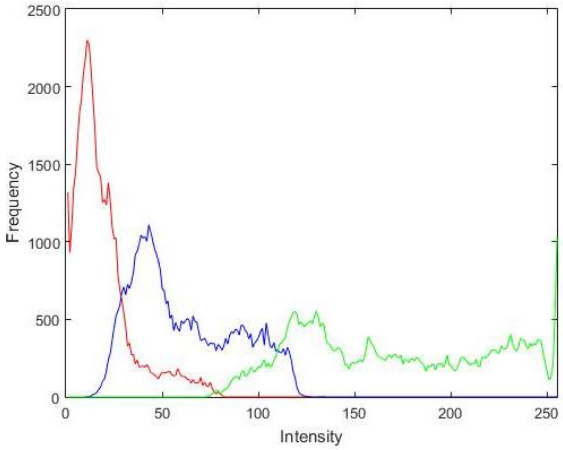

(a) Original Histogram

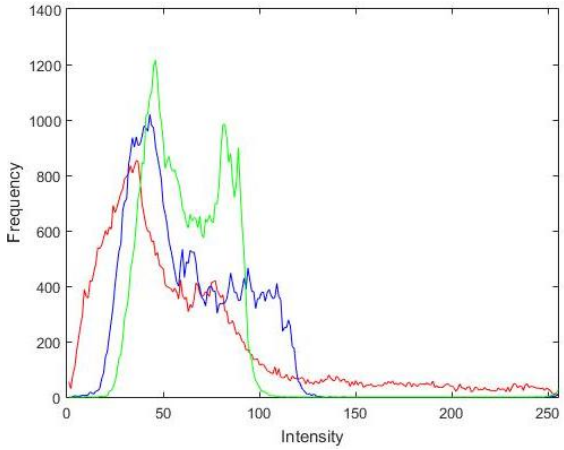

(b) [95]

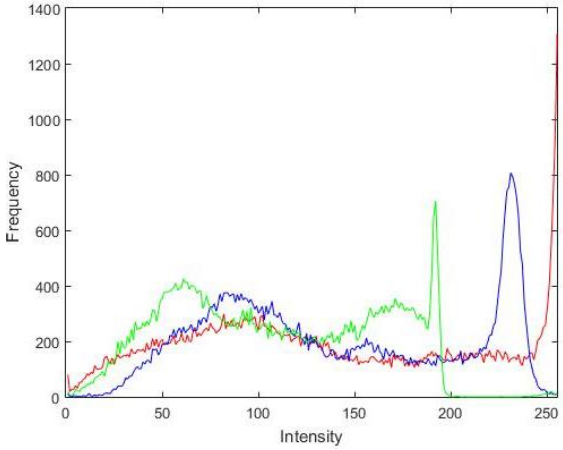

(c) [96]

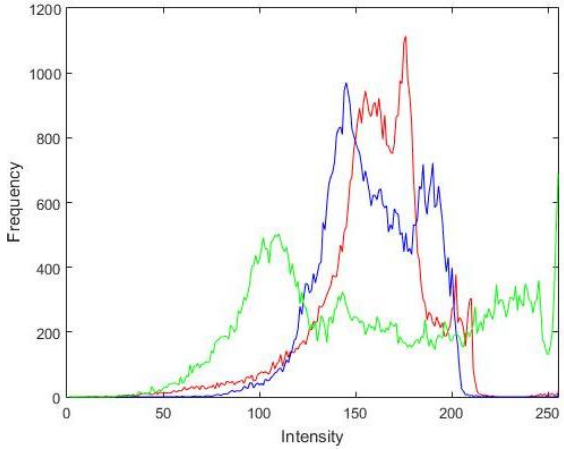

(d) [81]

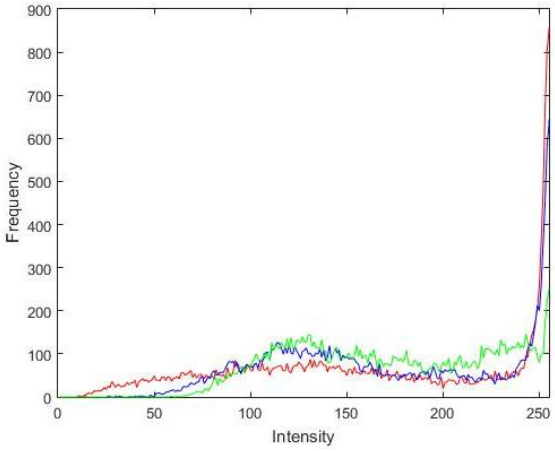

(e) [8]

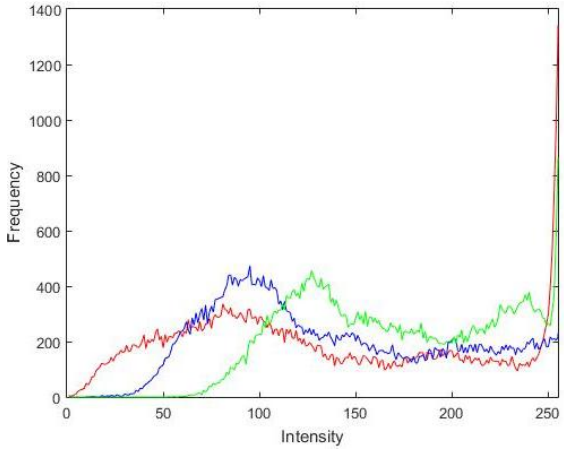

(f) CIEUI

Figure 3.10: Histograms of Drum Image for results obtained using different methods

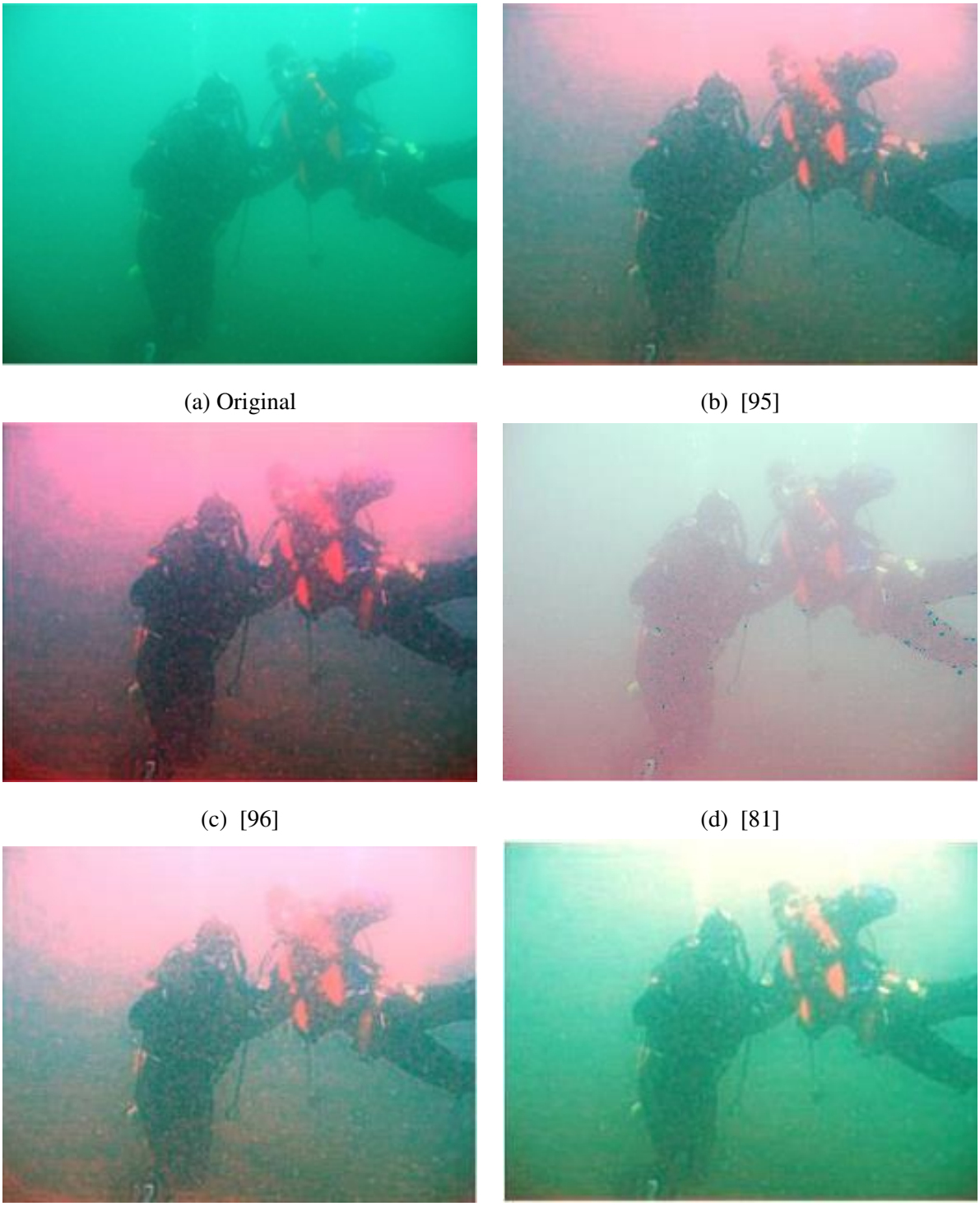

(a) Original (b) [95]

(c) [96] (d) [81]

(e) [8] (f) CIEUI

Figure 3.11: Results of Divers Image using different methods

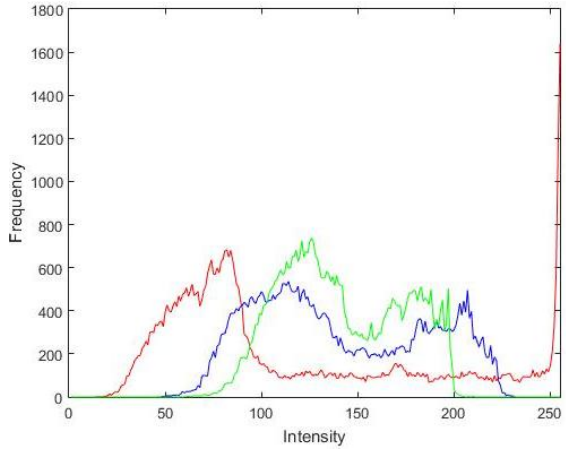

(a) Original Histogram

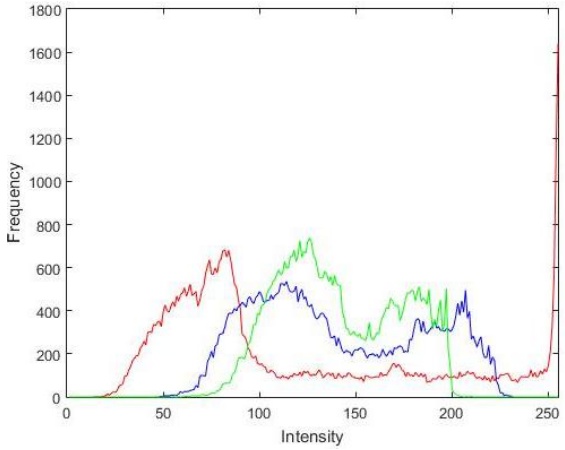

(b) [95]

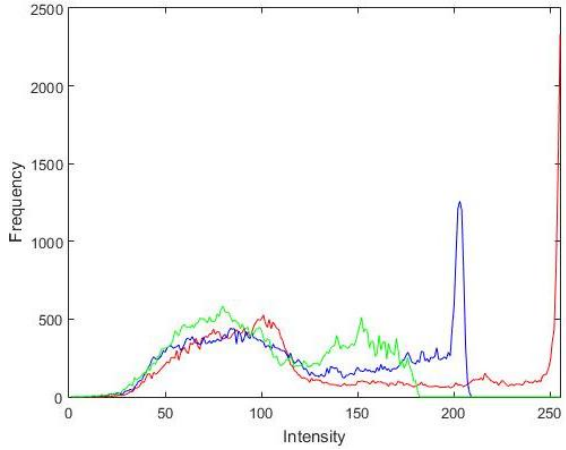

(c) [96]

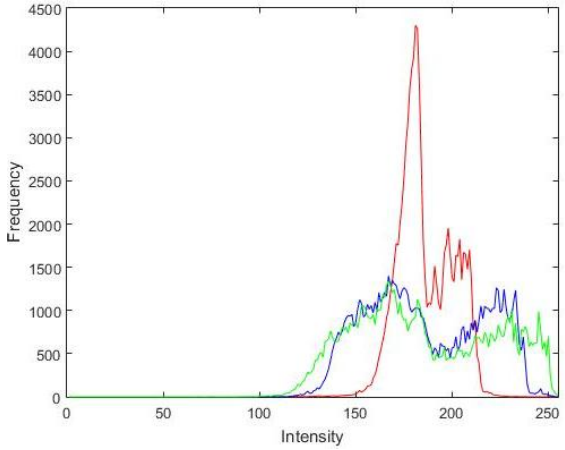

(d) [81]

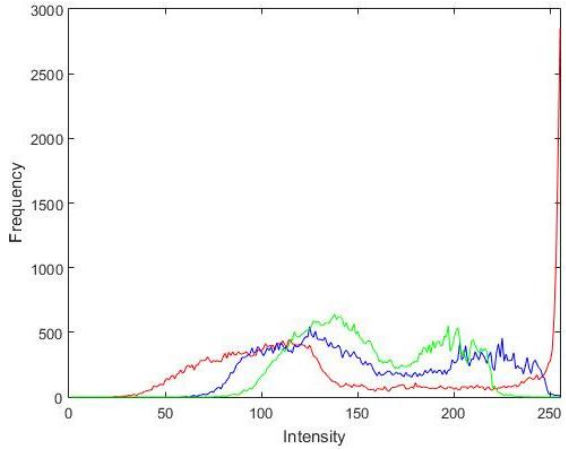

(e) [8]

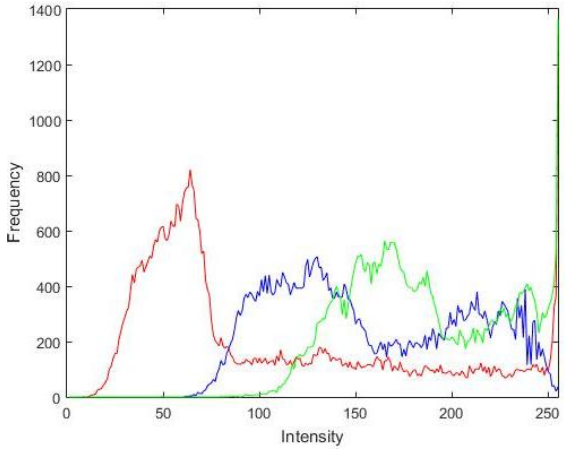

(f) CIEUI

Figure 3.12: Histograms of Divers Image for results obtained using the different methods

(a) Original (b) [95]

(c) [96] (d) [81]

(e) [8] (f) CIEUI

Figure 3.13: Results of Seal fish Image using different methods

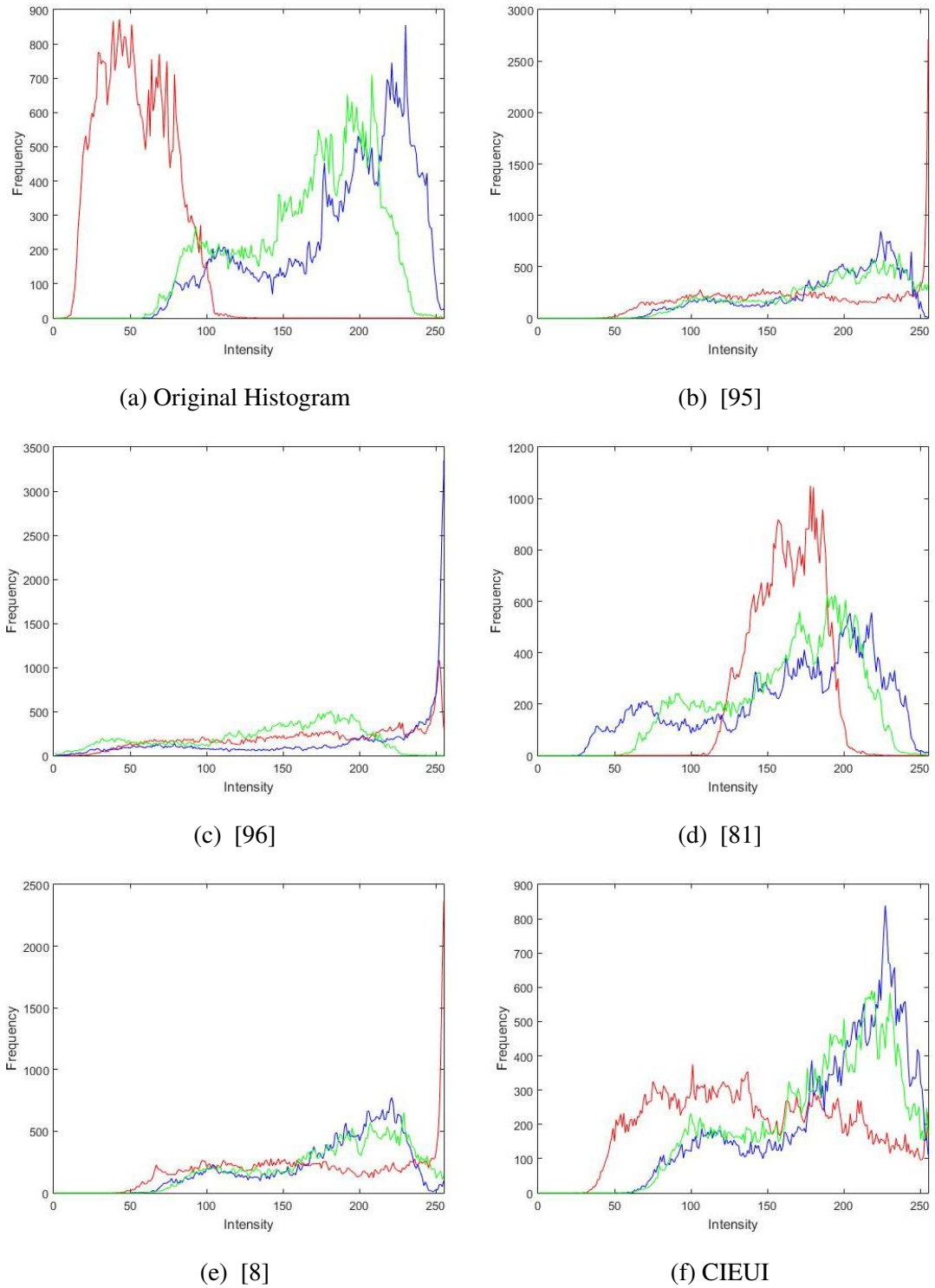

(a) Original Histogram

(b) [95]

(c) [96]

(d) [81]

(e) [8]

(f) CIEUI

Figure 3.14: Histograms of Seal Fish Image for results obtained using different methods

Histograms of images produced by gray world based technique [95] are either shifted towards lower intensities (low contrast) or towards higher intensities (high contrast). For the scuba diver image, histograms of three color channels span the whole dynamic range but the distribution of pixels is non-uniform.
Histograms of UCM [96] images span entire dynamic range but do not have uniform distribution and the histogram of blue channel usually shows a dip for higher intensity values due to which images have more reddish appearance.
Histograms of Kwok *et al.* [81] technique images are skewed towards higher intensities (high contrast) and have non-uniform distribution due to which resultant images are very light.
Histograms of the Sethi *et al.* [8] technique cover the whole range of intensities similar to UCM [96], but have more uniform distribution than UCM. the resultant images of the fish image for the Sethi *et al.* technique [8] and UCM [96] techniques are almost similar and give same entropy values but contrast of Sethi *et al.* [8] image is slightly better than UCM image which is validated by HS and UICM values of the resultant images of fish.
Some of the images of the Sethi *et al.* [8] method appear similar to that of CIEUI, e.g. scuba diver and fish image. But it can be seen from the highlighted red boxes in the resultant images of both the techniques, images of the Sethi *et al.* [8] method have a reddish tone. Histograms of blue and green channel of the scuba diver and fish images in [8] method show a dip for higher intensities as compared to corresponding histograms of CIEUI images, leading to the dominance of red channel in few regions of the image.

CIEUI produces images with histograms spanning the whole dynamic range. Distribution is not uniform but better than state-of-the-art techniques. Histograms of green and blue channels do not have pixels with lower intensities due to which few artifacts are present in the output images. The fish image has more artifacts due to presence of artificial light.
From Table 3.4, it can be seen that CIEUI improves the histogram spread value. However, it does not always outperform other techniques. It gives the best entropy value for all images except for the fish image. It gives the best UICM value for all the images except for the seal fish image. From the above analysis, it can be concluded that CIEUI always enhances the information content, color and contrast of the image and produces results that are visually more appealing and closer to reality when contrasted with state-of-the-art algorithms.

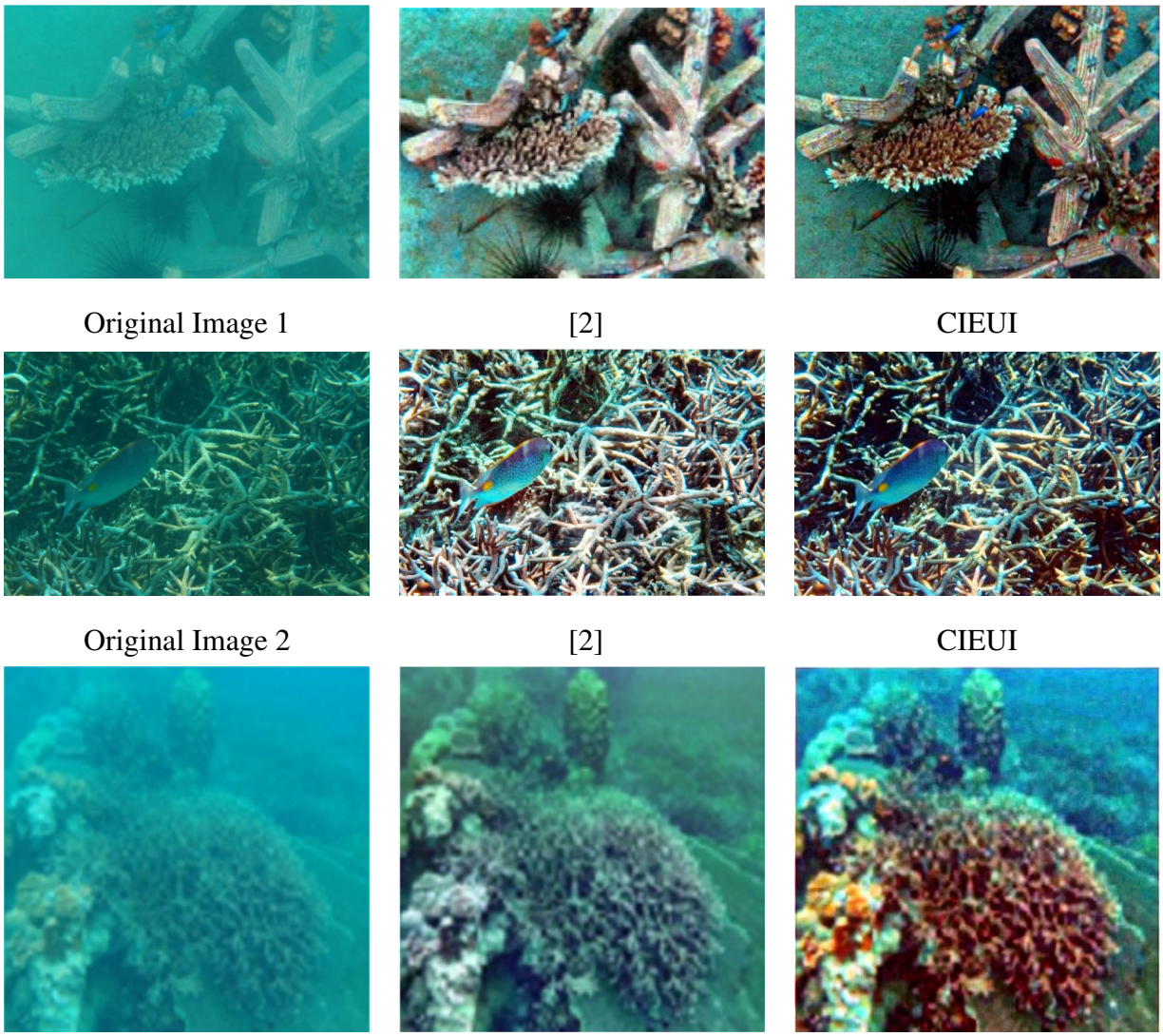

Figure 3.15: Images taken from articles [2] and [3]

Table 3.5: Values of Entropy, HS and UICM for Images shown in Fig. 3.15

Image	**Technique**	**Entropy**	**Histogram Spread**	**UICM**
Image 1	Original	5.93	0.1567	0.3229
	RAHIM [2]	7.65	0.3303	4.6511
	CIEUI	**7.76**	**0.3327**	**4.8951**
Image 2	Original	5.86	0.1779	2.8182
	RAHIM [2]	**7.88**	0.4566	4.859
	CIEUI	7.67	**0.4945**	**4.8761**
Image 3	Original	5.1087	0.1827	.4651
	Garg *et al.* Method [3]	6.78	**0.1610**	2.7318
	CIEUI	**7.27**	**0.2454**	**3.7905**

For more exhaustive comparison, The results of CIEUI have been compared with RAHIM [2] and the Garg *et al.* technique [3] which also try to tackle color and contrast issues together. A few images along with the results have been taken from the articles [2] and [3] are shown along with the results of CIEUI in Fig. 3.15.

From the visual results in Fig. 3.15, it is clear that the images of CIEUI are visually more pleasant than the images of RAHIM [2] and the Garg *et al.* technique [3]. The contrast of the images obtained by RAHIM [2] is on the higher side and colors are not visually appealing as compared to CIEUI. On the other hand, The images obtained by the Garg *et al.* technique still have bluish tone and color cast is still left. These facts are further proven by the quantitative measures values shown in Table 3.5. In Table 3.5, the values of quantitative measures prove that CIEUI has better information content, color and contrast as compared to RAHIM [2] and the Garg *et al.* technique [3]. However, for image 2, RAHIM has better information content but color (UICM) and contrast (HS) of CIEUI is better. However, images obtained using the Garg *et al.* technique does not possess better entropy, HS and UICM values which has been proven from the visual results also. Overall, CIEUI is better than RAHIM [2] and the Garg *et al.* technique [3] in terms of color, contrast and

information content of the image.

3.7 Conclusions

In this chapter, an adaptive enhancement technique for underwater images has been explained which does not require any parameter estimation. The main concern of underwater images is their poor quality due to bad contrast and color which results in poor information content. The major drawbacks of state-of-the-art algorithms are (1) these methods work either on improving contrast or color or both in underwater images (2) these methods do not scale to every type of underwater image which are captured at different depth or in water bodies with varying salinity and turbidity. The key contributions of CIEUI are: firstly, it not only improves contrast and color performance but also the information content of the underwater image and secondly, it works for all type of underwater images. It effectively avoids the artifacts (i.e. False colors and halos) caused by overstretching of the histogram. The major limitation of CIEUI is the slow execution time of MOPSO due to which it is not applicable in real time. One solution to apply the method in real time is to first get the optimized values of λ for a type of medium and then apply those values for other images captured in the same media. In this way, it can be applied in real time, and knowing the values of parameters in different type of underwater media, can be easily scaled to every type of underwater image. This method produces visually enhanced images with better color, contrast and object clarity, which is proven by quantitative measures as well. A few artifacts are still left in output images in which artificial lighting has been employed. In the next chapter, we will address the artifacts due to artificial lighting and also try to reduce the time required to pre-process the underwater image.

Chapter 4

Fuzzified Color and Contrast Correction of Underwater Images

4.1 Introduction

As discussed in previous chapter, underwater images suffer from poor contrast and color distortion. Poor contrast is mainly due to less penetration of light rays inside the water medium. Thus, artificial lighting is employed to compensate for the light. But, the solution i.e. CIEUI explained in the previous chapter, introduces artifacts in the images which are captured using artificial lighting. In this chapter, this drawback of CIEUI is removed by providing a local enhancement solution namely 'Fuzzified Color and Contrast Correction (FCCC)'.

A global enhancement technique considers the whole image equally affected by the underwater anomalies and thus applying such a technique leads to artifacts in the underwater image as the region in focus of artificial lighting will have better contrast and improved colors than the other regions. It can be seen in Fig. 4.1 that the fish focused with artificial lighting is clearer than other things in background.

(a) fish orignal image

(b) disc orignal image

(c) fish CIEUI image

(d) disc CIEUI image

(e) fish FCCC image

(f) disc FCCC image

Figure 4.1: Images with artificial lighting (a) Fish (b) disc

Similarly, disc near to camera is clearer than other objects in the image. Thus, it can be inferred that the objects in foreground i.e. near to camera are clearer than the objects in the background. Result of CIEUI (global enhancement) for these images and FCCC (local enhancement) are also shown in Fig. 4.1. From the results, it is clear that local enhancement of underwater images is required for desired results. Here, local enhancement means color and contrast correction of segments of images which have different color cast and contrast. Thus, In this chapter, to address the problems of poor contrast, color cast and non-uniform illumination of underwater images, we propose a novel local image enhancement technique named Fuzzified Color and Contrast Correction (FCCC) which employs type-2 fuzzy logic for color correction and Contrast Limited Adaptive Histogram Equalization (CLAHE) for contrast correction of the underwater image. These two versions of the same underwater image are then fused using wavelet decomposition based fusion to get the final enhanced image with better contrast and color performance.

4.2 Problem formulation

In this chapter, we are formulating an enhancement technique 'FCCC' which addresses the color and contrast correction problem of underwater images which can have different color cast and contrast in parts of image. FCCC corrects color and contrast of underwater images using single image captured by digital camera. Local enhancement is applied on blocks of images instead of whole image. Color correction is done to remove color cast by working on non-overlapping patches of images using an algorithm based on gray world assumption [33] and type-2 fuzzy logic [97]. Contrast correction is done by using Contrast Limited Adaptive Histogram Equalization (CLAHE) [98] which is a localized version of Histogram Equalization (HE). Finally, enhanced image is obtained by fusion of these two inputs i.e. color corrected image and contrast corrected image. FCCC effectively resolves the issues of underwater images by producing enhanced images with no or few artifacts. Type-2 fuzzy world algorithm is an enhancement of the fuzzy gray world algorithm [8] explained in previous chapter. We will understand this concept and the detailed steps of FCCC in further sections of this chapter.

4.3 Fuzzified Color and Contrast Correction

In this chapter, we have formulated a local hybrid image enhancement method named 'Fuzzified Color and Contrast Correction (FCCC)' to tackle the artifacts caused by global enhancement methods when applied on unevenly illuminated underwater images. It corrects the color and contrast of underwater images locally to handle the major problems (color cast, bad contrast and non-uniform illumination) in underwater images.

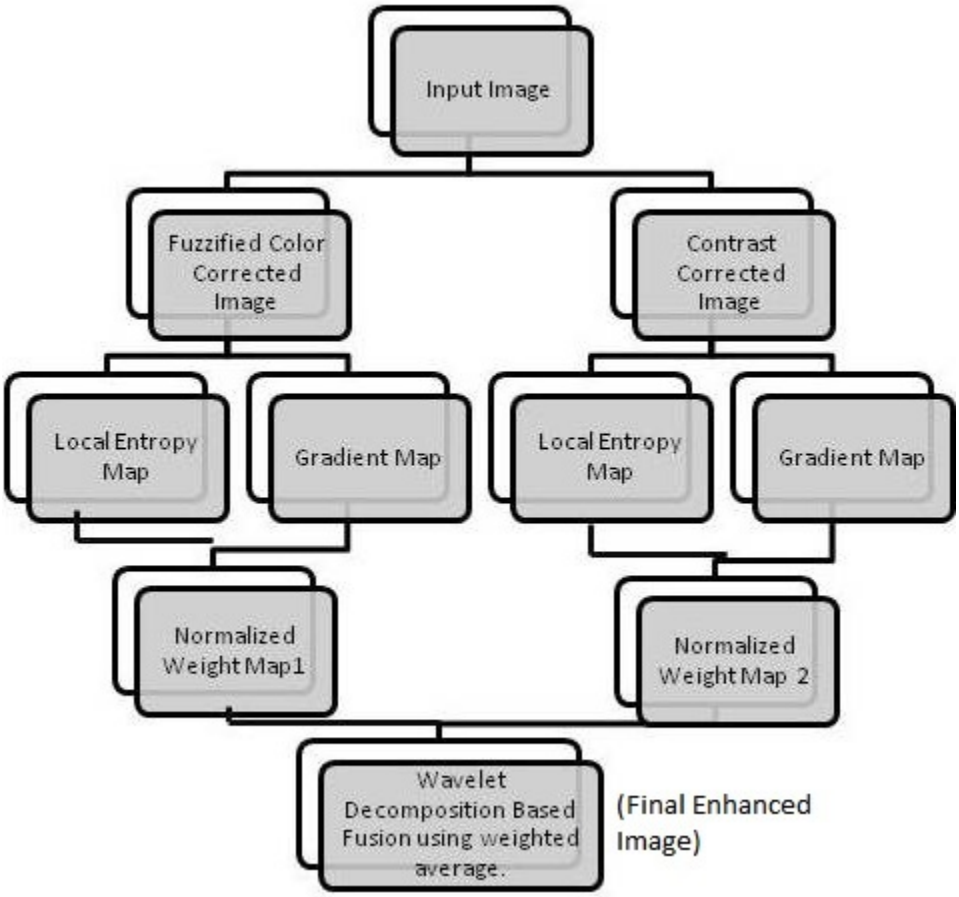

Figure 4.2: Processing Steps of FCCC

FCCC includes two parallel steps of 'color correction' and 'contrast correction' followed by finding the weight maps for each image and last step is to fuse these two images using weighted average of wavelet coefficients. It removes the color cast using an algorithm based on type-2 fuzzy logic and gray world based assumption and corrects contrast using CLAHE. Fuzzy logic is employed to find the color cast in different non-overlapping blocks of the image. Due to non-uniform lighting in underwater images, there can be different degree of color cast in the image. Fuzzy sets can easily handle the ambiguity regarding color cast as color cast is not always of blue color, sometimes it can be of green color or of greenish blue color and even no color cast if artificial lighting is employed. CLAHE is a local contrast correction method which performs histogram equalization on non-overlapping blocks of image. Size of block should not be too small or too big. In small block, there may be no change in color cast and contrast of the different adjacent blocks. In a single image, there can be different color cast and contrast in the sub-blocks of that image. Size of sub-block is taken as 16X16 for an image of size 256X256 after trying different values for sub-block size experimentally. FCCC delivers good results for almost all the images for this size of sub-block. The two versions of the original image are then fused using wavelet decomposition based fusion [99] which introduces few or no artifacts in the image. The key contributions of FCCC are (a) it is computationally inexpensive (b) It requires no parameter estimation and works for every type of underwater image (captured in media having different turbidity, salinity etc.) (c) It handles the major issues of underwater images (poor contrast, color cast, uneven illumination) efficiently. The different steps of FCCC are illustrated in Fig. 4.2 and are explained in the next subsections.

4.3.1 Type 2 Fuzzy Gray World Algorithm

There are lots of color correction algorithms available in literature, most of which are based on certain assumption and try to find some reference or standard value based on that assumption. That standard value is then used to find the correction factors which are then multiplied with the original image to find the color corrected version. Shades of Gray [4], Gray Edge [5] and Max-RGB [6] are examples of this class of algorithms which work on some specific assumption. Output images of the above-mentioned techniques are shown in

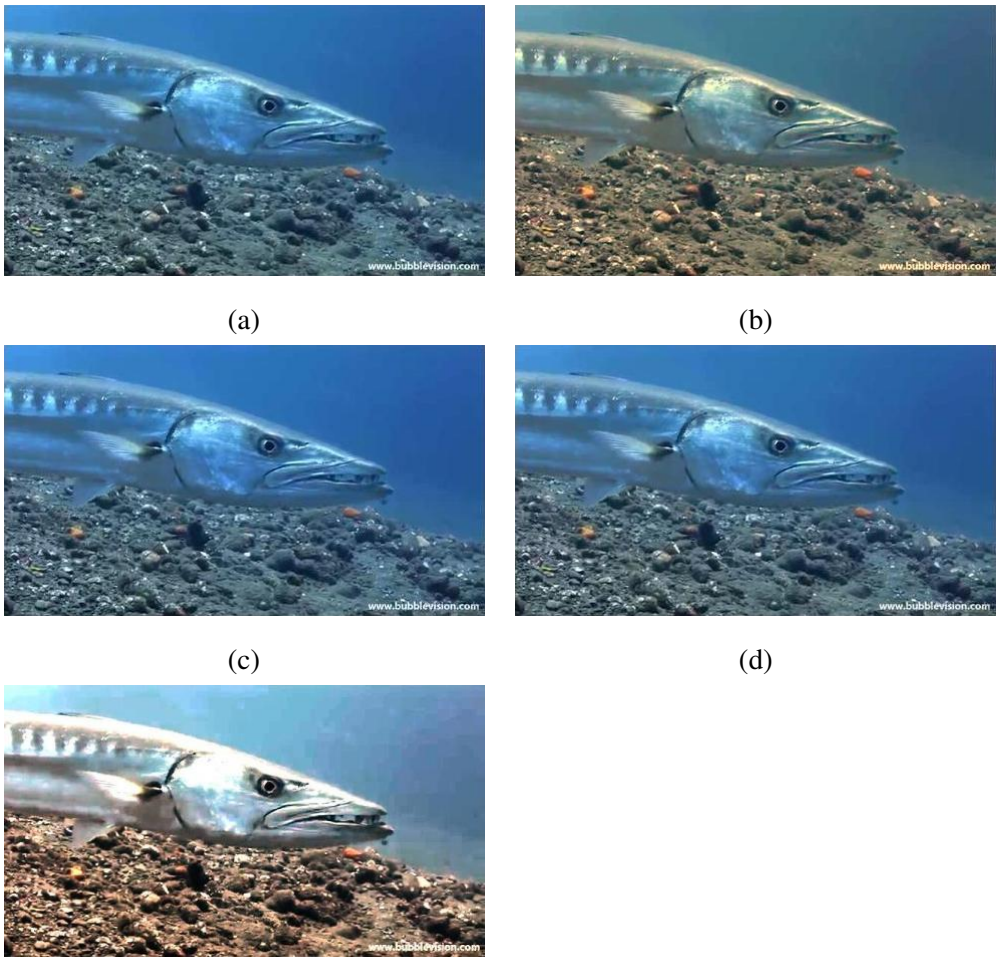

(a) (b)

(c) (d)

(e)

Figure 4.3: (a) Original Image (b) [4] (c) [5] (d) [6] (e) Proposed Type-2 fuzzy gray

Fig. 4.3.

Type 2 Fuzzy gray world algorithm used in this chapter has two concepts:

(a) **Gray World assumption**: Gray world assumption states that the average of three color channels should be achromatic and if the average is not achromatic, we need to adjust the color channels by the ratio defined by the algorithm.

(b) **Type-2 Fuzzy**: Application of fuzzy logic [100] for finding the color cast, as suggested by Sethi *et al.* [8], has been adopted in this chapter. But, in [8], there are two limitations (a) the parameter 'μ' has been fixed at 35, (b) there is no fuzzy rule to find the base if the pixel has low membership or high membership in all three channels. Thus, to fix the first limitation, Interval Type-2 Fuzzy Sets (IT2 FS) [97] has been employed to solve the uncertainty in the fuzzy set itself. Type-2 fuzzy set is an advancement over type-1 fuzzy set to handle more uncertainty. Interval Type-2 fuzzy sets minimizes the error due to membership function by using the concept of footprint of uncertainity (FOU). FOU gives the bound in which the membership function can vary. More the area under FOU, more is the uncertainty. To handle the second limitation, few fuzzy rules have been added.

The working of the algorithm is as follows:

First step of fuzzified color correction is to process image I = [R,G,B] in sub-blocks of size 16x16 so that the problem of non-uniform illumination can be handled. Each pixel in the sub-block is fuzzified using IT2 FS namely LOW and HIGH, which are defined in Eq. 4.1. Fig. 4.4 shows the membership functions (MFs) of fuzzy sets. thick blue line shows the upper membership function of LOW and thin blue line shows the lower membership function of LOW. Similarly, Thick red line shows the upper MF of HIGH and thin red line shows the lower MF of HIGH. Blue shaded region denotes footprint of uncertainty (FOU)

of LOW fuzzy set and Red shaded region denotes FOU of HIGH fuzzy set.

$$
\begin{aligned}
\overline{\mu}_{L\tilde{O}W}(x) &= \overline{FOU(L\tilde{O}W)} \\
&= gaussmf(x,[40,0]) \\
\underline{\mu}_{L\tilde{O}W}(x) &= \underline{FOU(L\tilde{O}W)} \\
&= gaussmf(x,[25,0]) \\
[H]\ \overline{\mu}_{H\tilde{I}GH}(x) &= \overline{FOU(H\tilde{I}GH)} \\
&= gaussmf(x,[40,255]) \\
\underline{\mu}_{H\tilde{I}GH}(x) &= \underline{FOU(H\tilde{I}GH)} \\
&= gaussmf(x,[25,255])
\end{aligned}
\tag{4.1}
$$

where, FOU is footprint of uncertainty.

Gaussian membership function has two parameters, 'center' and 'standard deviation (σ)'. The lower MF and upper MF for LOW are gaussian membership functions with center as zero for both and σ value equal to 25 for lower MF and 40 for upper MF. Similarly, the lower MF and upper MF for HIGH are gaussian membership functions with center as 255 for both and σ value equal to 25 for lower MF and 40 for upper MF. Center is zero for LOW fuzzy set so that membership value is highest at zero as it is the lowest possible intensity value. Similarly, center is 255 for HIGH fuzzy set as it is the highest possible intensity value for an 8-bit RGB image. The stated value of σ for upper MFs of both the fuzzy sets ensures that membership for LOW fuzzy set drops close to zero for intensity values greater than 128 (mid-point of dynamic range) and inverse for HIGH fuzzy set. If we choose upper MF with σ greater than 40, membership does not drop to zero for intensities greater than 128 for LOW fuzzy set and vice versa for HIGH fuzzy set. Value of σ for lower MF for both the fuzzy sets is 25, which implies that the membership of pixels drop close to zero for intensities greater than 75 for LOW fuzzy set and same pattern is followed for intensities lesser than 175 for HIGH fuzzy set. As all images do not cover the whole dynamic range so the lower MF ensures that for an image with poor contrast, the midpoint of the intensity values can be as low as 75 (intensities are on the lower side) as high as 175 (intensities are on the upper side) assuming artificial lighting has been employed for every image.

The inference mechanism of the fuzzy system computes the output 'Base' for each pixel

Table 4.1: Parameters of Type-2 Fuzzy System

Number of Inputs	3
Number of outputs	1
Number of Rules	8
Defuzzification Method	Weighted Average
Type Reduction Method	Karnik-Mendel
Output Type	Crisp
Input1 = Red Channel, Input2 = Green Channel, Input3 = Blue Channel	
Range	[0,255]
Number of Membership Functions	2 for each input
MF1U ($\overline{LOW}$)	'gaussmf',[40 0]
MF1L ($\underline{LOW}$)	'gaussmf',[25 0]
MF2U ($\overline{HIGH}$)	'gaussmf',[40 255]
MF2L ($\underline{HIGH}$)	'gaussmf',[25 255]
Output = 'Base'	
Range	[-1 1]
Number of Membership functions	7
MF1 (RED)	Linear, Base = input1
MF2 (GREEN)	Linear, Base = input2
MF3 (BLUE)	Linear, Base = input3
MF4 (RG)	Linear, Base = (input1+input2)/2
MF5 (GB)	Linear, Base = (input2+input3)/2
MF6 (RB)	Linear, Base = (input1+input3)/2
MF7 (RGB)	Constant, Base = 0.8

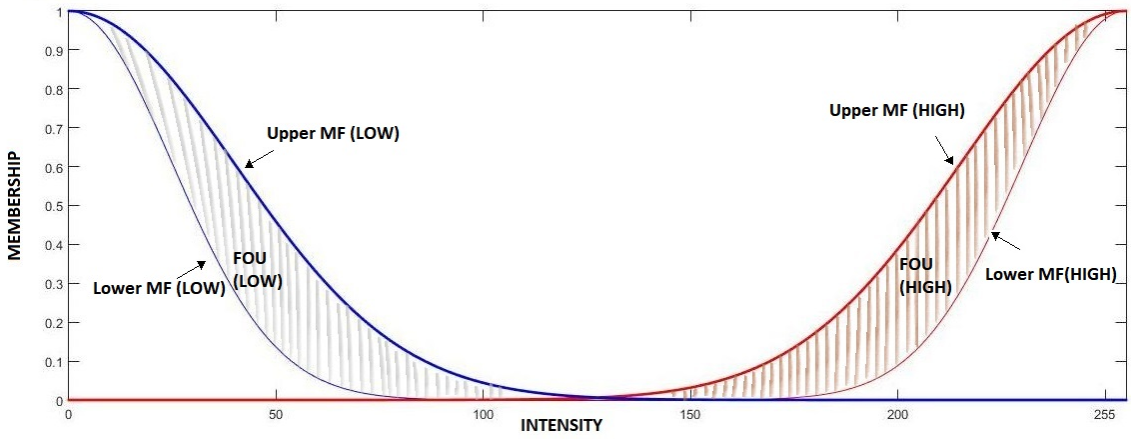

Figure 4.4: LOW and HIGH Type-2 fuzzy sets

in the segment. Table 4.1 states the values of parameters of the Type-2 fuzzy model. The designed type-2 fuzzy system is a Sugeno inference model [101] in which output is either linear or constant. Output processing is done using KM (Karnik-Mendel) defuzzification [102] which is one of the traditional defuzzification method. Table 4.2 states the eight fuzzy rules. The above Type-2 system has been implemented using an open source interval type-2 fuzzy toolbox [103]. After finding the value of 'Base' from the type-2 fuzzy toolbox, the correction factors for each pixel of three color channels are calculated using Eq. 4.2.

$$\alpha_r = \frac{Base}{\overline{R}} \quad \alpha_g = \frac{Base}{\overline{G}} \quad \alpha_b = \frac{Base}{\overline{B}} \tag{4.2}$$

where $\bar{R}, \bar{G}$ and $\bar{B}$ are mean intensities of red, green and blue channels respectively of image.

As we know underwater environment affect the three color channels in a non-linear manner. Hence, a factor of non-linearity has been added to the correction factors as shown in Eq. 4.3.

$$\begin{gathered} \gamma_r = \frac{\overline{SR}}{\overline{R}} \qquad \gamma_g = \frac{\overline{SG}}{\overline{G}} \qquad \gamma_b = \frac{\overline{SB}}{\overline{B}} \\ \hat{R} = (\alpha_r)^{\gamma_r} R \quad \hat{G} = (\alpha_g)^{\gamma_g} G \quad \hat{B} = (\alpha_b)^{\gamma_b} B \end{gathered} \tag{4.3}$$

$\overline{SR}, \overline{SG}$ and $\overline{SB}$ denotes the mean intensities of red, green and blue channels of segment respectively and $\hat{R}, \hat{G}$ and $\hat{B}$ are the intensity values of red, green and blue channels of

Table 4.2: Fuzzy Rules

IF			**Then**
Input1	**Input2**	**Input3**	**Output**
HIGH	LOW	LOW	RED
LOW	HIGH	LOW	GREEN
LOW	LOW	HIGH	BLUE
HIGH	HIGH	LOW	RG
LOW	HIGH	HIGH	GB
HIGH	LOW	HIGH	RB
LOW	LOW	LOW	RGB
HIGH	HIGH	HIGH	RGB

color corrected image respectively. Thus, color corrected image $\hat{I} = [\hat{R}, \hat{G}, \hat{B}]$ is obtained using the fuzzified color correction.

4.3.2 Contrast Limited Adaptive Histogram Equalization

While applying local color correction, local contrast correction is applied on the original image using Contrast Limited Adaptive Histogram Equalization (CLAHE) [98]. CLAHE is localized version of HE [24]. HE generates an output image having a histogram closer to uniform histogram by redistributing the probabilities of gray levels occurrences. HE considers just gray level distribution and no attention is paid on content. If the pixel values are distributed identically throughout the image, then the results are good. Since underwater images specifically with artificial lighting can have regions with significant darker or lighter pixels in comparison to other pixels within other region in the image, enhancement using HE does not give favorable results.

The Adaptive Histogram Equalization (AHE) algorithm proposed by Ketcham *et al.* [104] addresses this challenge by using a neighborhood pixel-derived conversion feature to con-

vert each pixel of the picture. HE is performed on blocks of size in the multiples of 2 e.g. 2x2, 4x4 and so on. Bi-linear interpolation is employed to merge the artificial boundaries created by equalization. The only parameter to be determined in this method is the block size. The major limitation of traditional AHE is that it amplifies noise which Contrast-Limited Adaptive Histogram Equalization (CLAHE) [105] does not. CLAHE operates just like AHE by applying HE to small blocks, but utilizes a contrast-limiting method to each neighborhood grid point within a specific region. Reduction of noise amplification is done by clipping the image histogram to a predefined value just before computing the Cumulative Distribution Function (CDF) for each region. With CLAHE, the parameters to be determined are block size, clip limit, type of distribution and its related parameter. Unlike HE, CLAHE gives the liberty to convert the histogram distribution not only to uniform but also rayleigh or normal distribution.

FCCC uses blocks of 16x16 for contrast correction to maintain uniformity with color correction. CLAHE is performed on three color channels using 'adapthisteq' which is an in-built function in Matlab. The values of various parameters of CLAHE are mentioned in Table 4.3. Distribution for CLAHE is chosen as 'Rayleigh' as it proved to be best distribution for underwater images [27], [106]. Algorithm 3 explains the steps of the proposed method FCCC.

Table 4.3: Parameter values of Matlab function 'adapthisteq' for CLAHE

Parameter	**Value**
Size of tiles	16x16
Distribution	Rayleigh
Clip Limit	0.01 (Default)
Distribution parameter	0.4 (Default)

Algorithm 3: Fuzzified Color and Contrast Correction

Input: RGB Image I

Result: EnhancedImage

Separate R,G,B channels of Image;
$[m, n] \leftarrow$ size of Each channel;
Compute Channel means using Eq. 3.1;
Finding the value of 'Base' from the type-2 fuzzy toolbox [103] using parameters defined in Table 4.2;
find the color corection factors using Eq.4.2;
for $segmentsize \leftarrow$ **to** $16X16$ **do**
    Compute for each segment $C_{col} = \hat{R}, \hat{G}, \hat{B}$ using Eq. 4.3;
end
find contrast corrected image C_{con} using 'adapthisteq' with CLAHE parameters mentioned in Table 4.3;
Calculate the weight map for C_{col} and C_{con} using Eq. 4.5;
Apply Wavelet Based fusion on the two versions of weighted images to find $EnhancedImage$;

4.3.3 Wavelet Based Fusion of Color and Contrast Corrected Images

Last step of FCCC is to fuse the color corrected and contrast corrected image to find the final enhanced image. Image fusion has applications in many domains like remote sens-

ing [107], medical image enhancement [108], night-time vision [109] etc. Image fusion can be primitive or based on pyramid decomposition or wavelet decomposition. In recent times, Fusion for underwater image enhancement is gaining popularity as it helps to incorporate required features from various different images into one without introducing any artifacts.

[47], [110] employed multi-scale laplacian pyramid based fusion with different weight maps for enhancement of underwater images and videos. [48] framed a white balance algorithm specifically for underwater images and created two versions from it. Then, it fused the two versions using multi-scale laplacian pyramid just like [47] did. [111] employed wavelet based fusion for enhancing the underwater images. Nowadays, wavelet based fusion is taking place of pyramid decomposition based fusion due its more compact theoretical base.

Color correction stage of FCCC results in images free from color cast but with few artifacts and poor contrast. On the other hand, contrast correction stage of FCCC results in images with good contrast but poor color quality. Fusion of essential features from color corrected and contrast corrected images results in an enhanced image which is free from artifacts. Wavelet Based fusion is a multi-scale fusion process which decomposes the image into different coefficients using discrete wavelet transform (DWT). This decomposition keeps the information content of image intact. The different coefficients of the images to be fused, are then merged in order to achieve new coefficients. These new coefficients have information of the images used for fusion and the resultant fused image is obtained by applying inverse wavelet transform (IWT). Thus, we can fuse multiple images with varied information into one with enhanced information content. The proposed wavelet fusion is carried out using steps mentioned below:

- Generation of weight maps for input images (Color corrected and Contrast corrected)
- Applying DWT on weight maps and input images to find the coefficients.
- Corresponding coefficients of weight maps are used for finding the weighted average of coefficients of input images to find the new coefficients.
- Applying IWT on new coefficients to find the enhanced image.

Each of these above-mentioned steps are explained in the further subsections.

4.3.3.1 Weight Map Generation

Unlike [48] only two weight maps have been defined for finding the relevant information from the images. Final enhanced image should have good information content (improved color) and contrast. So, we have used the following weight maps:

Local Entropy weight map Local entropy gives an estimate of variation of information in the local regions of image which reduces the effect of noise. Local entropy serves as an indicator in many applications like region extraction [112], saliency descriptor [113]. Local entropy is calculated by first converting RGB image into HSV format and using MATLAB function 'entropyfilt' with default neighborhood values on the value (V) component of the image. This weight map is estimating only one aspect, i.e., the information content of image. Thus, we need another weight map for estimation of contrast of image for which we have the another weight metric.

Gradient weight map Gradient weight map estimates the variance of color saturation level of the image. Gradient weight map is calculated using directional gradients of saturation (S) component of the HSV image. Gradient weight map (W_G) is calculated using Eq. 4.4.

$$\begin{aligned} G_x(x,y) &= S(x-1,y) - S(x+1,y) \\ G_y(x,y) &= S(x,y-1) - S(x,y+1) \\ W_G(x,y) &= \sqrt{G_x(x,y)^2 + G_y(x,y)^2} \end{aligned} \tag{4.4}$$

Finally, for each input k, a single weight map (w_k) is derived by summing up the two weight maps. Final weight map (W_k) is derived by normalizing value of each pixel in the range of [0,1] using Eq. 4.5

$$\begin{aligned} w_k(x,y) &= W_V(x,y) + W_G(x,y) \\ W_k(x,y) &= w_k(x,y)/(\sum_{j=1}^{2} w_j(x,y) + 0.001) \end{aligned} \tag{4.5}$$

where, w_j refers to weight maps of the two input images and a constant '0.001' is added to avoid divide by zero error.

4.3.3.2 Wavelet transform for Image fusion

The wavelet functions is a family of functions which operate on the concept of functions localized in both time and frequency. It decompose an image as a sum of wavelet functions with different locations and scales. When an image is decomposed using wavelet transform, it produces four sub images i.e. approximation details, horizontal details, vertical details and diagonal details in which there are two coefficients namely small coefficients and large coefficients. Small coefficients arises due to noise and can be thresholded without affecting the significant features of the image. Whereas large coefficients are generated due to essential signal features.The basis of the wavelet transform is the wavelet function family like Haar, Morlet, Symlet, Daubechies, etc. Daubechies are the most popular and has been used in the proposed method.
In this stage, DWT is applied on input images and their corresponding weight maps using Mallat's algorithm [99]. The corresponding wavelet coefficients of image and weight maps are multiplied and added to find the fused coefficients given by Eq. 4.6. Image fusion can be done using weighted addition of the two input images using Eq. 4.7 but such an addition leads to artifacts in final image. Wavelet based fusion of images ensures that such artifacts are not be present in the image.

$$C_{fused} = \sum_{k=1}^{K} C_k * C_{W_k} \tag{4.6}$$

where, C_k represents coefficients of k^{th} input image and C_{W_k} represents corresponding coefficients of weight map of k^{th} input image and K is the number of coefficients

$$Final(i,j) = \sum_{k=1}^{2} W_k(i,j) I_k(i,j) \tag{4.7}$$

where Final is the resultant image after weighted addition
Finally, an enhanced image is obtained by applying IWT on the fused coefficients (C_{fused}). Fig. 4.5 shows the original image which computes the two input images and corresponding

(a) Original Image

(b) Color corrected

(c) Contrast corrected

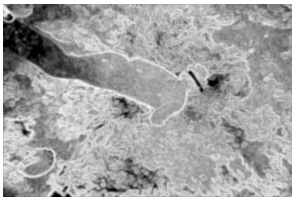

(d) Local Entropy map

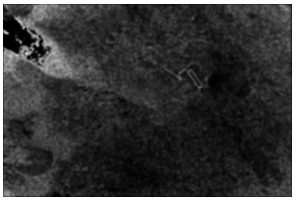

(e) Gradient Map

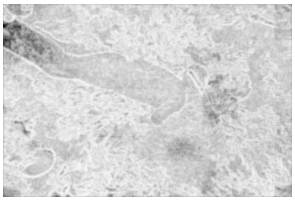

(f) Local Entropy Map

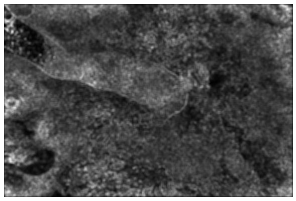

(g) Gradient Map

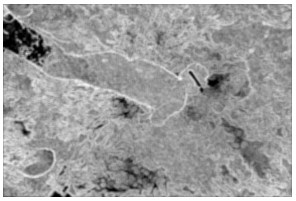

(h) Normalized Weight Map 1

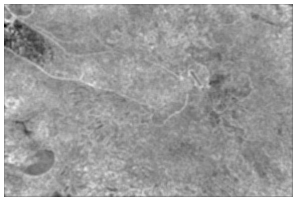

(i) Normalized Weight Map 2

(j) Final Image (Weighted average)

(k) Final Image (Wavelet fusion)

Figure 4.5: (a) Original image (b) Contrast corrected version (c) Color corrected version (d-g) Corresponding weight maps (h-i) normalized weight maps for weight maps and (j-k) final result using weighted average and using wavelet based fusion.

weight maps to obtain enhanced image using wavelet based fusion and weighted addition of images. Fused image obtained using weighted addition has good quality but have few artifacts which can be seen in the red boxes highlighted in the image, on the other hand, image obtained using wavelet based fusion has better quality. It can be seen from the weight maps, color corrected image has more information (entropy) but lesser contrast (gradient) as compared to contrast corrected image. Thus, the fused image has better information and contrast compared to original image and corresponding input images (color corrected and contrast corrected versions) using the weight maps.

4.4 Experimental Results

FCCC has been implemented using Matlab R2015a version on intel processor (i5, 2.60 GHz). FCCC has been tested on different images taken from internet, images from Ancuti *et al.* CVPR paper [47] and underwater images from SUN database [114]. It has been tested on more than 200 images for performance evaluation. As mentioned in the previous chapter, underwater images neither have any database with ground truth values nor any universally accepted quantitative measure for evaluating the extent of image enhancement. Thus, assessing the performance of underwater image enhancement methods is very challenging as reference based quantitative measures like PSNR (Peak Signal to Noise Ratio), MSE (Mean Squared Error) do not work for quantitative evaluation of underwater images. We have employed non-reference based qualitative measures namely Entropy [115], Histogram Spread [80], UIQM (Underwater Image Quality Measure) [91] and UCIQE (Underwater Color Image Quality Evaluation) Metric [116]. Entropy gives the estimate of information content of the image and its value should increase with improvement in image quality. Histogram Spread gives the estimate of spread of histogram over the entire range and its value should be equal to 0.5 for an image with uniform histogram. UIQM and UCIQE are specifically for underwater images. UIQM is combination of color, contrast and sharpness measure which contribute to overall quality of underwater image. UCIQE quantifies the extent to which contrast and blurriness of an image is reduced. Values of both UIQM and UCIQE increase as image quality enhances. The proposed type-2 fuzzy based color correction method is compared with different color correction methods based

on gray world assumption in the next subsection.

4.4.1 Quantitative and Qualitative Analysis of Color Correction Algorithm

Table 4.4 compares the different color correction techniques for various images on the basis of performance metrics mentioned in the previous section. Bold values in the table shows the best value of performance metric for each image. From the table values, it can be seen that *Gray Edge* and *Max-RGB* are not suitable for underwater images as the values of performance measures are not showing any significant improvement as compared to other algorithms. *Shades of Gray* and *Fuzzy Gray* are showing good results but proposed Type-2 fuzzy gray color correction algorithm is performing better than all the algorithms in terms of all performance metrics.

It is clear from the visual appearance as well as quantitative measures that proposed color correction algorithm gives best results. Fig. 4.6-4.11 shows the results of these mentioned color correction algorithms and proposed type-2 fuzzy gray algorithm for the images whose quantitative evaluation is stated in Table 4.4. From the images, *Gray Edge* and *Max-RGB* are not able to create any noticeable difference to the cast in image. *Shades of Gray* is adding red artifacts in most of the images. *Fuzzy Gray* is over-enhancing few regions of the image and introduces few red artifacts in images e.g. result of *fuzzy gray* in first row and sixth row are over-enhanced and have red artifacts in image in second row. Proposed type-2 fuzzy gray, on the other hand, produces fewer artifacts and has results with better clarity and more information as compared to other color correction algorithms. There are dimming or false color artifacts in images with prominent water regions by using proposed type-2 fuzzy gray. Reason for these artifacts is that the method assumes the block to be affected by blue color cast and processes it accordingly which is not required at all. This shortcoming of the method needs to be addressed.

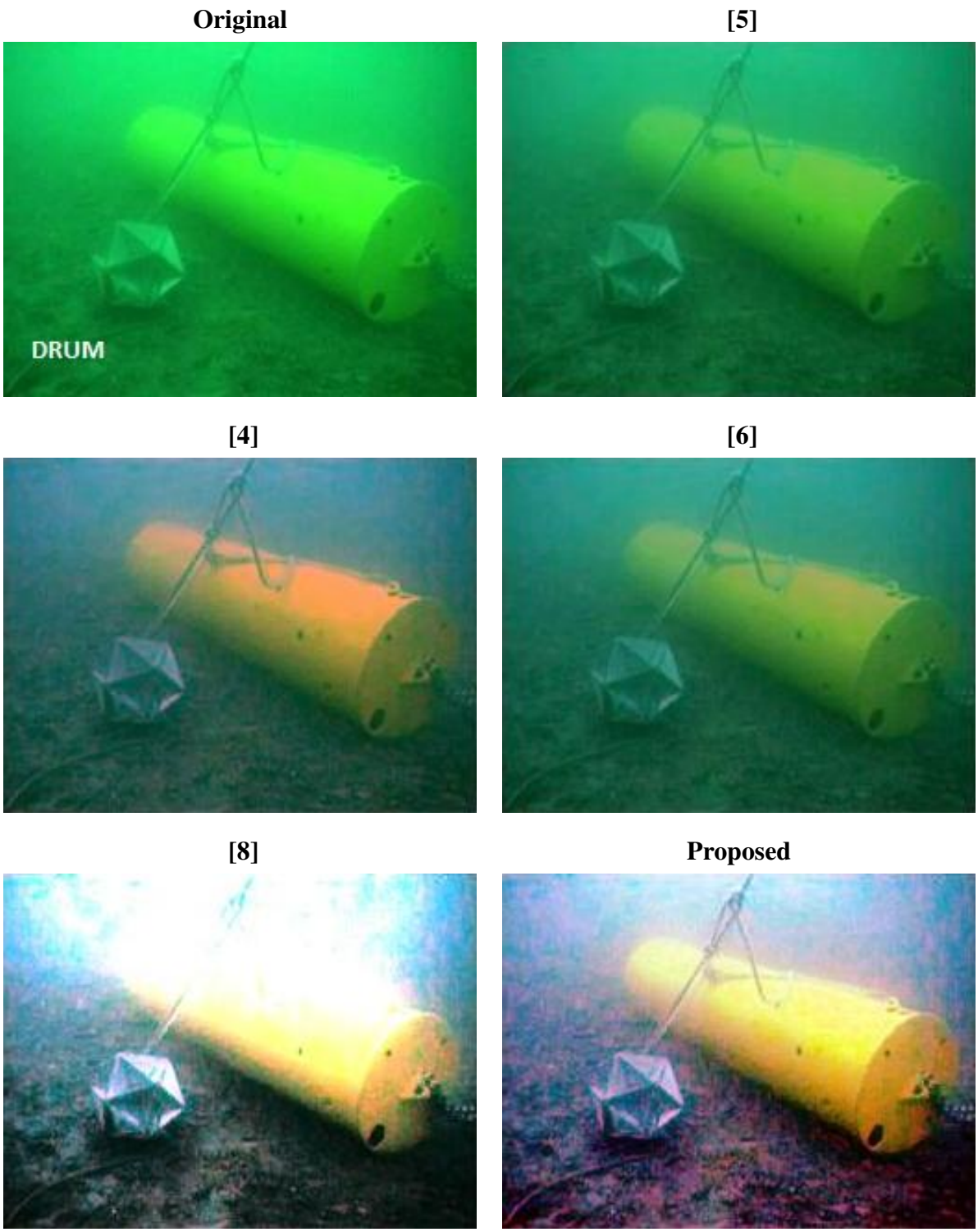

Figure 4.6: Results of Image Im1 for various color correction approaches based on Gray World Assumption

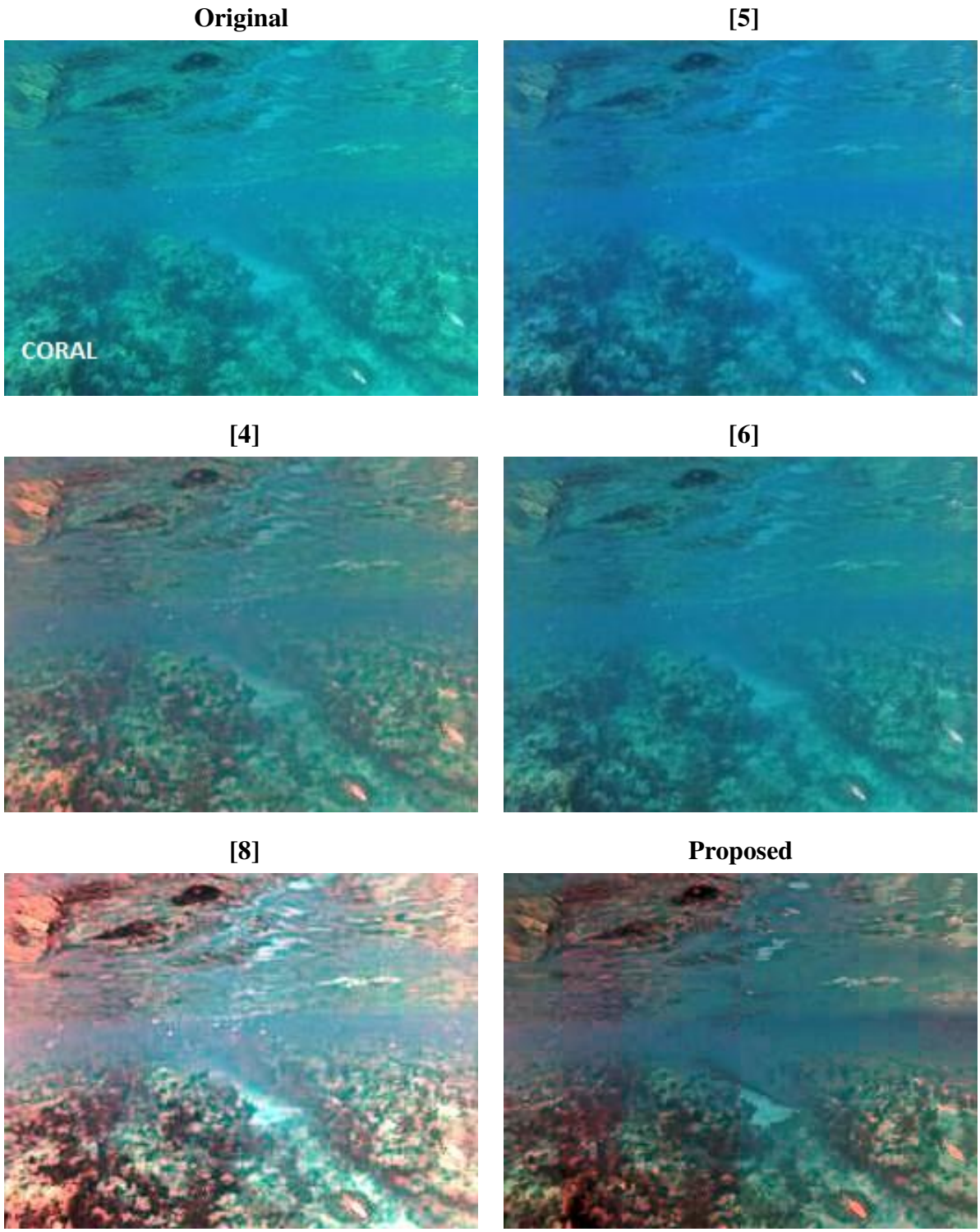

Figure 4.7: Results of Image Im2 for various color correction approaches based on Gray World Assumption

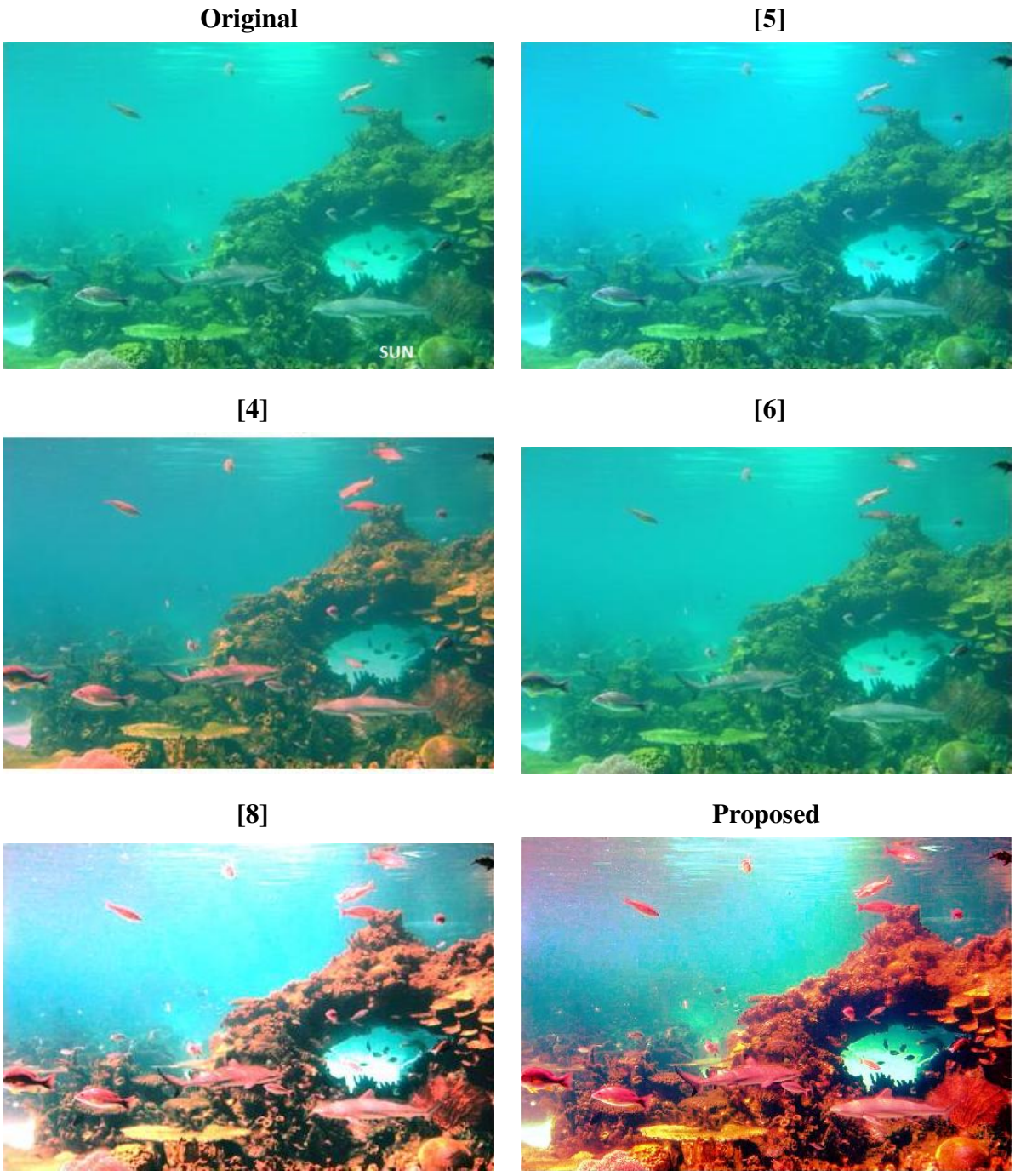

Figure 4.8: Results of Image Im3 for various color correction approaches based on Gray World Assumption

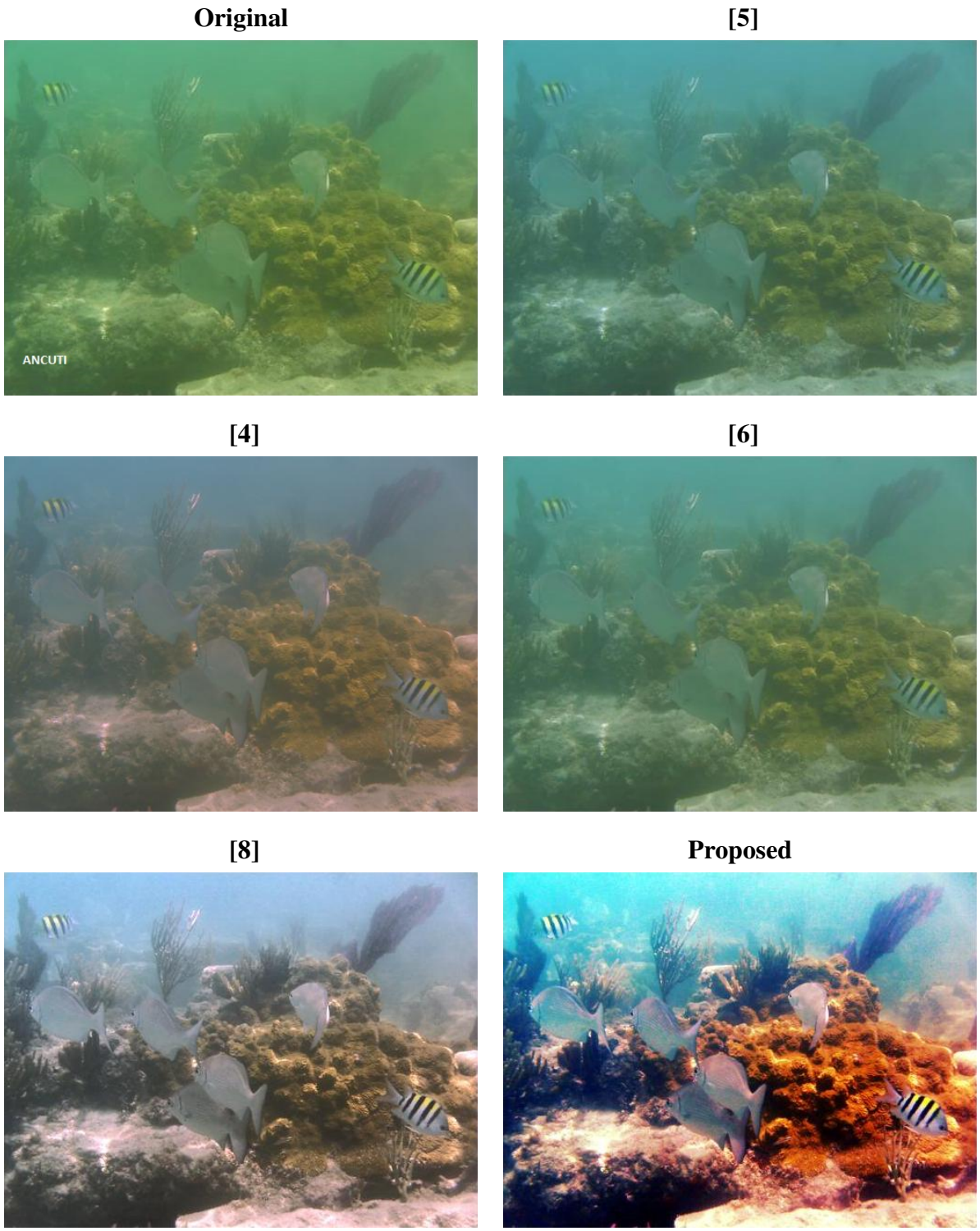

Figure 4.9: Results of Image Im4 for various color correction approaches based on Gray World Assumption

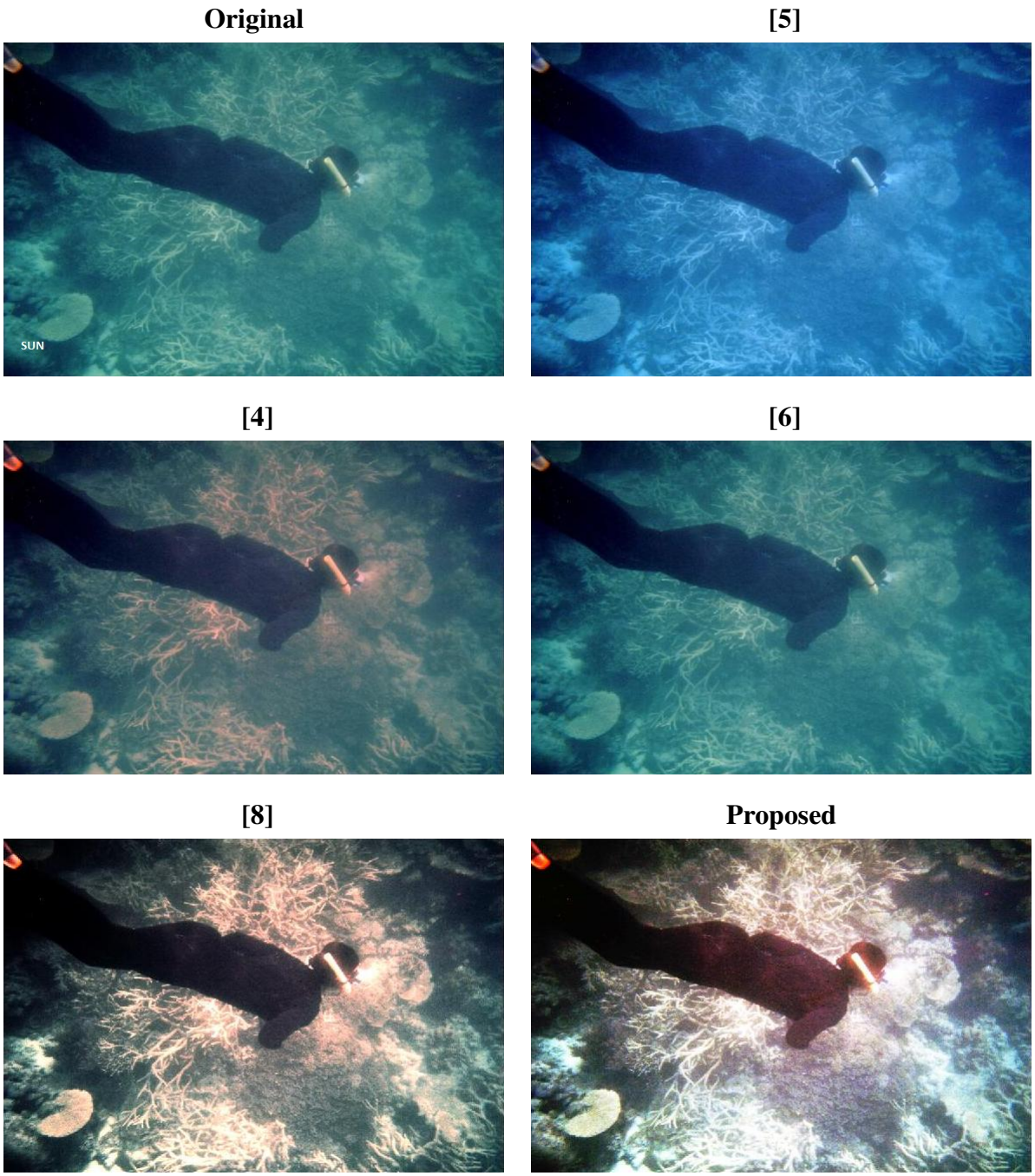

Figure 4.10: Results of Image Im5 for various color correction approaches based on Gray World Assumption

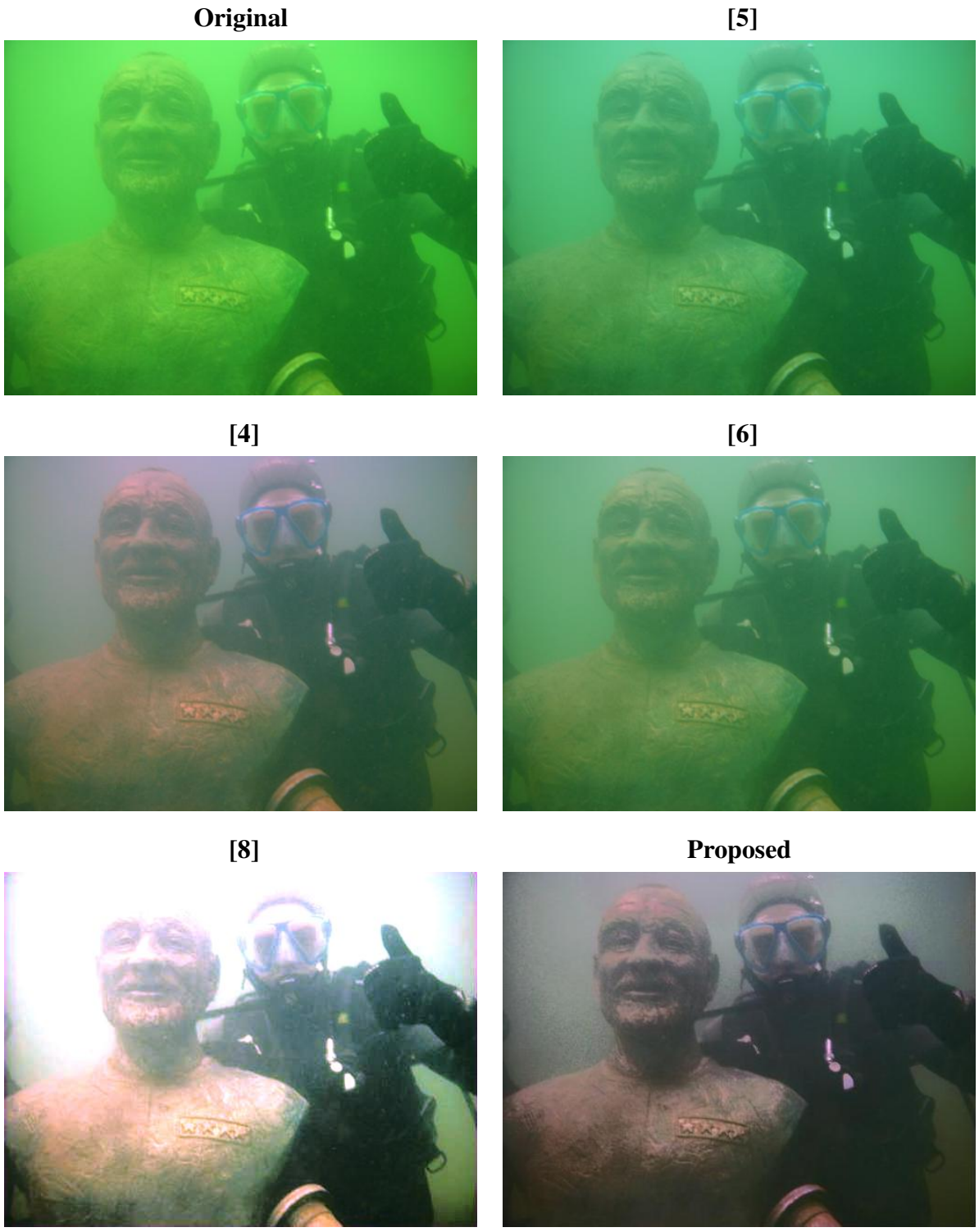

Figure 4.11: Results of Image Im6 for various color correction approaches based on Gray World Assumption

Table 4.4: Performance metrics of different color correction algorithms (Gray Edge [5], Shades of Gray [4], Max-RGB [6], Fuzzy Gray [8]) with proposed type-2 fuzzy gray algorithm for images shown in Fig. 4.6-4.11

	Image	**Original**	[4]	[5]	[6]	[8]	**FCCC**
Entropy	Im1	5.635	**7.334**	6.041	6.629	6.971	6.367
	Im2	4.867	6.797	5.044	5.543	7.636	**7.864**
	Im3	6.587	7.152	6.435	6.584	7.6447	**7.945**
	Im4	5.959	6.142	5.824	5.912	7.364	**7.545**
	Im5	5.876	6.927	5.773	5.995	7.6807	**7.870**
	Im6	6.523	**7.191**	6.473	6.746	6.704	7.097
HS	Im1	0.4005	0.3298	0.3708	0.3377	0.3814	**0.4742**
	Im2	0.1079	0.1388	0.1098	0.1011	0.1765	**0.3596**
	Im3	0.170	0.193	0.191	0.172	0.4521	**0.502**
	Im4	0.1702	0.1773	0.1789	0.1756	**0.3946**	0.3387
	Im5	0.2669	0.2799	0.3073	0.2574	3.066	**0.4837**
	Im6	0.2810	0.3007	0.2716	0.2671	0.7059	**0.3730**
UIQM	Im1	4.103	4.170	4.094	4.130	3.083	**4.716**
	Im2	4.283	4.419	4.298	4.322	4.597	**4.724**
	Im3	4.373	4.375	4.353	4.369	4.995	**41.735**
	Im4	3.979	4.035	3.992	3.998	4.5489	**4.980**
	Im5	0.0103	1.7532	0.2171	0.3019	3.065	**4.3391**
	Im6	3.673	3.776	3.696	3.706	3.2263	**3.805**
UCIQE	Im1	0.4918	0.6222	0.5385	0.5778	0.7689	**6.7943**
	Im2	0.3596	0.4426	0.3848	0.4049	0.5159	**3.2725**
	Im3	9.594	10.395	4.664	9.441	**17.063**	16.629
	Im4	0.446	0.491	0.4370	0.453	0.5802	**0.658**
	Im5	0.403	0.471	0.389	0.413	0.649	**1.180**
	Im6	0.452	0.534	0.461	0.497	0.6746	**0.836**

4.4.2 Quantitative and Qualitative Analysis of FCCC

FCCC has been compared with state-of-the-art approaches for underwater image enhancement (UCM [43], Ancuti *et al.* CVPR [47], Ghani *et al.* [44], Ancuti *et al.* transaction [48]). Performance measures for quantitative evaluation are same as used for evaluation of color correction algorithms. Few underwater images along with their results using the above-mentioned techniques and FCCC are shown in Fig. 4.12-4.19. Table 4.5 lists the value of performance metrics of those images for the above-mentioned algorithms. Bold value in each row highlights the best value of the mentioned performance metric for that image.

Entropy: From the table values, it can be seen that UCM [43], Ancuti *et al.* [47] and Ghani *et al.* [44] are not able to make any significant change in entropy values and it is evident from the visual results also that information content of the images is not improving as required. Ghani *et al.* [44], on the other hand, distorts the overall color and contrast of the images. FCCC increases the information content of all the images and gives best entropy values for 6 out of 8 images and for the 3 images, it gives the second best entropy value. In fishes images, there are false color and dimming artifacts due to the shortcoming of the type-2 fuzzy gray.

Histogram Spread (HS): UCM [43] mainly works on color adjustment, hence gives good results in terms of HS as histograms of all the three channels are uniformly distributed over the entire intensity range. Ghani *et al.* [44] also brings a negative change in HS values for some images due to its over-enhanced and under-enhanced regions. Both the techniques of Ancuti *et al.* are giving mixed results in terms of HS, i.e., these techniques may improve or degrade the HS value. Previous version of Ancuti *et al.* [47] is producing results with poor contrast as compared to new version [48] which is proven by the quantitative results. FCCC is overall improving the histogram spread values for all the images as it works on improvement of both color and contrast of the image. For some images, it is giving the best values also.

UIQM: Ghani *et al.* [44] is degrading the overall contrast, color and sharpness of image so it is lowering the UIQM values as compared to original image for most of the images. UCM [43], both the Ancuti *et al.* techniques [47] [48] and FCCC are improving the UIQM values. UIQM values are highest either for FCCC or Ancuti et al. [48] for all the images as these techniques are acting on all the three aspects: color, contrast and sharpness.

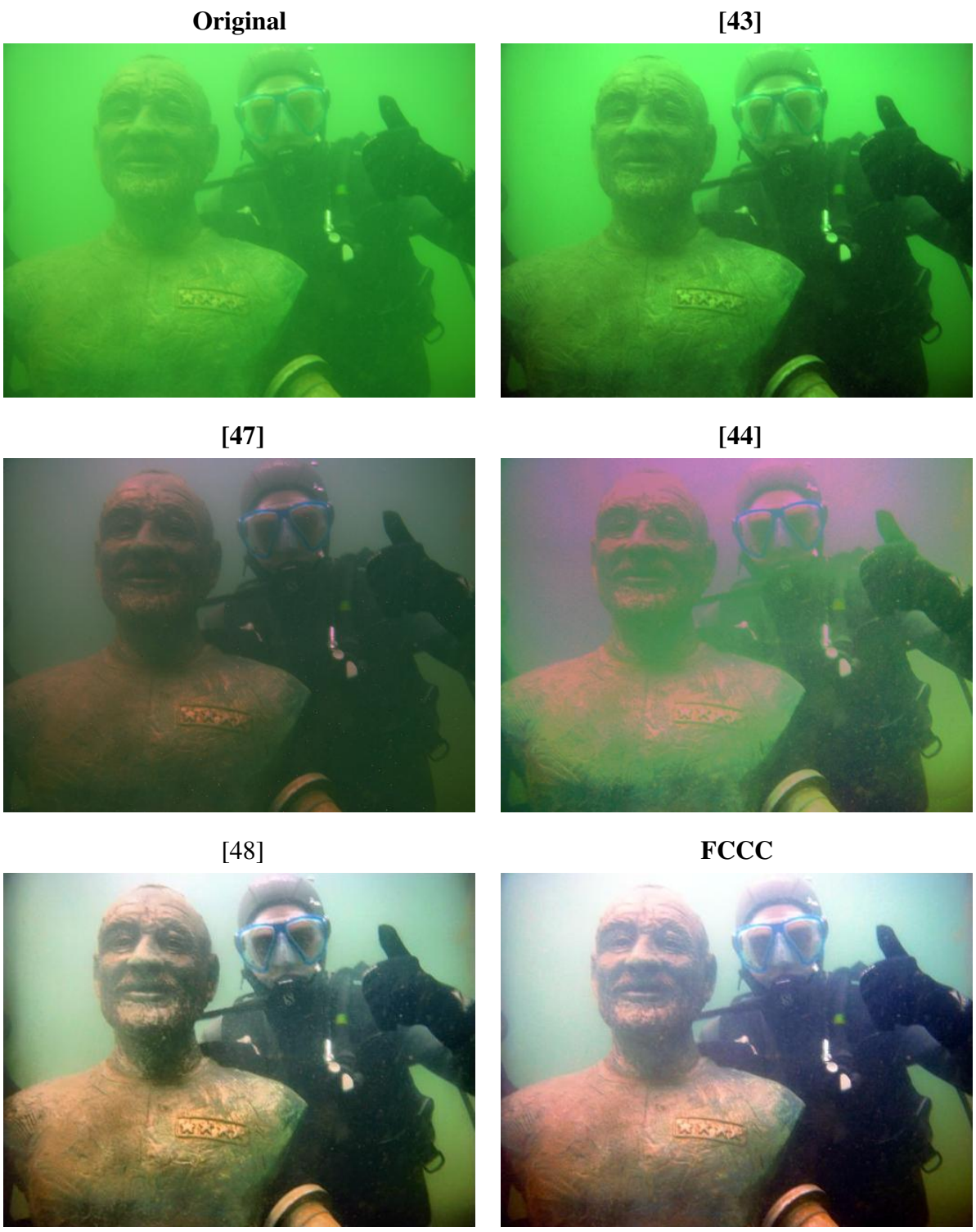

Figure 4.12: Results of Ancuti1 Image

Original **[43]**


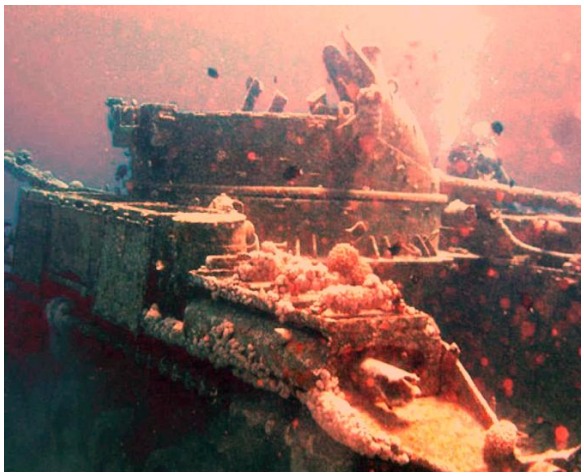

[47] **[44]**

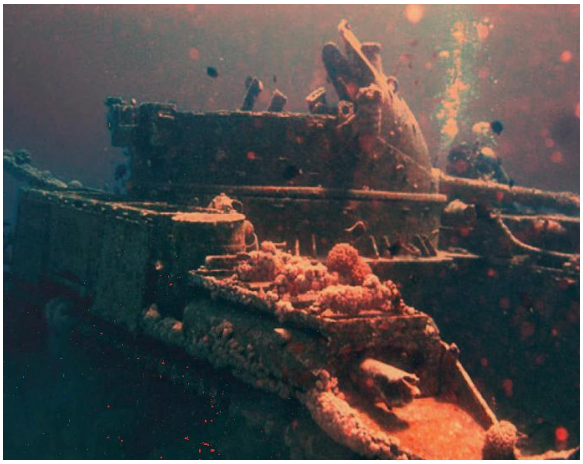


[48] **FCCC**


Figure 4.13: Results of Ship Image

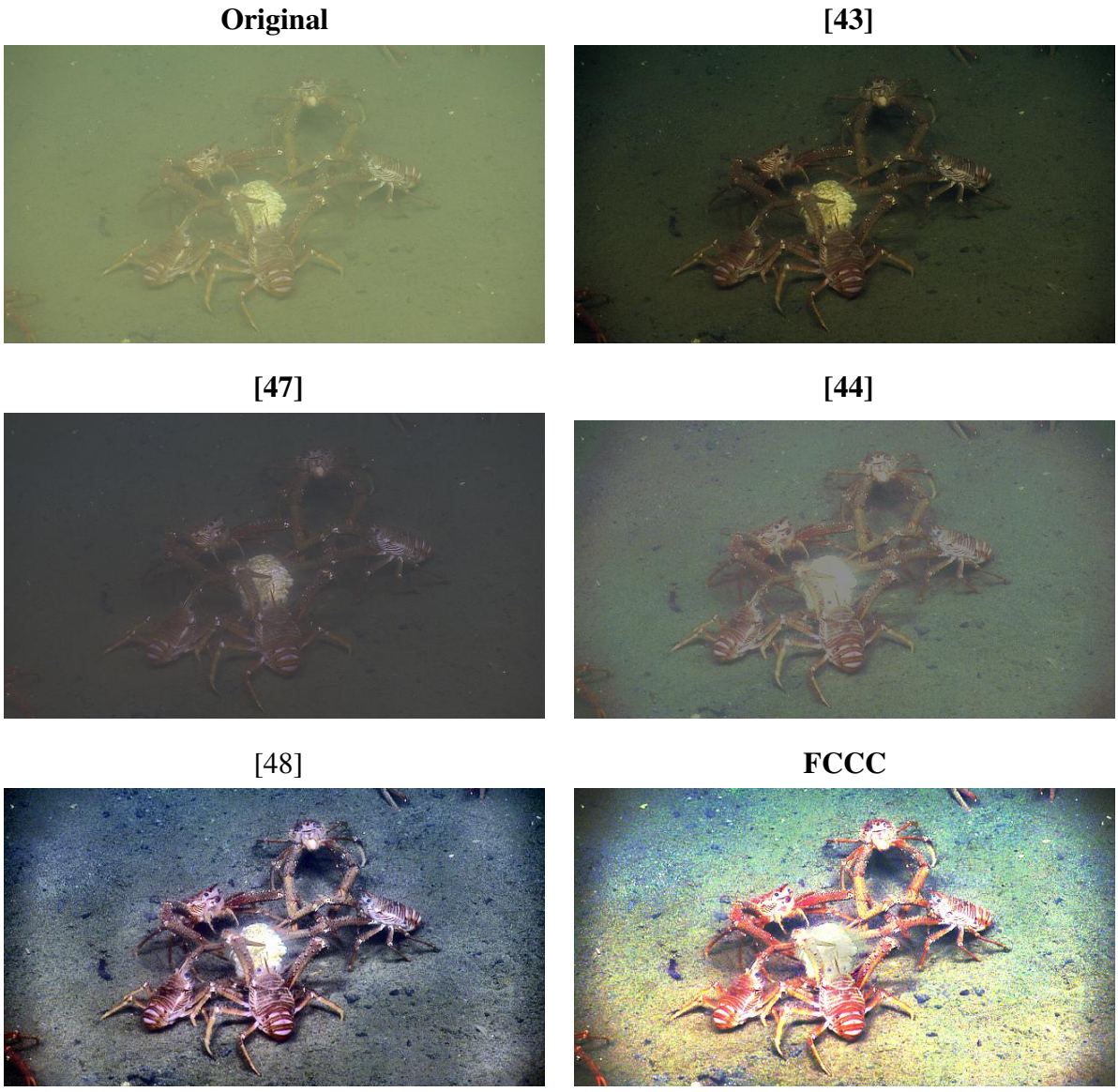

Figure 4.14: Results of Crabs Image

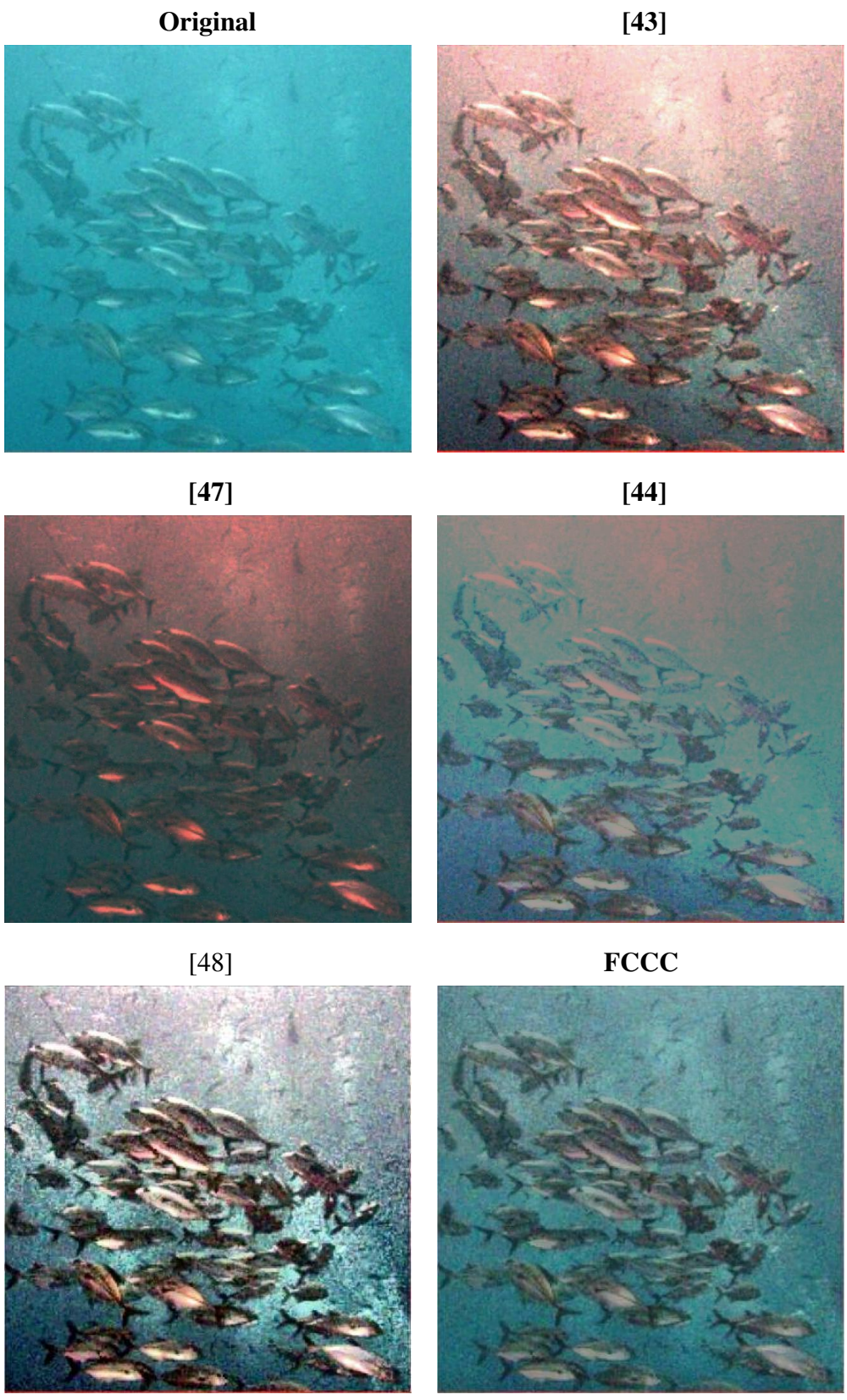

Figure 4.15: Results of Fishes Image

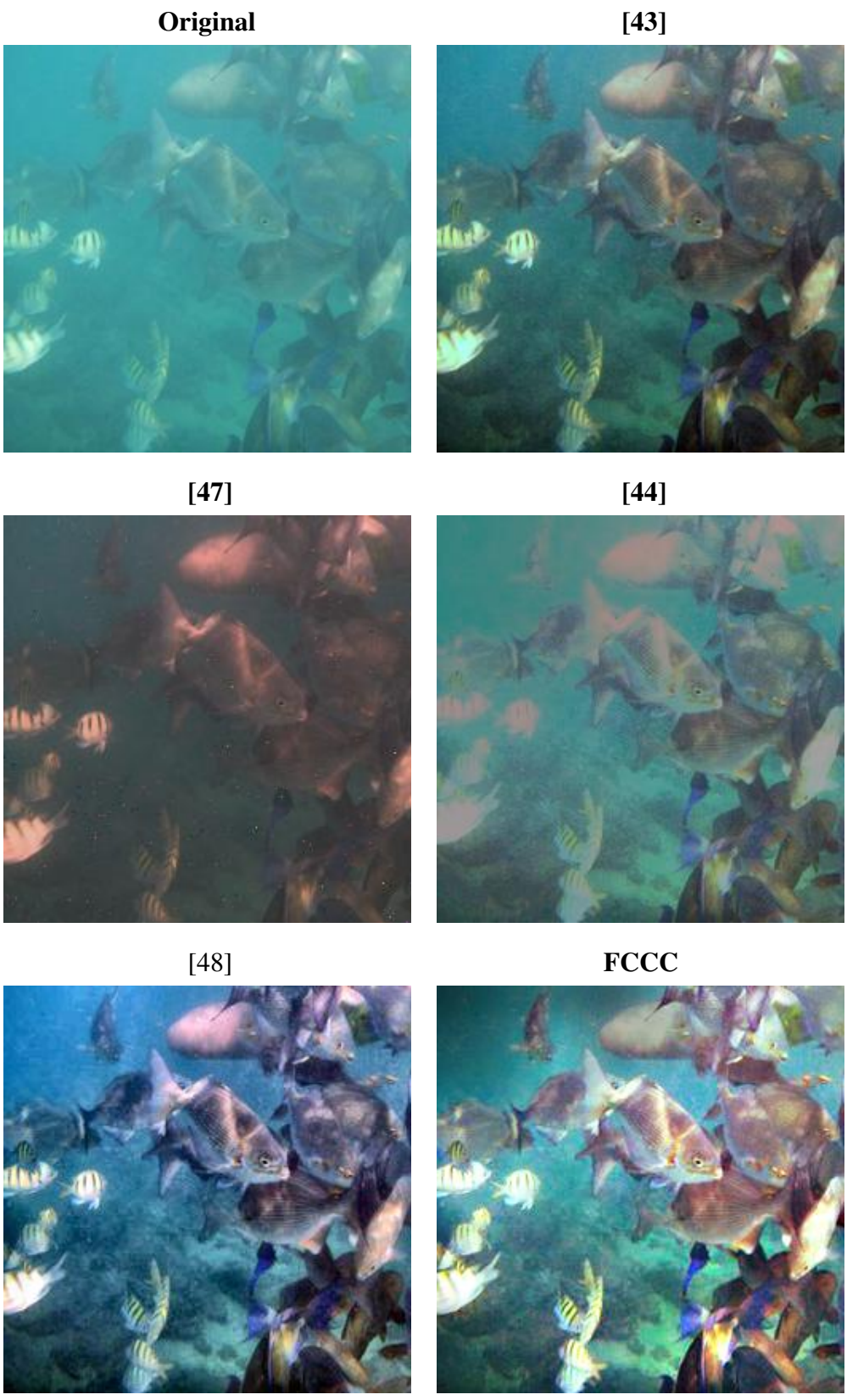

Figure 4.16: Results of SUN1 Image

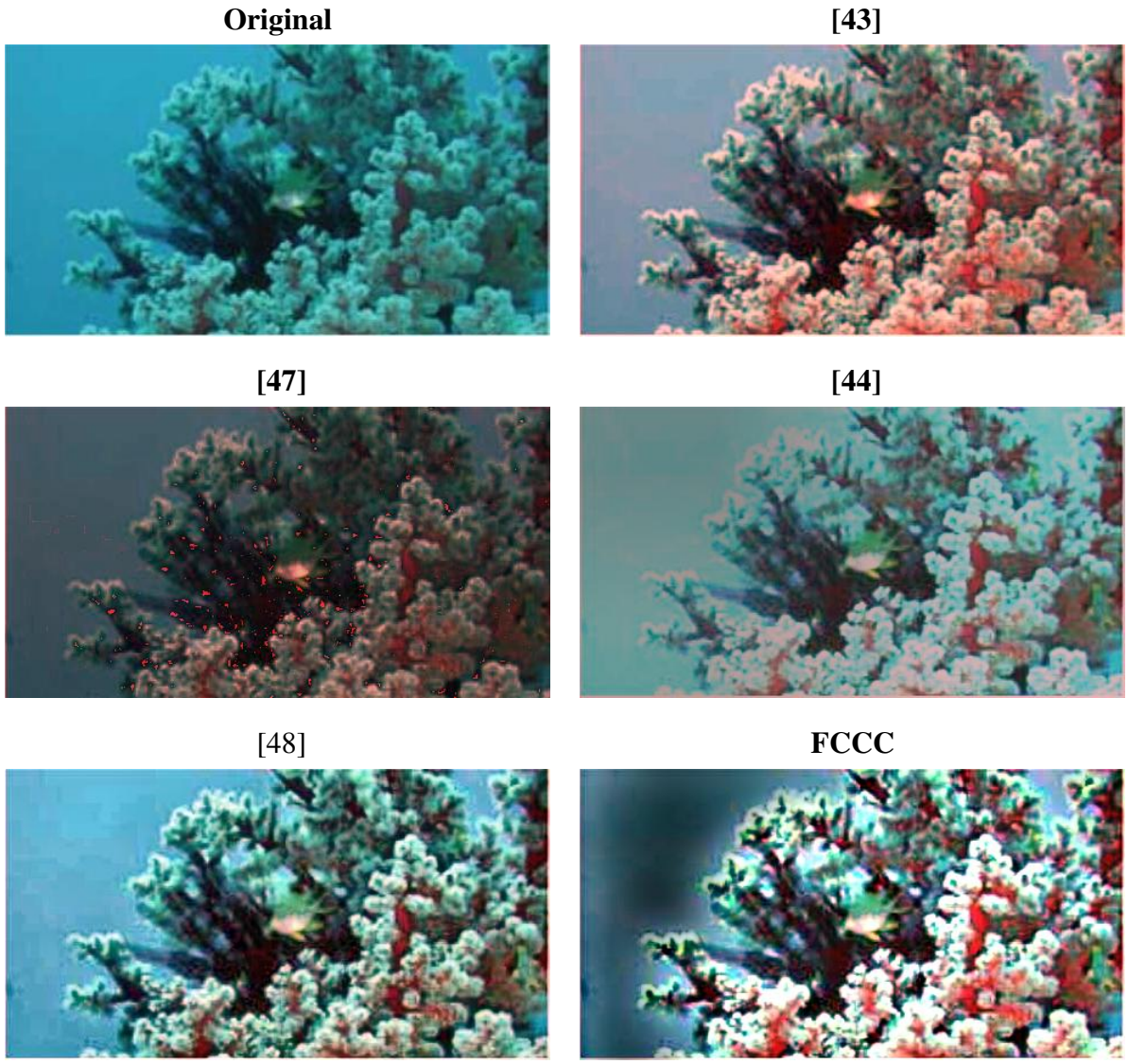

Figure 4.17: Results of SUN2 Image

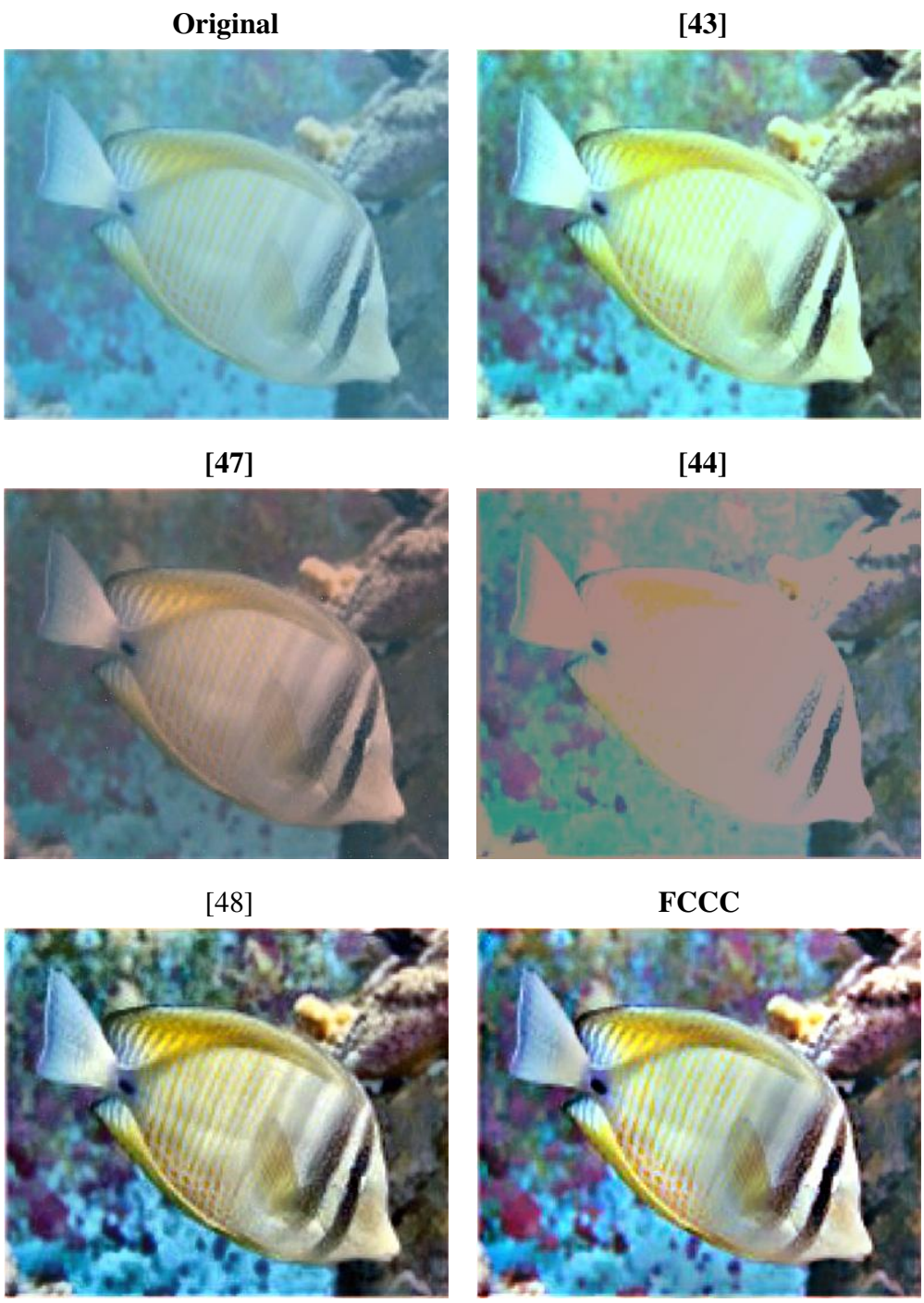

Figure 4.18: Results of SUN3 Image

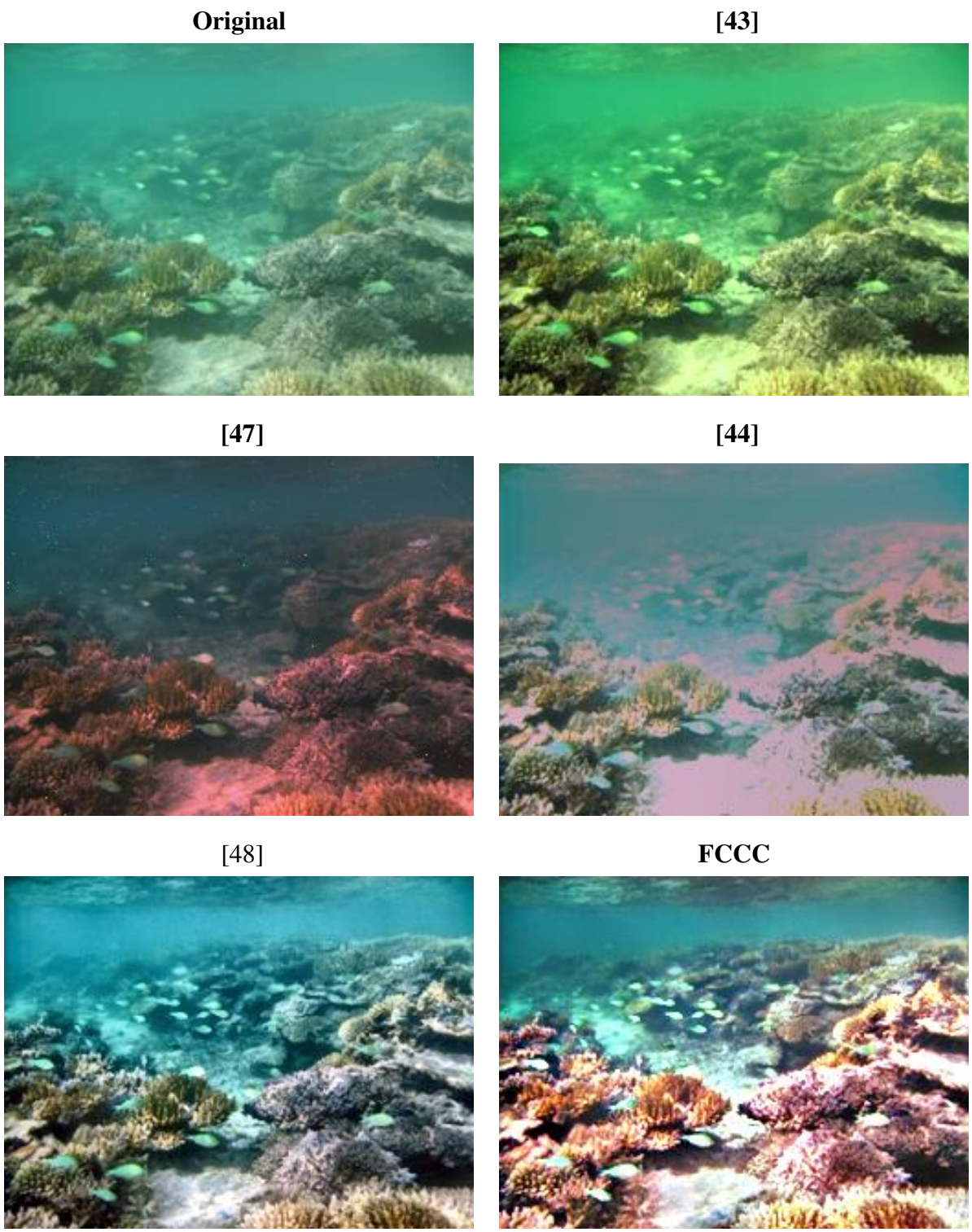

Figure 4.19: Results of Galdran1 Image

Table 4.5: Performance metric values for few images for different state-of-the-art techniques

Image	Metric	Original	[43]	[47]	[44]	[48]	FCCC
Ancuti1	**Entropy**	6.5248	6.5908	6.7296	7.3485	7.8433	**7.9503**
	HS	0.2816	0.3102	0.2254	0.2781	0.4196	**0.5072**
	UIQM	3.6941	3.7859	3.6786	3.8000	**4.2978**	4.0742
	UCIQE	0.4519	0.7646	0.7304	0.4910	0.8753	**2.7662**
Ship	**Entropy**	6.9697	7.4550	7.3877	7.2871	7.6911	**7.9705**
	HS	0.3882	0.5979	0.3197	0.3327	0.4575	**0.5033**
	UIQM	4.2983	4.6413	4.7459	3.9960	**4.9673**	4.2478
	UCIQE	0.5630	0.9827	0.9837	0.5487	1.3952	**1.7495**
Crabs	**Entropy**	4.8078	5.4126	4.2204	5.3897	7.3128	**7.6772**
	HS	0.0486	0.0490	0.0268	0.1569	0.1791	**0.3268**
	UIQM	3.6492	5.2427	3.4689	4.6656	5.5536	**5.7234**
	UCIQE	0.3728	0.6220	0.6889	0.4729	1.0552	**1.5218**
Fishes	**Entropy**	6.5324	6.7830	6.1696	6.9306	**7.8136**	7.7862
	HS	0.2530	0.2530	0.1982	**0.4694**	0.3739	0.4484
	UIQM	3.9228	5.2559	4.3864	4.3733	**5.4301**	5.2905
	UCIQE	0.4128	1.5013	0.6670	0.5105	**4.2828**	0.6745
SUN1	**Entropy**	5.7844	6.8056	6.0115	6.4395	7.4580	**7.6960**
	HS	0.1198	0.1851	0.1029	0.2406	0.2614	**0.2850**
	UIQM	3.6823	4.8914	4.2669	4.2116	5.2129	**5.2669**
	UCIQE	0.3512	0.8277	0.6687	0.4638	**1.4519**	0.5958
SUN2	**Entropy**	6.3700	7.5959	6.8058	7.1650	7.5948	**7.8292**
	HS	0.2340	0.3080	0.3725	0.2611	0.1951	**0.4641**
	UIQM	4.5231	4.7002	4.7405	4.3369	4.8297	**4.8932**
	UCIQE	0.6051	0.8202	1.2929	0.5351	1.0954	**1.4683**
SUN3	**Entropy**	6.8154	7.2994	7.0231	6.1260	**7.8287**	7.8267
	HS	0.2678	0.3844	0.2814	0.3003	**0.4000**	0.3922
	UIQM	3.6095	4.2130	4.0858	2.7284	4.3350	**4.8133**
	UCIQE	0.3634	0.5181	0.5413	0.4346	1.5654	**2.0578**
Galdran1	**Entropy**	6.7518	7.2867	6.7915	7.2489	7.6676	**7.7873**
	HS	0.2030	0.2396	0.1597	0.2404	0.3307	**0.3882**
	UIQM	4.8825	5.1963	5.2247	4.3185	5.0983	**5.2589**
	UCIQE	0.4576	0.6295	0.7936	0.4955	**2.0209**	1.7439

UCIQE: Since UCIQE measures the extent to which blurriness and contrast of an image is improved, Ghani *et al.* [44] technique lags in this factor also. UCM [43] on the other hand, increases the UCIQE values as it removes blurriness but contrast is not improved to a good extent. Ancuti *et al.* conference version [47] also performs better that UCM as it produces better contrast images compared to UCM. FCCC and Ancuti *et al.* [48] are improving contrast and blurriness of the images and hence are increasing UCIQE values for all the images.

On an average, FCCC is performing better than other techniques for every performance metric. From the visual results of different techniques, it can be seen that UCM either produces images with poor contrast or with reddish tone as it overcompensates the red channel. UCM results of shipwreck and fishes have reddish tone whereas only a little haze is removed in UCM results of Ancuti1, SUN1, Galdran images. Ghani *et al.* technique yields unsatisfactory results with under-enhanced and over-enhanced areas like in fishes image. Ancuti *et al.* [47] and Ancuti *et al.* [48] produce visually appealing results but has some haze left in the images which can be seen in sun1, sun2, Galdran images. Due to better choice of weight maps, FCCC gives good results with good contrast and color information along with better information content. In shipwreck, crabs, sun1 and Galdran image, the images are clear than results of other techniques. Only drawback in the results is that the regions with only water, sometime appear dark like in sun2 image, the corners are dark. Overall the results of FCCC are better than state-of-the-art methods in terms of qualitative and quantitative measures.

4.4.3 Applications of Enhanced Underwater Images

FCCC can be applied to many computer vision related fields like local feature matching, edge detection etc. In this chapter, application of FCCC in local feature matching has been depicted, which forms the basis for applications like classification, image registration etc. Local features are indifferent to rotation, scaling and motion changes. We have employed SURF [117] operator to compute and match feature blobs for a pair of underwater images and repeated the same process for the enhanced versions of the corresponding pair of im-

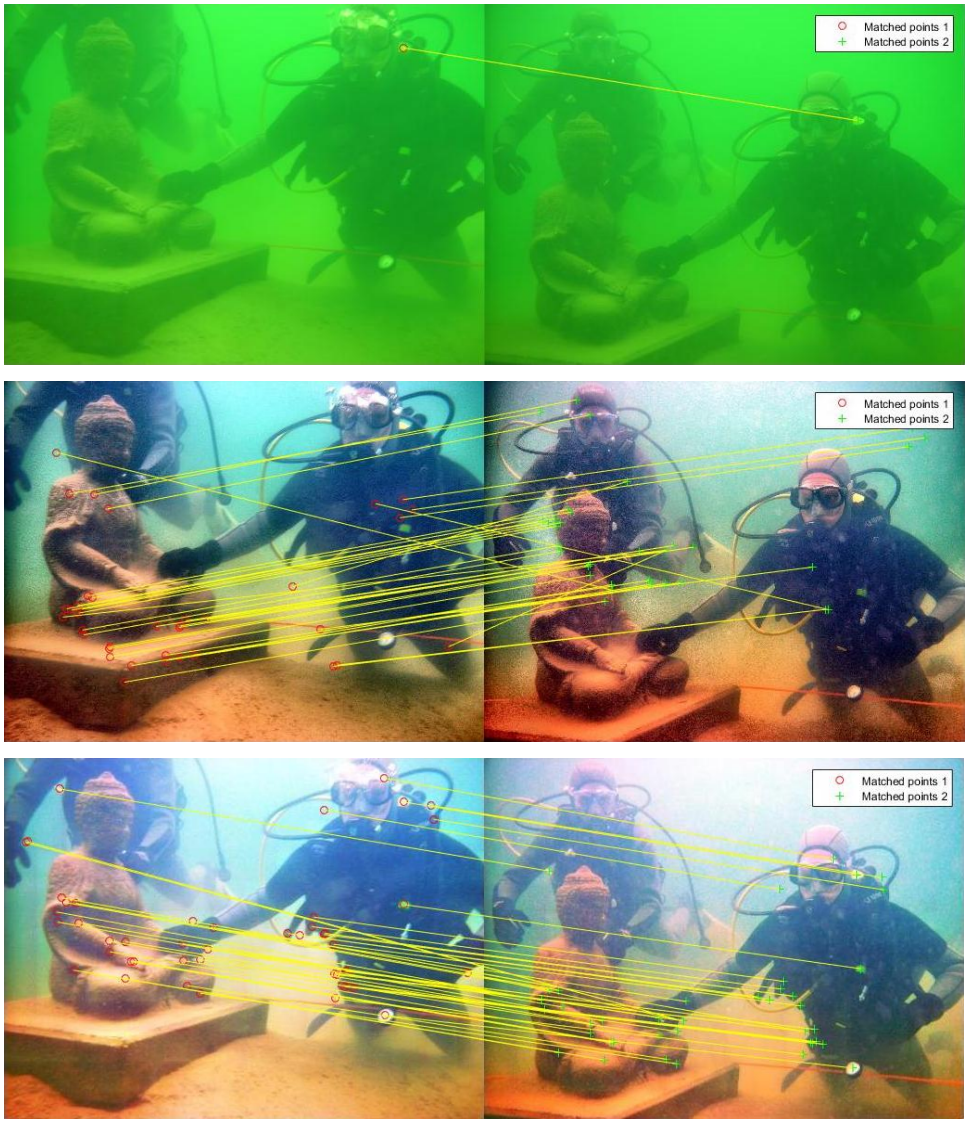

Figure 4.20: First row contains Original pair of images with only 2 SURF features are matching, second row contains enhanced pair of images using Ancuti *et al*. technique with 37 SURF features are matching and third row contains enhanced pair of images using FCCC with 48 SURF features are matching.

Figure 4.21: First row contains Original pair of images with only one SURF feature, second row contains enhanced pair of images using Ancuti *et al*. technique with 2 SURF features and third row contains enhanced pair of images using FCCC with 4 SURF features matching.

ages. We used the SURF feature matching provided by MATLAB. We enhanced the pair of images using Ancuti *et al.* [48] results and FCCC. Results are very promising which shows that the number of local feature points increase significantly by FCCC as compared to Ancuti *et al.* [48] and are shown in Fig. 4.20 and Fig. 4.21.

4.5 Conclusions

In this chapter, A novel approach named FCCC, based on fusion of color corrected and contrast corrected versions of a single underwater image, has been proposed. Novelty of the technique lies in the use of type-2 fuzzy logic to handle the fuzzy nature of color cast (greenish blue or blue or uneven cast) and the choice of weight maps to extract the relevant features required for an enhanced underwater image. It does not require any information other than the image itself and no parameter tuning is required for enhancing the image. It removes the color cast and contrast related problems in underwater images. Limitations of FCCC are: a little haze remains in case of deep dense haze, e.g. a little haze is left in case of fishes image and dark region in water region in few images e.g. dark corners in water region of SUN2 image and size of sub-blocks can be adaptive depending on the image which can further improve the enhancement results. Since it produces good results for underwater images captured in different environment and the darkness is usually observed in water area and not in the objects in focus, this limitation can be ignored. Overall, the results are better than state-of-the-art techniques as it is enhancing contrast, color information and sharpness of the image. Since FCCC is not able to deliver good results for images with dense haze, this issue has been taken in the next chapter.

Chapter 5

Fusion of Underwater Image Enhancement and Restoration

5.1 Introduction

FCCC encounters the artifacts caused by artificial lighting well but introduces dark colors in water region and fails to improve images with dense haze. In this chapter, we will address the removal of issue of hazy appearance in underwater images along with color and contrast issues. Since we have focused on the major problems i.e., color and contrast through simple image enhancement based solutions like histogram stretching. Haze can be handled only through image restoration based solutions. In this chapter, a novel technique named Fusion of Underwater Image Enhancement and Restoration (FUIER) has been proposed which enhances as well as restores underwater images with a target to act on all major issues in underwater images, i.e., color cast removal, contrast enhancement and dehazing. It generates two versions of the single input image and these two versions are fused using Laplacian pyramid based fusion to get the enhanced image. The proposed method works efficiently for all types of underwater images captured in different conditions (turbidity, depth, salinity etc.). Results obtained using the proposed method are better than those for state-of-the-art methods.

5.2 Problem Formulation

There is a plethora of work present in the literature which either performs intensity manipulation using spatial domain filters or tries to restore the original image from captured image using the image formation model. Some of them apply image restoration technique followed by image enhancement. In this way, they try to remove all the problems in underwater images, but the result has disadvantages of both, i.e., increased computational complexity and artifacts in the output image. As we know both types of techniques have their advantages and disadvantages, the motivation behind this work is to develop an algorithm which tackles all the major problems in underwater images and is computationally less intensive. FUIER combines the color and contrast correction ability of image enhancement based methods and haze removal property of image restoration based methods. Furthermore, image restoration technique is chosen in a way that computation and time complexity of the overall algorithm is low and artifacts of image enhancement methods can be avoided. Multi-scale weighted Laplacian pyramid based fusion has been employed which ensures that only desired features are taken in the final image.

In FUIER, two versions of the input image are created. the first version is a histogram equalized version of the input image which leads to color correction. The second version is contrast stretched version of the input image followed by dehazing using dark channel prior based method. Two weight maps, namely local entropy weight map and gradient weight map have been calculated for both the versions. Now, these two versions are fused using multi-scale weighted Laplacian pyramid decomposition [118] based fusion. These weights control the contribution of each version towards the final enhanced image without introducing artifacts and halos. The main contributions of FUIER are as follows:

(a) It employs simple and computationally less intensive techniques which produce results possessing the qualities required in underwater images.

(b) It is an adaptive method which works for every type of underwater image captured at any depth, in any saline or turbid medium.

The next sections explain FUIER in detail.

5.3 Working of FUIER

FUIER employs computationally simple image enhancement and image restoration methods to achieve the aim of removing the problem of color cast (by histogram equalization), poor contrast (by contrast correction) and hazy appearance (by dark channel prior based method).

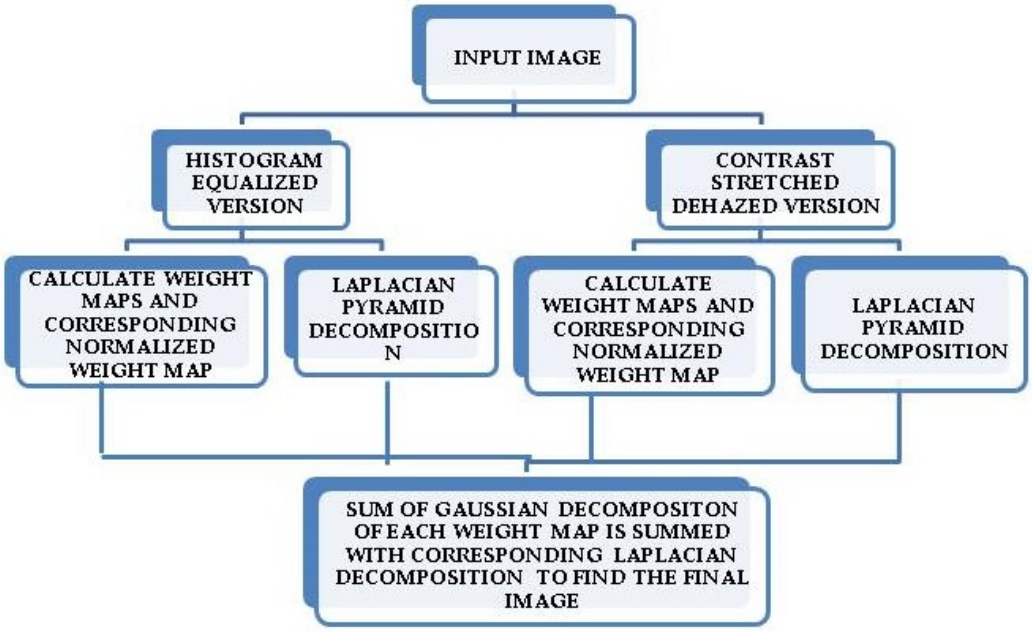

Figure 5.1: Work Flow of FUIER

The basic workflow of FUIER is shown in Fig. 5.1. FUIER works at three levels: deriving two versions of the input image, calculating weight maps and fusion of the two versions with corresponding weight maps at multiple scales.

5.3.1 Generation of Two Versions for Fusion

The first version for fusion process is a color corrected version which is generated by a traditional image enhancement method named Histogram Equalization (HE) [24]. HE is

a simple method to enhance the contrast when applied on a grayscale image but when it is applied on three color channels individually in case of underwater images, it uniformly distributes the intensity value over the whole dynamic range thereby removing the color cast.

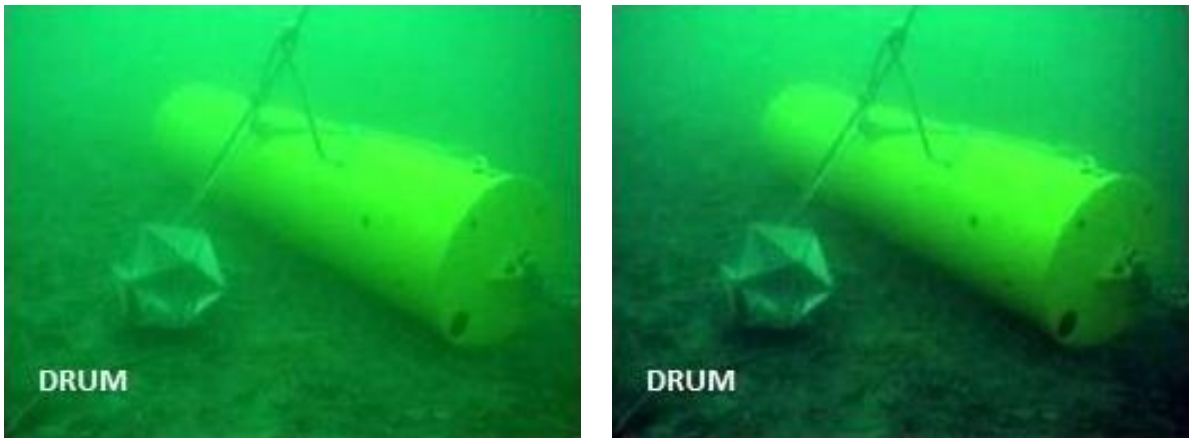

(a) Drum Image

(b) Drum Image after contrast stretching

(c) Drum Image after contrast stretching and dehazing

Figure 5.2: Drum image after applying contrast stretching and dehazing to obtain the second version for fusion

The reason behind this phenomenon is that it removes the domination of a single color channel in the image by spreading the intensities of all color channels over the dynamic range of intensities which can be seen in Fig. 5.3. Fig. 5.3 shows an underwater image and its histogram before and after applying HE.
The second version for the fusion process is a contrast corrected dehazed image. Contrast correction is done by simply stretching the histogram of all the color channels to span the whole dynamic range using Eq. 5.1.

$$CI_c(x,y) = (I_c(x,y) - minI_c) * (Max - Min)/(maxI_c - minI_c) \tag{5.1}$$

where $CI_cc \in$ [r,g,b] is the contrast corrected image, $maxI_c$ and $minI_c$ is the maximum and minimum intensity value respectively of each color channel and Max and Min denotes the maximum and minimum possible intensity value respectively for an image e.g. 255 and 0 are the maximum and minimum possible value for an 8 bit RGB image.

After contrast stretching, dehazing of the image is done by dark channel prior [62]. As mentioned earlier, a lot of work has been done in the field of underwater images using either the original dark channel prior or its modified versions, but we have chosen the original dark channel prior because it is a simple yet powerful method for dehazing to remove the haze present in underwater images. For a hazy image, the image is modeled as in Eq. 5.2.

$$I(x) = J(x)t(x) + A(1 - t(x)) \tag{5.2}$$

where I(x) is the observed radiance, J(x) is the actual radiance, t(x) is the transmission map and A is the atmospheric light
The above equation is same as Eq. 1.2, which is the image formation model for underwater images. In this approach, we first find the dark channel using the assumption that the dark channel of a haze-free image is zero which can be defined as shown in Eq. 5.3.

$$J^{dark}(x) = \min_{c\epsilon r,g,b}(\min_{y\epsilon\Omega(x)}(J^c(y))) \tag{5.3}$$

where J^{dark} is the dark channel and Ω is 15X15 neighborhood is chosen for estimating the dark channel.

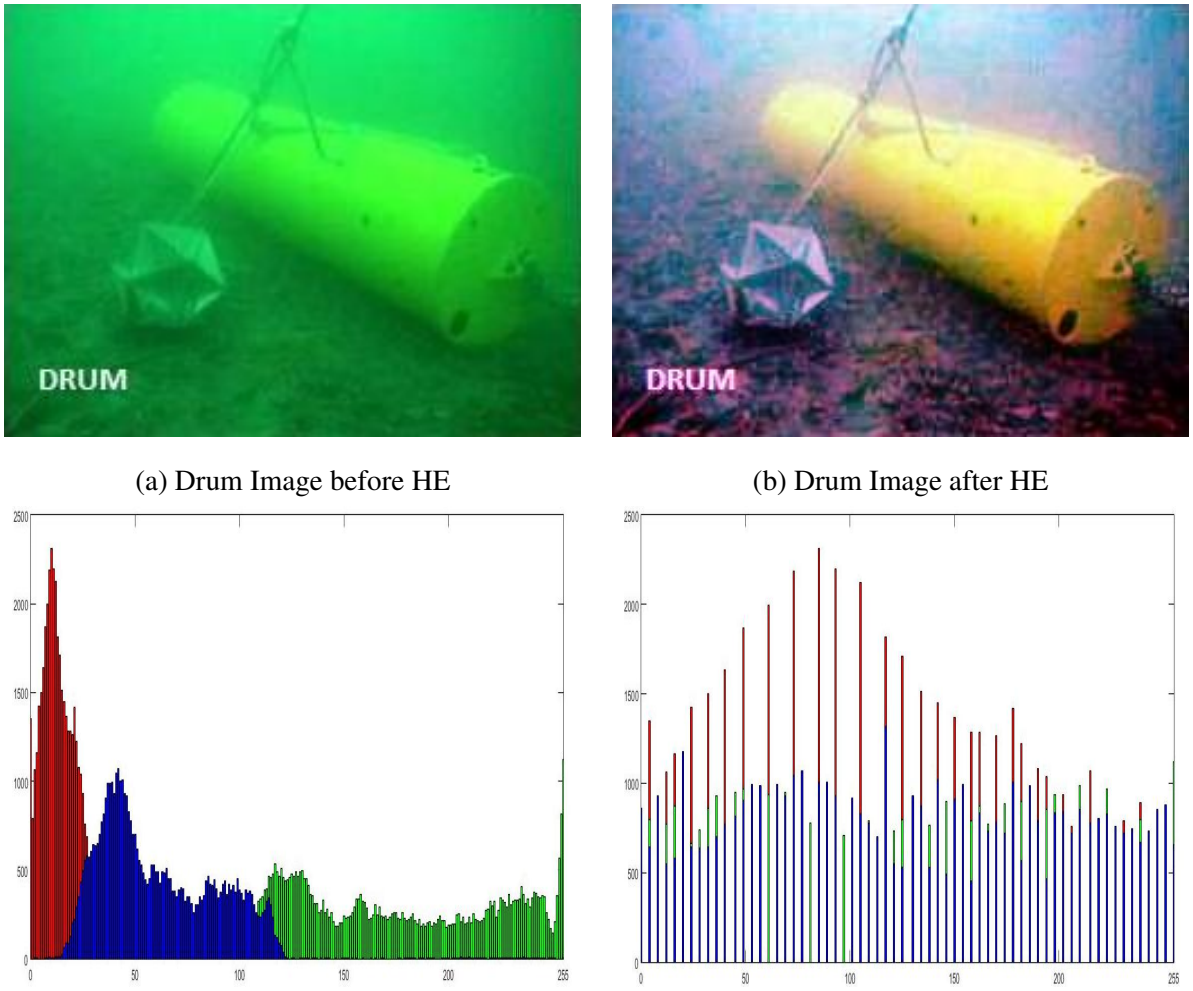

(a) Drum Image before HE

(b) Drum Image after HE

(c) Histogram of Drum Image before HE

(d) Histogram of Drum Image after HE

Figure 5.3: Drum image and its histogram before and after applying HE

Firstly, the atmospheric light is estimated by using this dark channel. The top 0.1 % percent of the brightest pixels are chosen from the dark channel and then among these pixels, the highest intensity pixel from the image I is chosen to represent 'A' (atmospheric light). We then compute the raw transmission map $\tilde{t}(x)$ by using Eq. 5.4.

$$\tilde{t}(x) = 1 - \min_{c}(\min_{y \epsilon \Omega(x)} \frac{I^c(y)}{A}) \tag{5.4}$$

$\min_c(\min_{y\epsilon\Omega(x)} \frac{I^c(y)}{A})$ *denotes dark channel of the normalized haze image* $\frac{I_c(y)}{A}$ *which directly provides the estimation of the transmission.*

Then, the raw transmission map is refined by using guided filter [119] to speed up computation instead of soft matting used in [62]. Finally, haze-free image is recovered using Eq. 5.5 from the refined transmission map (t(x)) and estimated atmospheric light (A).

$$J(x) = \frac{(I(x) - A)}{max(t(x), t_0)} + A \tag{5.5}$$

t_0 is chosen 0.1 as mentioned in [62]. Fig. 5.2 shows the contrast stretched and dehazed image version of the drum image.

5.3.2 Weight Maps for fusion

Local entropy weight map and gradient weight maps are computed in the same manner as mentioned in section 4.3.3.1 in order to incorporate the desired features in the final image. We want the final image to have good contrast along with better information content. Depending on the weight values, a pixel with higher weight is given priority over other to appear in the final enhanced image. Final normalized weight map (W_k) for each input image k is derived using Eq. 4.5 as explained in previous chapter.

5.3.3 Multi-scale Pyramid decomposition based fusion

As mentioned earlier weighted addition leads to artifacts, we opt for multi-scale Laplacian pyramid decomposition based fusion [118]. Fig. 5.4 shows the result of drum image using simple weighted addition, multi-scale Laplacian pyramid decomposition based fusion and result using FCCC. Red boxes in the weighed fusion image show the artifacts and halos in the resultant image. It is also clear from the results of FCCC and FUIER, FCCC result is hazy and blurred as compared to FUIER although same weight maps have been used in both the techniques.

Multi-scale Laplacian pyramid decomposition of each version of the input image is per-

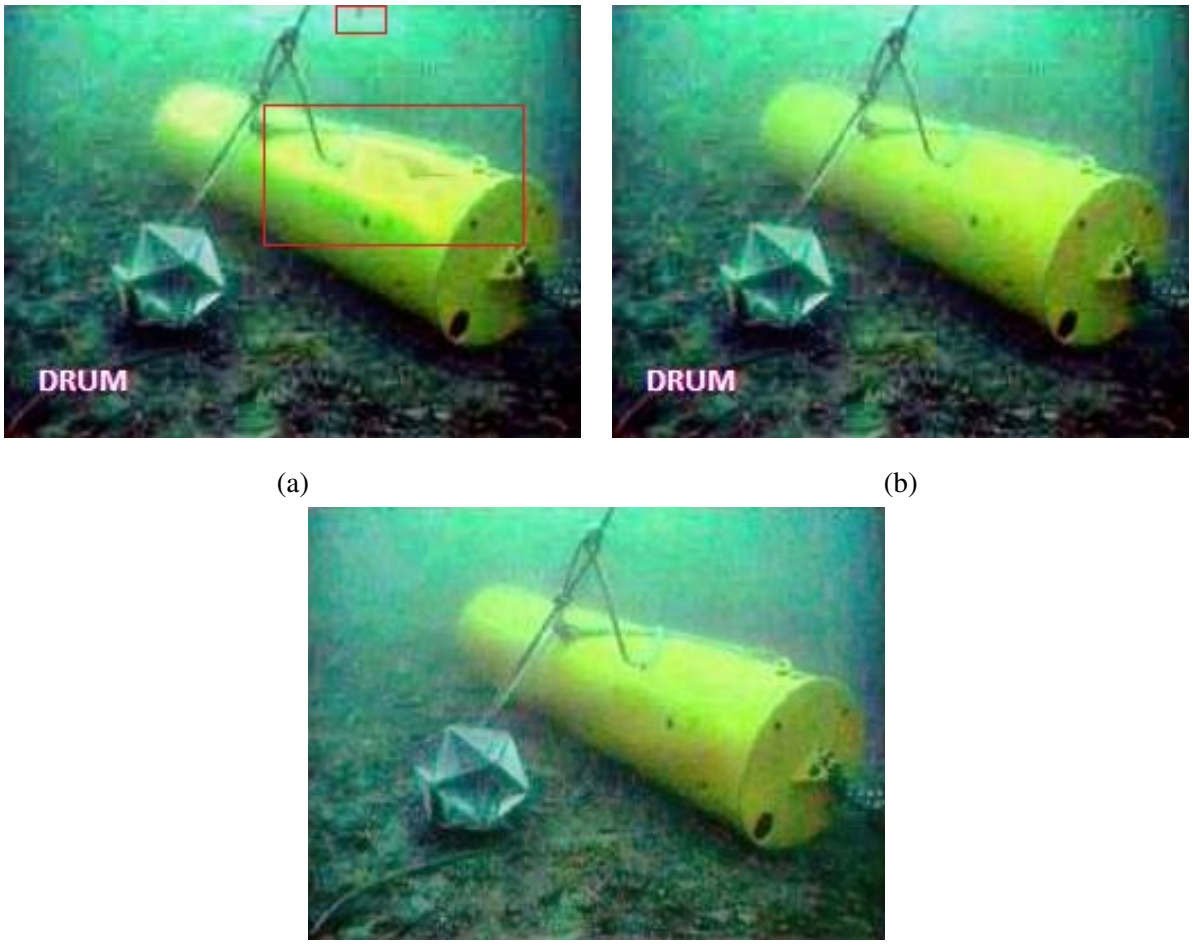

(a) (b)

(c)

Figure 5.4: Enhanced drum image using (a) weighted addition (b) Multi-scale Laplacian pyramid decomposition based fusion (c) Image using FCCC

formed at 5 levels. This means if the image size is 256X256, Laplacian operator is applied on it to obtain the first level of pyramid and then the image is scaled down by 2 for next level and Laplacian operator is applied again to find that level. Image is scaled down and same process is followed till image reaches the size of 16X16. Similarly, Gaussian pyramid of normalized weight map is found out by convolving with Gaussian kernel at the same number of levels as Laplacian pyramid. Now, the corresponding levels of each version are fused to form the fused pyramid using Eq. 5.6.

$$pyramid^l(i,j) = \sum_{k=1}^{2} G^l(W_k(i,j))L^l(I_k(i,j)) \tag{5.6}$$

where, $pyramid^l$ is the fused pyramid at level l, G^l indicates Gaussian pyramid level l, L^l indicates Laplacian pyramid level l.

The different levels of the fused pyramid are then composed starting from the highest level, i.e., the pyramid layer at level 5 is upscaled by 2 and then added to level 4, then the resultant is upscaled by 2 and added to level 3 and this process continues till level 1 is reached to find the final fused image. This multi-scale Laplacian fusion process is relatively simple and fast. Algorithm **??** explains all the steps of FUIER. The results tend to be free from artifacts as fusing at multiple scales suppress sharp transitions.

5.4 Results and Discussion

For establishing the technique, we have compared FUIER with state-of-the-art techniques, i.e., dehazing by dark channel prior [62], WCID [66], automatic red channel (ARC) underwater restoration [69] and the Ancuti *et al.* [48] technique. FUIER is implemented in MATLAB version 2015a on an Intel i5 2.60 GHz processor.

5.4.1 Datasets and Performance Metrics

FUIER has been tested on different images taken from the internet, images from the Ancuti *et al.* CVPR paper [47] and underwater images from SUN database [114]. It has been tested on more than 200 images for performance evaluation. Recently, a few underwater image databases have been developed namely TURBID dataset [92] and WHOI color correction dataset [93]. The pictures of TURBID dataset are generated by experimentation for simulation of images in the turbid water body and WHOI (Woods Hole Oceanographic Institution) color correction dataset have original images along with reference images generated by the color correction method developed by scientists of WHOI. Thus, a comparison can be done with the results given on WHOI website [93] using reference based performance measures like PSNR (Peak Signal to Noise Ratio) and MSE (Mean Squared Error) but these reference based performance measures cannot be used for quantitative evaluation of other underwater images. Other than these datasets, underwater images neither have any database with ground truth values nor any universally accepted quantitative measure for evaluating the extent of image enhancement. Thus, assessing the performance of underwater image enhancement methods is very challenging.

There are few non-reference based quantitative performance measures which have been used to evaluate the quality of the results namely, Entropy [24], Δ (difference) [81], HS (Histogram Spread) [80], UIQM (Underwater Image Quality measure) [91] and UCIQE (Underwater Color Image Quality Measure) [116]. Entropy is general performance metric which indicates the information content of the image. The entropy of an image should increase with improvement in image quality. Δ indicates how closely the image follows gray world assumption [120]. Gray world assumption states that the average of the three color channels should be a gray value. Value of Δ should be zero for an image following the gray world assumption. Histogram spread measures the contrast of an image. If the value of histogram spread is 0.5, then the image is considered to have uniform contrast. UIQM and UCIQE are the two performance measures specifically for underwater images. UIQM is combination of color, contrast and sharpness measure which contribute to overall quality of an

underwater image. UCIQE quantifies the extent to which contrast and blurriness of an image is reduced. Values of both UIQM and UCIQE increase as image quality enhances.

5.4.2 Qualitative and Quantitative evaluation of FUIER

For qualitative evaluation of FUIER, few underwater images are shown along with their results obtained using the techniques stated earlier for comparison in Fig. 5.5-5.10. Table 5.1 lists the values of these performance measures for the images shown in Fig. 5.5-5.10, for comparison of all the mentioned techniques. For quantitative evaluation, Table 5.2 lists the average value of mentioned non-reference based performance metrics and average execution time for 200 images tested for evaluation of FUIER and other state-of-the-art-techniques. Bold values in each column of both the tables indicate the best value of that particular metric for an image and underlined value indicates the second best value for that image.

From the visual appearance of images shown in Fig. 5.5 - 5.10, it can be seen that DCP [62] does not bring any noticeable change in the image as it tries to remove the haze only. WCID [66] is removing haze as well as trying to improve the contrast and color of the image but is degrading the overall quality by introducing artifacts in some images, e.g. red color artifact in diver image, green color artifact in diver with rocks image and creation of uneven darker and lighter regions in sea walker image. ARC [69], the Ancuti *et al.* [48] technique and FUIER gives visually good results but on the comparison of the images, it can be seen that details are much better in case of latter than both the former techniques for almost all images, for example, in fishes image, corals in the background are clearly visible as compared to any other results. The Ancuti *et al.* technique is giving better image quality for diver image as this technique is specifically designed for Malaysian water in which diver image is captured.

Following conclusions can be drawn from value of Table 5.2 and Table 5.1 for different performance metrics:

Entropy [24]: FUIER is performing best in terms of entropy for all the images which means it is

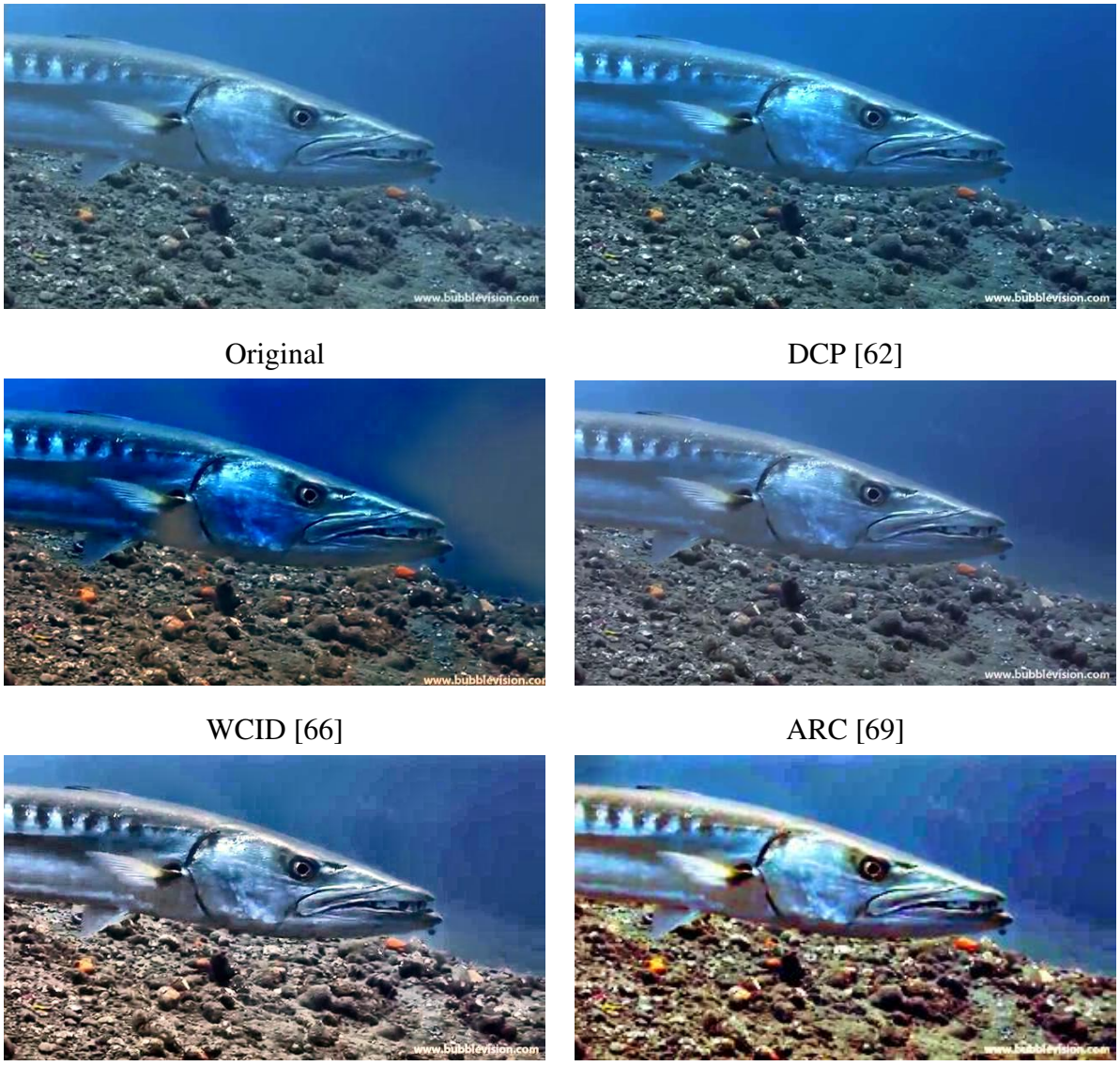

Figure 5.5: Results of fish image using state-of-the-art techniques and FUIER. Images are in this order: first row: original image, results using DCP, second row: results using WCID, results using ARC, third row: results using the Ancuti *et al.* technique and FUIER

Original DCP [62]

WCID [66] ARC [69]

Ancuti *et al.* [48] FUIER

Figure 5.6: Results of corals image using state-of-the-art techniques and FUIER. Images are in this order: first row: original image, results using DCP, second row: results using WCID, results using ARC, third row: results using the Ancuti *et al.* technique and FUIER

Original

DCP [62]

WCID [66]

ARC [69]

Ancuti *et al.* [48]

FUIER

Figure 5.7: Results of diver with rocks image using the state-of-the-art techniques and FUIER. Images are in this order: first row: original image, results using DCP, second row: results using WCID, results using ARC, third row: results using the Ancuti *et al.* technique and FUIER

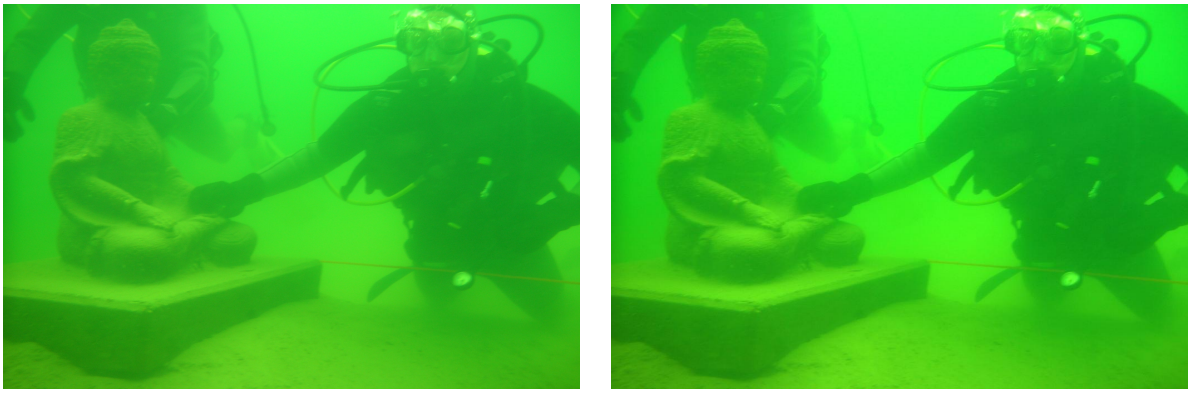

Original DCP [62]

WCID [66] ARC [69]

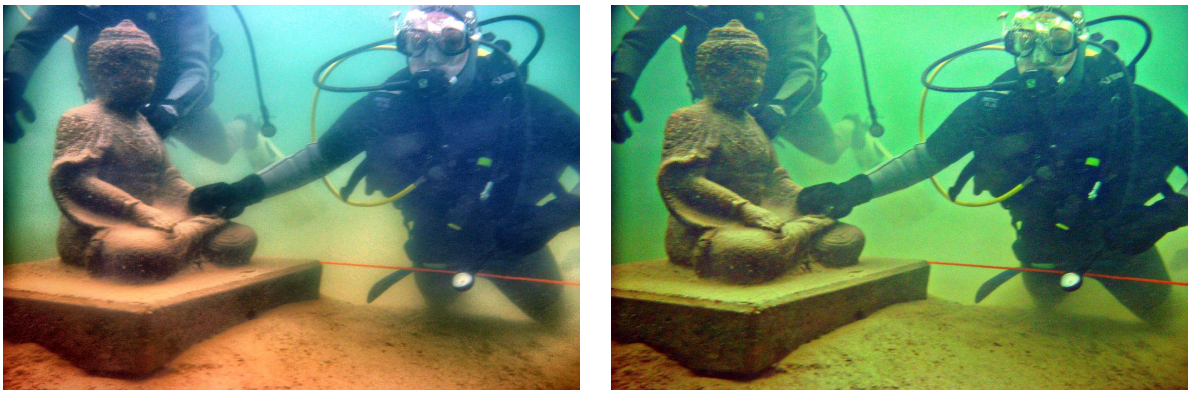

Ancuti *et al.* [48] FUIER

Figure 5.8: Results of diver image using the state-of-the-art techniques and FUIER. Images are in this order: first row: original image, results using DCP, second row: results using WCID, results using ARC, third row: results using the Ancuti *et al.* technique and FUIER

Original DCP [62]

WCID [66] ARC [69]

Ancuti *et al.* [48] FUIER

Figure 5.9: Results of sea walker image using state-of-the-art techniques and FUIER. Images are in this order: first row: original image, results using DCP, second row: results using WCID, results using ARC, third row: results using the Ancuti *et al.* technique and FUIER

Original DCP [62]

WCID [66] ARC [69]

Ancuti *et al.* [48] FUIER

Figure 5.10: Results of fishes image using state-of-the-art techniques and FUIER. Images are in this order: first row: original image, results using DCP, second row: results using WCID, results using ARC, third row: results using the Ancuti *et al.* technique and FUIER

enhancing information content of the image better than other techniques which can be seen in the results, For example, In Fig. 5.5, details of fish and terrain below it are clearer in the FUIER fish image than in the results of other techniques and in Fig. 5.6 image, details of the corals in result of the FUIER are better than in other results. DCP and WCID, on the other hand, sometimes reducing the entropy values of a few images, For example, Diver with rocks (Fig, 5.7) and sea walker image (Fig. 5.9). ARC is enhancing the information content but not as much as Ancuti *et al.* technique and FUIER. The Ancuti *et al.* technique is giving the second best entropy values for most of the images.

Difference (Δ) [81]: FUIER has the best values for this performance metric for almost all the images which mean there is a balance of colors, i.e., three color channels are averaging to a same gray value. The Ancuti *et al.* technique and ARC are also performing well in terms of this performance measure. DCP and WCID, however, are creating a imbalance in colors by increasing the value of this performance metric for some images. For instance, in Fig. 5.7, WCID has introduced false colors and in Fig. 5.6, DCP and WCID image has increased the blue color in the background.

Histogram Spread (HS) [80]: Histogram spread indicates the contrast performance of an image, i.e., if histogram spreads over the whole dynamic range uniformly. FUIER gives the best results for almost all images for this performance measure also. It can be proven from the visual results also that FUIER gives results with improved contrast. The Ancuti *et al.* technique performs well in terms of contrast but not better than FUIER, e.g., the result of Fig. 5.5 using the Ancuti *et al.* technique has poor contrast as compared to the result of FUIER. However, DCP, WCID and ARC lag in terms of contrast for most of the images which can be seen from the results also as the contrast of the images are not improving to a great extent.

UIQM [91]: FUIER always gives results with increased UIQM value. For some images, it gives the best values. From the results, it can be seen that FUIER increases the overall quality of the image by improving the color, contrast and sharpness of the image. DCP is able to improve only the sharpness of the image. WCID, on the other hand, improves the color, contrast and sharpness for few images for example, images shown in Fig. 5.5, 5.6 and 5.10, but it distorts the colors of few

Table 5.1: Value of non-reference based performance metric for the images shown in Fig. 5.5 - 5.9

Metric	Technique	Fish	Corals	Diver	Diver with rocks	Sea Walker	Fishes
Entropy [24]	Original	7.303	7.347	6.711	6.634	7.184	7.481
	DCP [62]	7.475	7.660	6.636	6.625	6.897	7.344
	WCID [66]	7.483	7.368	7.050	6.488	7.522	7.569
	ARC [69]	7.304	7.521	7.696	7.265	7.249	7.549
	Ancuti [48]	7.687	7.786	7.679	7.267	7.717	7.621
	FUIER	**7.730**	**7.920**	**7.745**	**7.584**	**7.783**	**7.848**
Δ [81]	Original	41.99	14.78	97.80	103.34	45.84	80.86
	DCP [62]	51.47	31.56	108.05	103.36	25.23	87.89
	WCID [66]	33.51	26.22	31.93	148.44	35.05	44.04
	ARC [69]	31.01	18.65	40.67	68.73	22.88	**11.45**
	Ancuti [48]	19.95	19.32	**9.06**	84.19	14.42	20.95
	FUIER	**19.06**	**10.31**	31.18	**44.01**	**14.02**	20.72
HS* [80]	Original	0.1680	0.2500	0.1554	0.1180	0.2333	0.3106
	DCP [62]	0.1908	0.2286	0.1558	0.1317	0.2780	0.3232
	WCID [66]	0.2118	0.2461	0.2434	0.0777	0.2731	0.2921
	ARC [69]	0.1725	0.2431	0.1880	0.1664	0.2397	0.3500
	Ancuti [48]	0.2967	0.3072	**0.3725**	0.2726	**0.3673**	0.3356
	FUIER	**0.3464**	**0.4052**	0.3548	**0.3020**	0.3373	**0.4747**
UIQM [91]	Original	3.362	4.538	3.559	1.512	3.491	1.455
	DCP [62]	3.462	**5.268**	3.559	1.342	4.059	0.646
	WCID [66]	**4.312**	4.485	3.575	1.716	4.025	3.084
	ARC [69]	3.512	4.693	4.205	2.385	3.537	**5.034**
	Ancuti [48]	3.812	5.029	**4.833**	3.287	4.712	4.129
	FUIER	3.901	4.717	4.820	**4.566**	**4.887**	3.761
UCIQE [116]	Original	5.189	7.367	1.466	2.929	3.257	7.380
	DCP [62]	7.595	11.298	1.264	2.766	5.388	6.958
	WCID [66]	**12.306**	10.471	5.647	**6.007**	**5.845**	8.408
	ARC [69]	5.635	7.142	3.660	5.020	3.597	10.765
	Ancuti [48]	7.486	9.732	**10.237**	5.716	5.195	3.290
	FUIER	9.482	**11.310**	9.421	4.623	3.938	**13.621**

**HS stands for Histogram Spread*

images like those shown in Fig. 5.7, 5.8 and 5.9. Contrast and sharpness of ARC images, except for the image shown in Fig. 5.5 are not better than the results of the Ancuti *et al.* technique and FUIER, resulting in lower UIQM values than the latter two. In terms of average UIQM values, the Ancuti *et al.* technique is giving the best and FUIER is giving the second best results, but from visual results, it can be seen that sharpness and brightness of results of FUIER are better than the results of the Ancuti *et al.* technique.

UCIQE [116]: From Table 5.2, it can be seen that FUIER again performs better than all the other techniques. WCID is performing well in terms of this performance metric as it removes the blur effectively but lags in terms of other performance measures leading to poor visual results. ARC and the Ancuti *et al.* technique also perform well, but it can be seen from the visual results as well as the overall values of quantitative measures that FUIER delivers visually appealing results as compared to other techniques.

Execution Time: From Table 5.2, it is clear that average execution time is in the following increasing order, DCP, ARC, FUIER, Ancuti *et al.* technique, WCID. Thus, DCP takes the least time but it is not suitable for underwater images. WCID does not produce good results and has the highest average execution time. Out of ARC, FUIER and Ancuti *et al.* technique, ARC is the best in terms of execution time but does not produce very good quality images as discussed earlier. There is very little difference in the average execution time of ARC and FUIER. Thus, we can say that FUIER gives good quality results with lesser time complexity as compared to all other state-of-the-art techniques.

As mentioned earlier, there are two datasets for underwater images i.e. WHOI dataset [93] and TURBID dataset [92], so for further comparison of FUIER with state-of-the-art methods, we have shown a few images from these databases in Fig. 5.11 and Fig. 5.12. Table 5.3 gives the value of reference based PSNR(Peak Signal to Noise Ratio) and MSE(Mean Squared Error) along with the non-reference based performance metric values for these images. PSNR should be higher and MSE should be lower for a better image.

From the table values, it can be seen that FUIER has the best PSNR and MSE values among all

Table 5.2: Average Value of performance metrics and execution time for 200 underwater images for comparison of FUIER and state-of-the-art techniques

Technique	**Entropy** [24]	Δ [81]	**HS** [80]	**UIQM** [91]	**UCIQE** [116]	**Time (in sec)**
Original	6.970	47.04	0.1867	3.750	4.059	-
DCP [62]	6.928	50.46	0.1844	3.750	4.954	**0.078**
WCID [66]	6.965	43.05	0.2183	3.760	7.199	4.19
ARC [69]	6.994	24.63	0.1996	4.3228	5.885	0.94
Ancuti [48]	7.671	19.34	0.3240	**4.690**	7.441	1.89
FUIER	**7.774**	**16.90**	**0.3552**	4.648	**7.923**	1.07

techniques. Visual results of FUIER and the Ancuti *et al.* technique have better information content and are more appealing as compared to other techniques which is also proven by the performance measure values. However, the Ancuti *et al.* technique is not performing consistently for every type of image. It is not improving contrast of few images (e.g., fishes image., (Fig.5.10)) and not able to remove haze properly for few other images (e.g., corals image (Fig.5.6)). From quantitative and qualitative analysis, we can say that FUIER performs well for underwater images captured in different conditions (turbidity, depth, salinity etc.) using computationally less intensive approach, as proven by the average execution time.

For a more exhaustive comparison, comparative analysis has been done with a CNN based technique [7]. A few images along with the results have been taken from the article [7] and are shown along with the results of FUIER in Fig. 5.13. The values of various performance metrics of the images are depicted in table 5.4.

It is clear from the images shown in Fig. 5.13 that the CNN based technique [7] produces good results but the contrast is poor whereas FUIER produces better images with more clarity.

In terms of quantitative measures, Entropy, HS and UCIQE values of FUIER are always better than for the CNN based technique [7]. This means information content, contrast and blurriness of

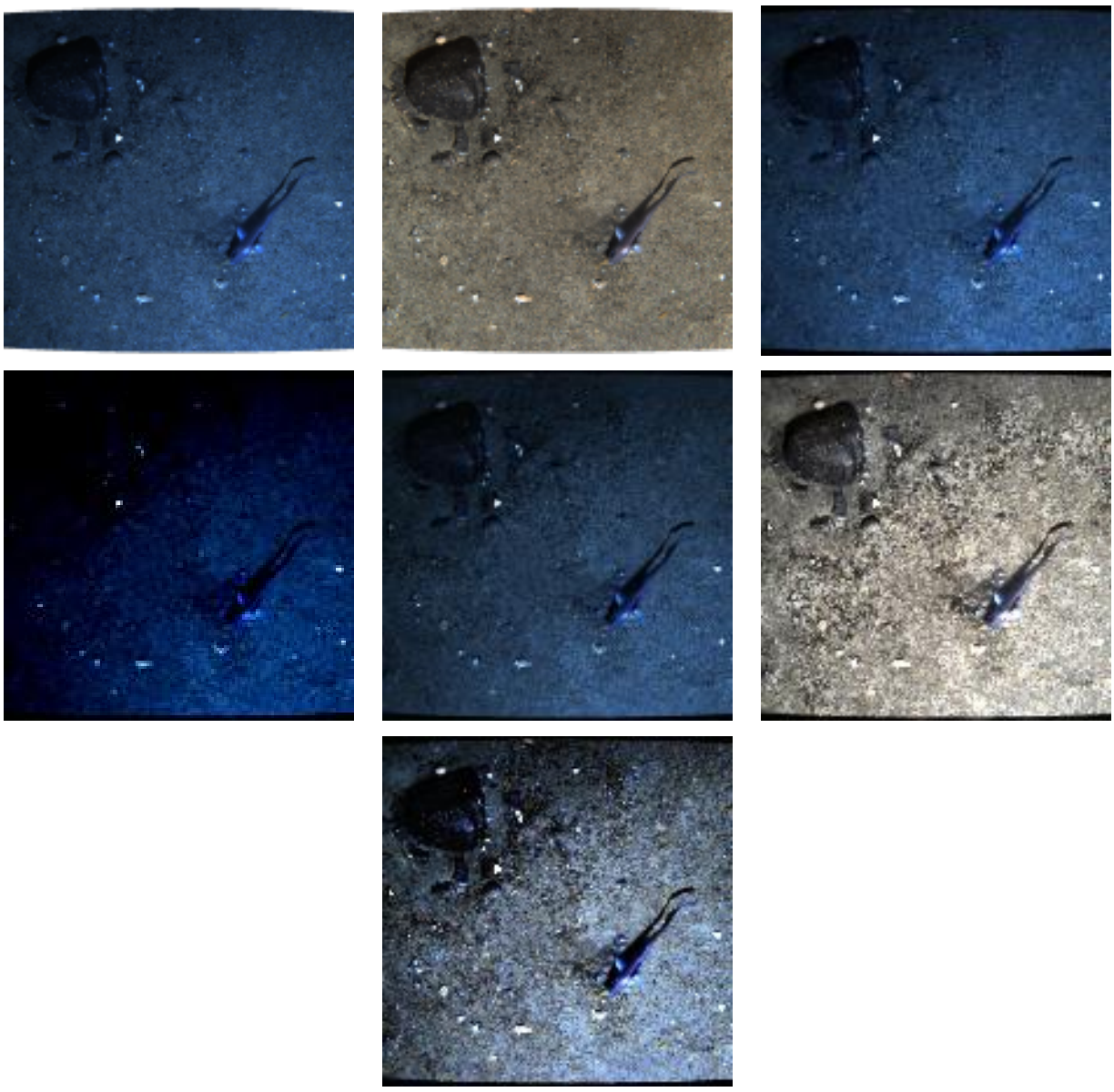

(a) Image1 From WHOI [93]

Figure 5.11: Results of image 1 using the state-of-the-art techniques and FUIER. For each type of image, images are in this order : first row: original image, results using DCP, results using WCID, , second row: results using ARC and Ancuti *et al.* technique and third row: results using FUIER.

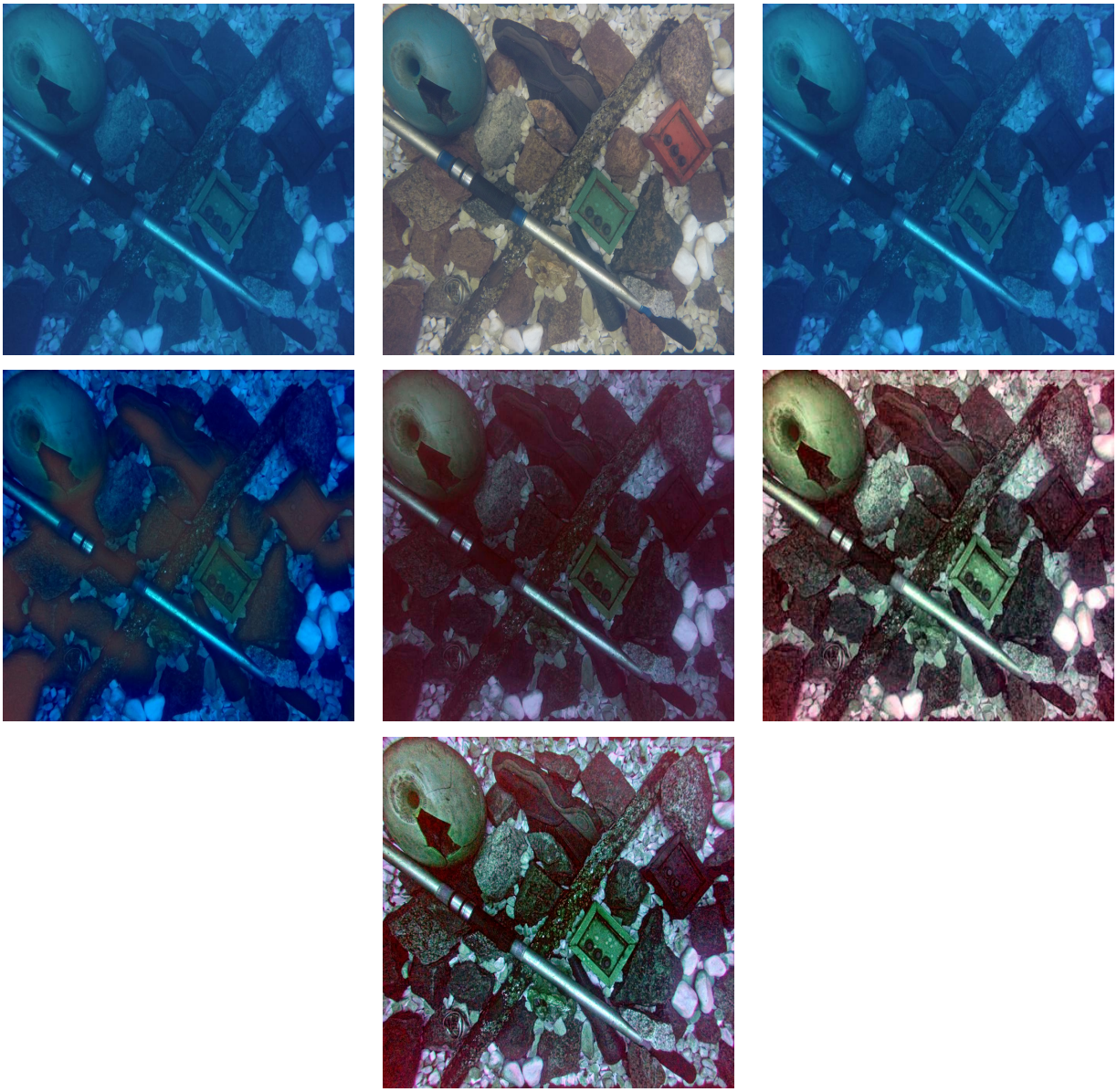

(a) Image2 From TURBID dataset [92]

Figure 5.12: Results of image 2 using the state-of-the-art techniques and FUIER. For each type of image, images are in this order : first row: original image, results using DCP, results using WCID, , second row: results using ARC and Ancuti *et al.* technique and third row: results using FUIER.

Table 5.3: Value of reference based performance metrics for images shown in Fig. 5.11 and Fig. 5.12

Image	**Technique**	**PSNR**	**MSE**	**Entropy**	**Δ**	**HS**	**UIQM**	**UCIQE**
Image1	Original	-	-	5.911	26.68	0.1244	3.383	0.352
	Reference	-	-	6.798	8.943	0.1404	4.971	1.009
	DCP [62]	14.42	2349.6	7.295	30.69	0.1493	4.4018	1.179
	WCID [66]	10.62	6129.1	6.852	27.89	0.1242	2.176	**3.438**
	ARC [69]	13.85	2676.4	7.034	20.93	0.1423	4.388	0.831
	Ancuti [48]	13.92	2635.3	7.780	**5.57**	0.3124	**5.372**	2.516
	FUIER	**16.48**	**1461.6**	**7.809**	14.59	**0.3360**	4.655	1.211
Image2	Original	-	-	5.157	52.12	0.1832	2.786	0.6711
	Reference	-	-	6.807	**3.29**	0.2066	4.430	4.056
	DCP [62]	12.89	3339.3	6.678	55.60	0.1775	4.270	3.207
	WCID [66]	10.52	5772	6.762	42.09	0.1528	4.171	7.216
	ARC [69]	13.24	3080.8	6.610	12.52	0.1632	4.984	3.522
	Ancuti [48]	15.53	1820	7.670	6.36	**0.3320**	**5.143**	7.480
	FUIER	**15.76**	**1724.3**	**7.689**	4.51	0.3216	5.020	**9.803**

Table 5.4: Value of performance metrics for images shown in Fig. 5.13

Image	Technique	Entropy	Δ	HS	UIQM	UCIQE
Rocks	**Original**	3.73	10.35	0.0365	4.56	1.49
	CNN based [7]	6.14	**4.23**	0.1232	**5.08**	0.79
	FUIER	**7.12**	5.72	**0.2615**	5.04	**4.43**
Medium	**Original**	4.93	15.00	0.093	4.95	0.27
	CNN based [7]	6.37	**1.50**	0.1475	5.28	0.33
	FUIER	**7.44**	4.05	**0.3211**	**5.86**	**1.78**
Shallow	**Original**	4.30	10.13	0.1455	2.70	1.01
	CNN based [7]	5.56	**1.24**	0.1589	3.39	0.48
	FUIER	**7.73**	2.19	**0.3699**	**4.66**	**5.71**

the image are improved better in images obtained using FUIER. UIQM values of the CNN based technique [7] are better for a few images but again FUIER outperforms it for most of the images. Both the CNN based technique [7] and FUIER lower the Δ values close to zero but gray world assumption is being followed more closely by the results of the former. CNN based technique [7] has tested various types of underwater images (sands, rocks, kelp [7]) taken at different depths (shallow, medium and deep corals [7]). FUIER gives good results for all of them. CNN requires training for adjusting the parameters of image restoration techniques whereas FUIER requires no parameter adjustment or training. Therefore, FUIER is suitable for all types of underwater images.

5.4.3 Applications

FUIER finds its applicability in the following computer vision related fields:

Local Feature Matching:One of the basic tasks of computer vision algorithms is local feature points matching, which forms the basis for underwater studies like classification of marine animals,

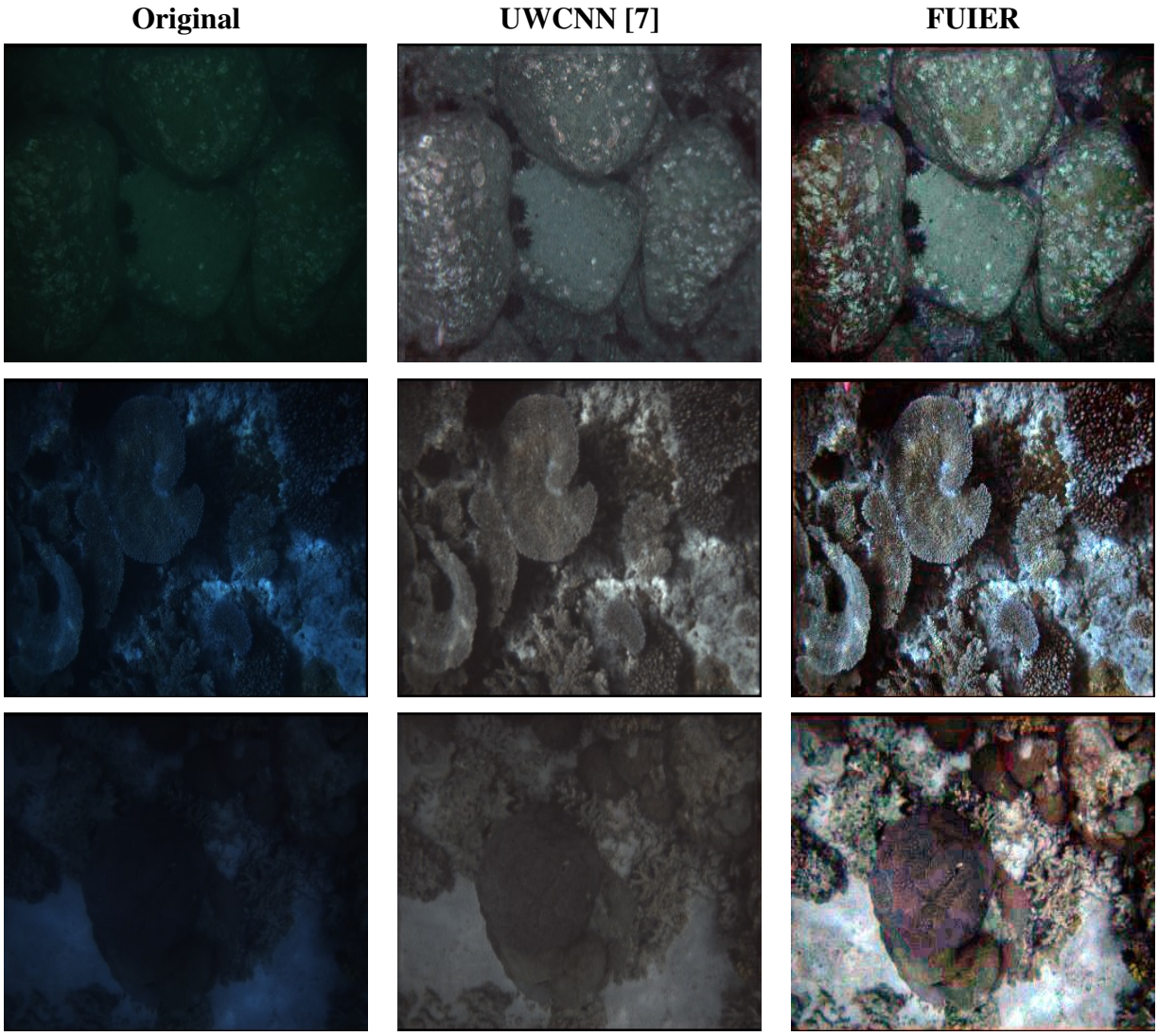

Figure 5.13: Results of images first row: Rocks, second row: Medium and third row: Shallow; taken from [7] and results using FUIER.

fish species recognition etc. Local features are indifferent to rotation, scaling and motion changes. We have employed SURF [117] operator to compute and match feature blobs for a pair of underwater images and repeated the same process for the enhanced versions of the corresponding pair of images. We used the SURF feature matching provided by MATLAB. We enhanced the pair of images using the Ancuti *et al.* [48] technique results and FUIER. The results are very promising which shows that the number of local feature points increase significantly by FUIER as compared to Ancuti *et al.* [48] and are shown in Fig. 5.14 and Fig. 5.15.

Edge Detection: Edge detection is an important processing task in image processing which further assists in various fields of computer vision related to underwater studies like segmentation in order to localize coral reefs. We have employed Laplacian of Gaussian (LoG) [121] to find the edges in the images. Edge detection results of the original image and enhanced images using Ancuti *et al.* technique and FUIER are shown in Fig. 5.16. It is clear from these results that both FUIER and the Ancuti *et al.* technique generate enhanced images with more edges as compared to the original image. However, images of FUIER have more edge pixel count than the Ancuti *et al.* technique [48] for most of the images.

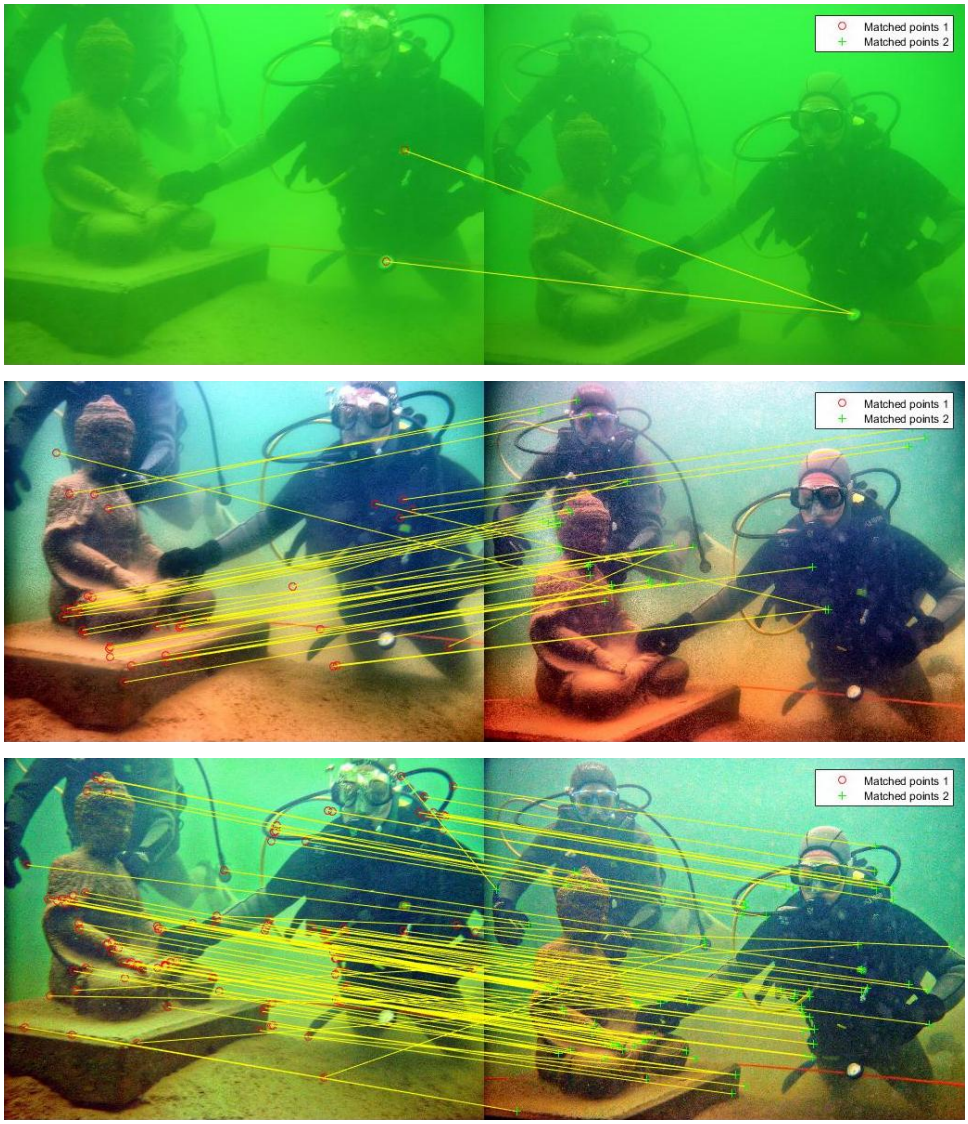

Figure 5.14: First row contains the original pair of images with only 2 SURF features are matching, second row contains the enhanced pair of images using the Ancuti *et al.*. technique with 37 SURF features are matching and third row contains the enhanced pair of images using FUIER with 104 SURF features are matching.

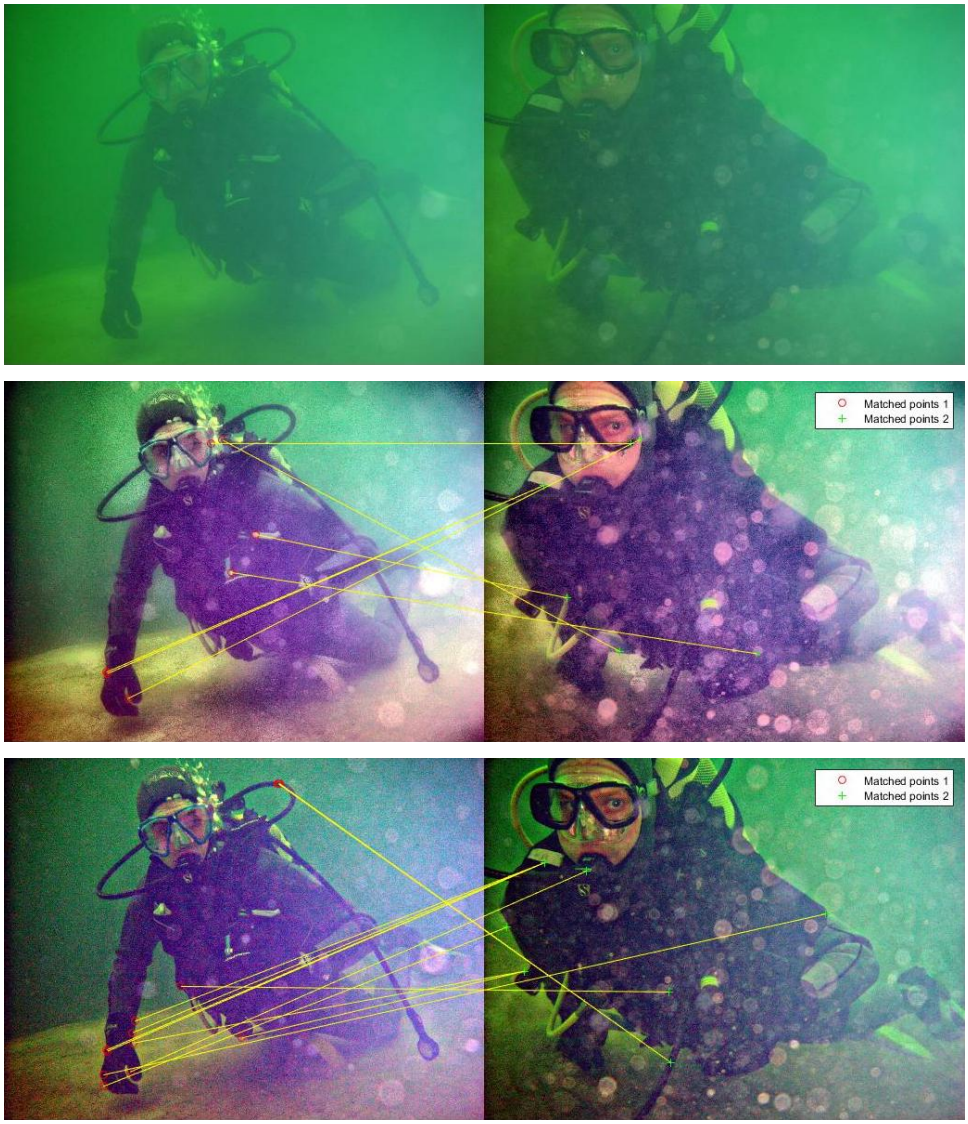

Figure 5.15: First row contains the original pair of images with no SURF features are matching, second row contains the enhanced pair of images using the Ancuti *et al.*. technique with 7 SURF features and third row contains the enhanced pair of images using FUIER with 13 SURF features are matching.

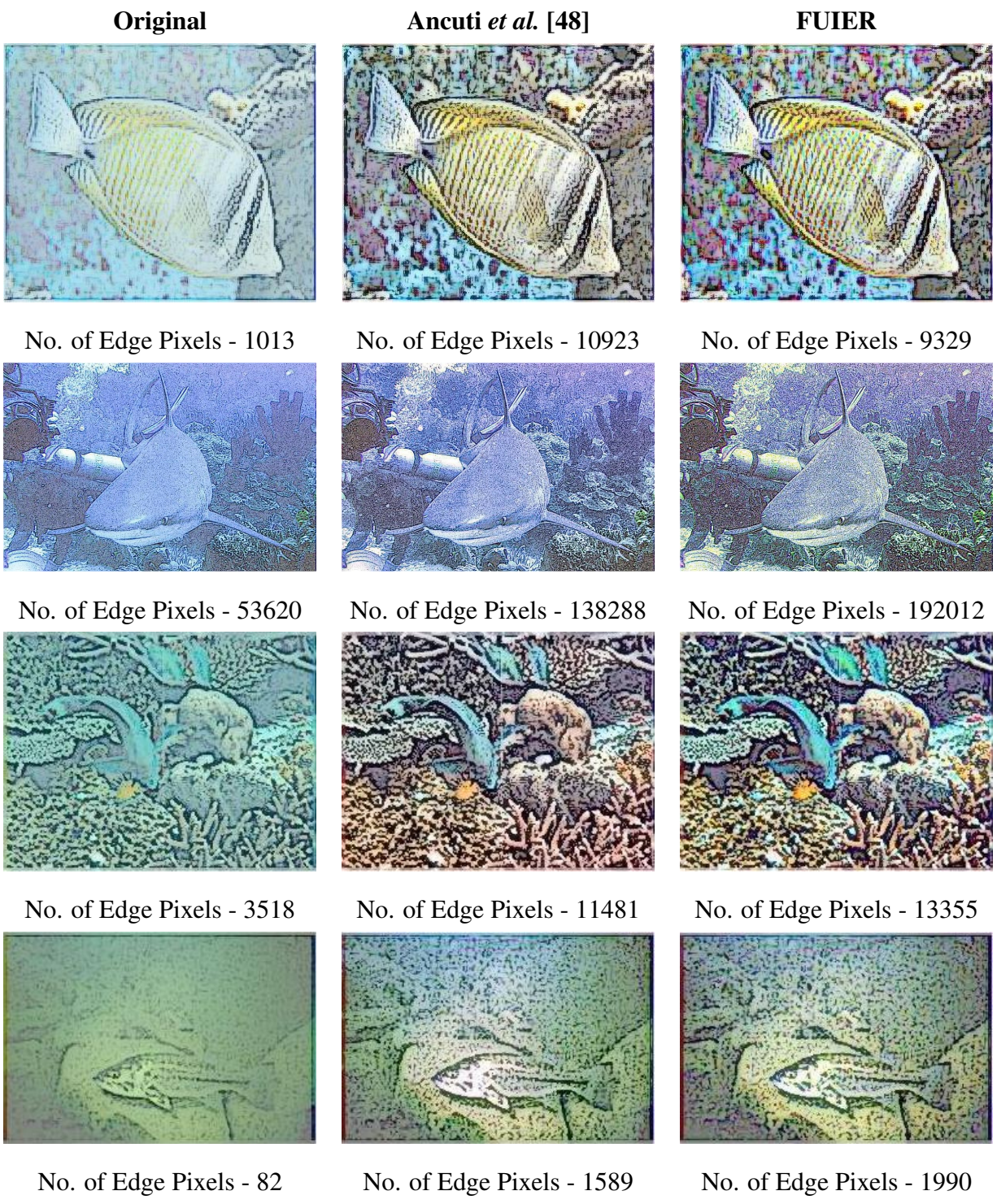

Figure 5.16: Different images blended with their edge detection results and the number of edge pixels found using Ancuti *et al.* technique and FUIER.

5.5 Conclusions

In this chapter, a fusion of underwater image enhancement and restoration has been presented. FUIER is a simple yet powerful method for improving the visual quality of every type of underwater image. Simple and basic techniques like HE, contrast stretching and DCP have been employed but with effective and meaningful weight maps so that the required features are taken and fused to derive resultant image. The resultant image has improved color, contrast and visibility. The advantage of FUIER is that it incorporates color correction, contrast correction and dehazing into two versions and takes essential features based on weights so as to generate an enhanced output image. All the major issues in underwater images have been handled using simple and computationally less intensive techniques employed in FUIER. The results of FUIER are visually appealing and better as compared to state-of-the-art techniques and are easily applicable in many computer vision algorithms. However, FUIER lags, in terms of color reproduction when there is deep haze in the underwater images. The future scope may include an attempt to tackle this problem.

Chapter 6

Conclusions and Future work

In this thesis, we formulated algorithms for enhancement and restoration of the underwater images so as to make them suitable for the purpose of various scientific studies like coral life monitoring, aquatic species survey etc.

These algorithms have been compared with state-of-the-art techniques and have given significant results for different non-reference based performance metrics (entropy, histogram spread, difference, UCIQE, UICM, UIQM) for all the techniques being compared. We performed enhancement of underwater images using these algorithms and then compared the values of performance measures. Proposed methods have given enhanced images not only in terms of the visual appearance but also in terms of the quantitative measures.

6.1 Summary of the work done in the thesis

To address the problem of color cast and information loss while capturing underwater images, we devised an algorithm called 'Contrast and Information Enhancement of Underwater Images' (CIEUI) which finds the color cast in underwater images captured in different water bodies using fuzzy rules and removes that color cast using a non-linear gray world based algorithm. Factors

which add non-linearity have been found using MOPSO. The algorithm gives good results for most of the images but has slow execution time due to MOPSO. Moreover, it produces artifacts for images with artificial lighting.

Thus, to address the artifacts caused by artificial lighting in CIEUI, we proposed an algorithm named 'Fuzzified Color and Contrast Correction (FCCC)' in which we refined the fuzzy gray world algorithm to type-II fuzzy algorithm and instead of using global enhancement, applied color correction on local level by applying it on segments and similarly applied contrast correction on local level by using CLAHE. Finally the features are color and contrast corrected images are fused using wavelet based fusion using appropriate weight maps which capture the required features in the resultant image. Now, the problem of artifacts in artificial lit underwater images was resolved but the hazy appearance in the underwater images is still present in results of FCCC.

Lastly, we developed a simple fusion based algorithm named 'Fusion of Underwater Image Enhancement and Restoration (FUIER)' which fuses the histogram equalized version (color corrected) and contrast stretched dehazed version which uses the simple dark channel prior so as to reduce the computational complexity of the algorithm. All the three major problems of underwater images i.e. color cast, poor contrast and haze are addressed and furthermore, FUIER gives good results for every type of underwater image whether captured at shallow, medium or deep depths.

6.2 Contributions

Underwater images are instrumental in understanding the world beneath water. The work in the thesis helps in pre-processing the images for the scientific studies. Following are the contributions of the thesis:

- We formulated fuzzy gray world based algorithm for finding the color cast in the underwater images. The proposed method enhances the images captured in different types of underwater

media.

- We developed a method which removes all the major issues i.e. color cast, poor contrast and hazy appearance of underwater images.
- We created appropriate weight maps for extracting required information from the underwater images.
- We developed a local enhancement method which handles the non-uniform illumination in underwater images.

6.2.1 Future Scope

1. Creating a database for underwater images which covers all types of underwater images captured in different turbidity, depth, salinity.
2. Handling the images with deep haze more effectively.
3. Enhancing the underwater images in real time.

Publications Related to the Thesis

Papers Published/Accepted for Publication

Journal papers

1. **Rajni Sethi**, and Indu Sreedevi. "Fusion of Underwater Image Enhancement and Restoration" International Journal of Pattern Recognition and Artificial Intelligence [SCIE] (2019) doi:10.1142/S0218001420540075.

2. **Rajni Sethi**, and Indu Sreedevi "Adaptive Enhancement of Underwater Images using Multi-objective PSO", Multimedia Tools and Applications (Springer) [SCIE] (2019) doi:10.1007/s11042-019-07938-x.

Conference Papers

1. **Rajni Sethi**, I. Sreedevi, O. P. Verma and V. Jain, "An optimal underwater image enhancement based on fuzzy gray world algorithm and Bacterial Foraging algorithm," 2015 Fifth National Conference on Computer Vision, Pattern Recognition, Image Processing and Graphics (NCVPRIPG), Patna, 2015, pp. 1-4. doi:10.1109/NCVPRIPG.2015.7490004

2. **Rajni Sethi** and I. Sreedevi, "Local Enhancement of SLIC Segmented Underwater Images using Gray World based Algorithm," 2017 Ninth International Conference on Advances in

Pattern Recognition (ICAPR), Bangalore, 2017, pp. 1-6. doi: 10.1109/ICAPR.2017.8593151

Papers Communicated to Journals/In Review

1. ”Fuzzified Color and Contrast Correction of Underwater Images” a paper communicated to The Visual Computers (Springer) journal for publication.

Bibliography

[1] J. F. Anthoni, "Water and light in underwater photography," www.seafriends.org.nz/phgraph/water.htm, 2005.

[2] A. S. Abdul Ghani and N. A. Mat Isa, "Automatic system for improving underwater image contrast and color through recursive adaptive histogram modification," *Comput. Electron. Agric.*, vol. 141, no. C, pp. 181–195, Sep. 2017. [Online]. Available: https://doi.org/10.1016/j.compag.2017.07.021

[3] D. Garg, N. K. Garg, and M. Kumar, "Underwater image enhancement using blending of clahe and percentile methodologies," *Multimedia Tools and Applications*, vol. 77, no. 20, pp. 26 545–26 561, Oct 2018. [Online]. Available: https://doi.org/10.1007/s11042-018-5878-8

[4] G. D. Finlayson and E. Trezzi, "Shades of gray and colour constancy," in *Color and Imaging Conference*, vol. 2004, no. 1. Society for Imaging Science and Technology, 2004, pp. 37–41.

[5] J. Van De Weijer, T. Gevers, and A. Gijsenij, "Edge-based color constancy," *IEEE Transactions on image processing*, vol. 16, no. 9, pp. 2207–2214, 2007.

[6] A. Gijsenij and T. Gevers, "Color constancy using natural image statistics and scene semantics," *IEEE Transactions on Pattern Analysis and Machine Intelligence*, vol. 33, no. 4, pp. 687–698, 2011.

[7] Y. Wang, J. Zhang, Y. Cao, and Z. Wang, "A deep cnn method for underwater image enhancement," in *2017 IEEE International Conference on Image Processing (ICIP)*, Sept 2017, pp. 1382–1386.

[8] R. Sethi, I. Sreedevi, O. Verma, and V. Jain, "An optimal underwater image enhancement based on fuzzy gray world algorithm and bacterial foraging algorithm," in *2015 Fifth National Conference on Computer Vision, Pattern Recognition, Image Processing and Graphics (NCVPRIPG)*. IEEE, 2015, pp. 1–4.

[9] Z. Willis, "Chapter 2 - national ocean observing systems in a global context," in *Coastal Ocean Observing Systems*, Y. Liu, H. Kerkering, and R. H. Weisberg, Eds. Boston: Academic Press, 2015, pp. 11 – 25. [Online]. Available: http://www.sciencedirect.com/science/article/pii/B978012802022700002X

[10] W. E. Watson, S. R. Benson, and J. T. Harvey, "An application of underwater imaging for marine vertebrate ecology," in *OCEANS 2010 MTS*, Seattle, USA, Sept 2010, pp. 1–6.

[11] L. A. Torres-Méndez and G. Dudek, "Color correction of underwater images for aquatic robot inspection," in *Energy Minimization Methods in Computer Vision and Pattern Recognition*, A. Rangarajan, B. Vemuri, and A. L. Yuille, Eds. Berlin, Heidelberg: Springer Berlin Heidelberg, 2005, pp. 60–73.

[12] D. R. Yoerger, A. M. Bradley, B. B. Walden, M. H. Cormier, and W. B. F. Ryan, "Fine-scale seafloor survey in rugged deep-ocean terrain with an autonomous robot," in *Proceedings 2000 ICRA. Millennium Conference. IEEE International Conference on Robotics and Automation. Symposia Proceedings (Cat. No.00CH37065)*, vol. 2, 2000, pp. 1787–1792 vol.2.

[13] H. Qin, X. Li, J. Liang, Y. Peng, and C. Zhang, "DeepFish: Accurate underwater live fish recognition with a deep architecture," *Neurocomputing*, 2016.

[14] B. N. White, C. R. Booth, and J. H. Morrow, "Detecting substances in drinking water reservoirs," Oct. 10 2006, uS Patent 7,119,891.

[15] A. Ortiz, M. Simó, and G. Oliver, "Image sequence analysis for real-time underwater cable tracking," in *Proceedings Fifth IEEE Workshop on Applications of Computer Vision*. IEEE, 2000, pp. 230–236.

[16] R. Garcia, T. Nicosevici, and X. Cufí, "On the way to solve lighting problems in underwater imaging," in *OCEANS'02 MTS/IEEE*, vol. 2. IEEE, 2002, pp. 1018–1024.

[17] C. Funk, S. Bryant, and P. Heckman Jr, "Handbook of underwater imaging system design," NAVAL UNDERSEA CENTER SAN DIEGO CA, Tech. Rep., 1972.

[18] R. Schettini and S. Corchs, "Underwater image processing: state of the art of restoration and image enhancement methods," *EURASIP Journal on Advances in Signal Processing*, vol. 2010, p. 14, 2010.

[19] L. A. Torres-Méndez and G. Dudek, "Color correction of underwater images for aquatic robot inspection," in *International Workshop on Energy Minimization Methods in Computer Vision and Pattern Recognition*. Springer, 2005, pp. 60–73.

[20] B. McGlamery, "A computer model for underwater camera systems," in *Ocean Optics VI*, vol. 208. International Society for Optics and Photonics, 1980, pp. 221–232.

[21] J. S. Jaffe, "Computer modeling and the design of optimal underwater imaging systems," *Oceanic Engineering, IEEE Journal of*, 1990.

[22] J. Ott, "Concepts of underwater experimentation," *Helgoländer wissenschaftliche Meeresuntersuchungen*, vol. 24, no. 1, p. 54, 1973.

[23] R. B. Wynn, V. A. Huvenne, T. P. L. Bas, B. J. Murton, D. P. Connelly, B. J. Bett, H. A. Ruhl, K. J. Morris, J. Peakall, D. R. Parsons, E. J. Sumner, S. E. Darby, R. M.

Dorrell, and J. E. Hunt, "Autonomous underwater vehicles (auvs): Their past, present and future contributions to the advancement of marine geoscience," *Marine Geology*, vol. 352, pp. 451 – 468, 2014, 50th Anniversary Special Issue. [Online]. Available: http://www.sciencedirect.com/science/article/pii/S0025322714000747

[24] R. C. Gonzalez and R. E. Woods, *Digital Image Processing (3rd Edition)*. Upper Saddle River, NJ, USA: Prentice-Hall, Inc., 2006.

[25] R. Dale-Jones and T. Tjahjadi, "A study and modification of the local histogram equalization algorithm," *Pattern Recognition*, vol. 26, no. 9, pp. 1373 – 1381, 1993. [Online]. Available: http://www.sciencedirect.com/science/article/pii/003132039390143K

[26] K. Iqbal, R. A. Salam, A. Osman, and A. Z. Talib, "Underwater Image Enhancement Using an Integrated Colour Model," *International Journal of Computer Science*, vol. 34, no. 2, pp. 239–244, 2007.

[27] M. S. Hitam, E. A. Awalludin, W. N. Jawahir Hj Wan Yussof, and Z. Bachok, "Mixture contrast limited adaptive histogram equalization for underwater image enhancement," *International Conference on Computer Applications Technology, ICCAT 2013*, 2013.

[28] A. S. A. Ghani and N. A. M. Isa, "Underwater image quality enhancement through rayleigh-stretching and averaging image planes," *International Journal of Naval Architecture and Ocean Engineering*, vol. 6, no. 4, pp. 840 – 866, 2014. [Online]. Available: http://www.sciencedirect.com/science/article/pii/S2092678216302588

[29] K. Srividhya and M. Ramya, "Fuzzy based adaptive contrast enhancement of underwater images," *Res J Inf Technol*, vol. 8, pp. 29–38, 2016.

[30] J. Ma, X. Fan, S. X. Yang, X. Zhang, and X. Zhu, "Contrast limited adaptive histogram equalization-based fusion in yiq and hsi color spaces for underwater image enhancement,"

International Journal of Pattern Recognition and Artificial Intelligence, vol. 32, no. 07, p. 1854018, 2018.

[31] Y. Fan, S. Wang, T. Yu, and B. L. Hu, "Underwater image enhancement algorithm based on rgb channels histogram equalization," in *Optical Sensing and Imaging Technologies and Applications*, vol. 10846. International Society for Optics and Photonics, 2018, p. 108460G.

[32] P. Mathur, K. Monica, and B. Soni, "Improved fusion-based technique for underwater image enhancement," in *2018 4th International Conference on Computing Communication and Automation (ICCCA)*, Dec 2018, pp. 1–6.

[33] G. Buchsbaum, "A spatial processor model for object colour perception," *Journal of the Franklin Institute*, vol. 310, no. 1, pp. 1–26, jul 1980. [Online]. Available: https://www.sciencedirect.com/science/article/pii/0016003280900587

[34] V. C. Cardei and B. Funt, "Committee-based color constancy," in *Color and Imaging Conference*, vol. 1999, no. 1. Society for Imaging Science and Technology, 1999, pp. 311–313.

[35] E. H. Land, "The retinex theory of color vision," *Scientific American*, vol. 237, no. 6, pp. 108–129, 1977.

[36] G. Bianco, M. Muzzupappa, F. Bruno, R. Garcia, and L. Neumann, "A new color correction method for underwater imaging," *The International Archives of Photogrammetry, Remote Sensing and Spatial Information Sciences*, vol. 40, no. 5, p. 25, 2015.

[37] M. Chambah, D. Semani, A. Renouf, P. Courtellemont, and A. Rizzi, "Underwater color constancy: enhancement of automatic live fish recognition," in *Electronic Imaging 2004*. International Society for Optics and Photonics, 2003, pp. 157–168.

[38] A. Rizzi, C. Gatta, and D. Marini, "From retinex to automatic color equalization: issues in developing a new algorithm for unsupervised color equalization," *Journal of Electronic Imaging*, vol. 13, no. 1, pp. 75–84, 2004.

[39] A. T. Çelebi and S. Ertürk, "Visual enhancement of underwater images using empirical mode decomposition," *Expert Systems with Applications*, vol. 39, no. 1, pp. 800 – 805, 2012. [Online]. Available: http://www.sciencedirect.com/science/article/pii/S0957417411010396

[40] X. Fu, P. Zhuang, Y. Huang, Y. Liao, X. Zhang, and X. Ding, "A retinex-based enhancing approach for single underwater image," in *2014 IEEE International Conference on Image Processing (ICIP)*, Oct 2014, pp. 4572–4576.

[41] G. Hou, Z. Pan, B. Huang, G. , and X. Luan, "Hue preserving-based approach for underwater colour image enhancement," *IET Image Processing*, vol. 12, no. 2, 2017.

[42] H. H. kareem, H. G. Daway, and E. G. Daway, "Underwater image enhancement using colour restoration based on YCbCr colour model," *IOP Conference Series: Materials Science and Engineering*, vol. 571, p. 012125, aug 2019. [Online]. Available: https://doi.org/10.1088%2F1757-899x%2F571%2F1%2F012125

[43] K. Iqbal, M. Odetayo, A. James, R. A. Salam, and A. Z. H. Talib, "Enhancing the low quality images using unsupervised colour correction method," *Conference Proceedings - IEEE International Conference on Systems, Man and Cybernetics*, pp. 1703–1709, 2010.

[44] A. S. Abdul Ghani and N. A. Mat Isa, "Underwater image quality enhancement through integrated color model with Rayleigh distribution," *Applied Soft Computing Journal*, vol. 27, pp. 219–230, 2015. [Online]. Available: http://dx.doi.org/10.1016/j.asoc.2014.11.020

[45] A. S. Abdul Ghani and N. A. Mat Isa, "Underwater image quality enhancement through composition of dual-intensity images and rayleigh-stretching," *SpringerPlus*, vol. 3, no. 1, p. 757, Dec 2014. [Online]. Available: https://doi.org/10.1186/2193-1801-3-757

[46] R. Ramanath and M. S. Drew, *von Kries Hypothesis*. Boston, MA: Springer US, 2014, pp. 874–875. [Online]. Available: https://doi.org/10.1007/978-0-387-31439-6_455

[47] C. Ancuti, C. O. Ancuti, T. Haber, and P. Bekaert, "Enhancing underwater images and videos by fusion," in *Computer Vision and Pattern Recognition (CVPR), 2012 IEEE Conference on*. IEEE, 2012, pp. 81–88.

[48] C. O. Ancuti, C. Ancuti, C. D. Vleeschouwer, and P. Bekaert, "Color balance and fusion for underwater image enhancement," *IEEE Transactions on Image Processing*, vol. 27, no. 1, pp. 379–393, Jan 2018.

[49] C. Zhang, X. Zhang, and D. Tu, "Underwater image enhancement by fusion," in *International Workshop of Advanced Manufacturing and Automation*. Springer, 2017, pp. 81–92.

[50] S.-L. Wong, R. Paramesran, and A. Taguchi, "Underwater image enhancement by adaptive gray world and differential gray-levels histogram equalization," *Advances in Electrical and Computer Engineering*, vol. 18, no. 2, pp. 109–117, 2018.

[51] K. Z. M. Azmi, A. S. A. Ghani, Z. M. Yusof, and Z. Ibrahim, "Deep underwater image enhancement through colour cast removal and optimization algorithm," *The Imaging Science Journal*, vol. 67, no. 6, pp. 330–342, 2019. [Online]. Available: https://doi.org/10.1080/13682199.2019.1660484

[52] S. Bazeille, I. Quidu, L. Jaulin, and J. P. Malkasse, "Automatic underwater image pre-processing," *Proceedings of*, vol. 1900, no. 1, p. 8, 2006. [Online]. Available: http://hal.archives-ouvertes.fr/hal-00504893/

[53] H. Lu, Y. Li, and S. Serikawa, "Underwater image enhancement using guided trigonometric bilateral filter and fast automatic color correction," *2013 IEEE International Conference on Image Processing, ICIP 2013 - Proceedings*, pp. 3412–3416, 2013.

[54] M. Sheng, Y. Pang, L. Wan, and H. Huang, "Underwater images enhancement using multi-wavelet transform and median filter," *TELKOMNIKA Indonesian Journal of Electrical Engineering*, vol. 12, no. 3, pp. 2306–2313, 2014.

[55] S. Zhang, T. Wang, J. Dong, and H. Yu, "Underwater image enhancement via extended multi-scale retinex," *Neurocomputing*, vol. 245, pp. 1 – 9, 2017. [Online]. Available: http://www.sciencedirect.com/science/article/pii/S0925231217305246

[56] D. J. Jobson, Z. Rahman, and G. A. Woodell, "A multiscale retinex for bridging the gap between color images and the human observation of scenes," *IEEE Transactions on Image Processing*, vol. 6, no. 7, pp. 965–976, Jul 1997.

[57] U. A. Nnolim, "Smoothing and enhancement algorithms for underwater images based on partial differential equations," *Journal of Electronic Imaging*, vol. 26, pp. 26 – 26 – 21, 2017. [Online]. Available: https://doi.org/10.1117/1.JEI.26.2.023009

[58] A. AbuNaser, I. A. Doush, N. Mansour, and S. Alshattnawi, "Underwater image enhancement using particle swarm optimization," *Journal of Intelligent Systems*, vol. 24, no. 1, pp. 99–115, 2015.

[59] J. Perez, A. C. Attanasio, N. Nechyporenko, and P. J. Sanz, "A deep learning approach for underwater image enhancement," in *International Work-Conference on the Interplay Between Natural and Artificial Computation*. Springer, 2017, pp. 183–192.

[60] S. Anwar, C. Li, and F. Porikli, "Deep underwater image enhancement," *arXiv preprint arXiv:1807.03528*, 2018.

[61] R. Fattal, "Single image dehazing," in *ACM SIGGRAPH 2008 Papers*, ser. SIGGRAPH '08. New York, NY, USA: ACM, 2008, pp. 72:1–72:9. [Online]. Available: http://doi.acm.org/10.1145/1399504.1360671

[62] K. He, J. Sun, and X. Tang, "Single image haze removal using dark channel prior," *IEEE transactions on pattern analysis and machine intelligence*, vol. 33, no. 12, pp. 2341–2353, 2011.

[63] L. Chao and M. Wang, "Removal of water scattering," *ICCET 2010 - 2010 International Conference on Computer Engineering and Technology, Proceedings*, vol. 2, pp. 35–39, 2010.

[64] N. Carlevaris-Bianco, A. Mohan, and R. M. Eustice, "Initial results in underwater single image dehazing," *MTS/IEEE Seattle, OCEANS 2010*, 2010.

[65] H. Y. Yang, P. Y. Chen, C. C. Huang, Y. Z. Zhuang, and Y. H. Shiau, "Low complexity underwater image enhancement based on dark channel prior," *Proceedings - 2011 2nd International Conference on Innovations in Bio-Inspired Computing and Applications, IBICA 2011*, pp. 17–20, 2011.

[66] J. Y. Chiang and Y. C. Chen, "Underwater image enhancement by wavelength compensation and dehazing," *IEEE Transactions on Image Processing*, vol. 21, no. 4, pp. 1756–1769, 2012.

[67] L. Jolla, "SINGLE UNDERWATER IMAGE ENHANCEMENT USING DEPTH ESTIMATION BASED ON BLURRINESS," *International Conference on Image Processing (ICIP)*, pp. 2–6, 2015.

[68] Y. Gao, H. Li, and S. Wen, "Restoration and Enhancement of Underwater Images Based on Bright Channel Prior," *Mathematical Problems in Engineering*, vol. 2016, 2016.

[69] A. Galdran, D. Pardo, A. Picón, and A. Alvarez-Gila, "Automatic Red-Channel underwater image restoration," *Journal of Visual Communication and Image Representation*, vol. 26, pp. 132–145, 2015. [Online]. Available: http://dx.doi.org/10.1016/j.jvcir.2014.11.006

[70] C. Y. Li, J. C. Guo, R. M. Cong, Y. W. Pang, and B. Wang, "Underwater image enhancement by Dehazing with minimum information loss and histogram distribution prior," *IEEE Transactions on Image Processing*, vol. 25, no. 12, pp. 5664–5677, 2016.

[71] Y. T. Peng and P. C. Cosman, "Underwater image restoration based on image blurriness and light absorption," *IEEE Transactions on Image Processing*, vol. 26, no. 4, pp. 1579–1594, April 2017.

[72] Y. Wang, H. Liu, and L. P. Chau, "Single Underwater Image Restoration Using Adaptive Attenuation-Curve Prior," *IEEE Transactions on Circuits and Systems I: Regular Papers*, vol. 65, no. 3, 2018.

[73] K. O. Amer, M. Elbouz, A. Alfalou, C. Brosseau, and J. Hajjami, "Enhancing underwater optical imaging by using a low-pass polarization filter," *Opt. Express*, vol. 27, no. 2, pp. 621–643, Jan 2019. [Online]. Available: http://www.opticsexpress.org/abstract.cfm?URI=oe-27-2-621

[74] K. Purohit, S. Mandal, and A. N. Rajagopalan, "Multilevel weighted enhancement for underwater image dehazing," *J. Opt. Soc. Am. A*, vol. 36, no. 6, pp. 1098–1108, Jun 2019. [Online]. Available: http://josaa.osa.org/abstract.cfm?URI=josaa-36-6-1098

[75] X. Deng, H. Wang, and X. Liu, "Underwater image enhancement based on removing light source color and dehazing," *IEEE Access*, vol. 7, pp. 114 297–114 309, 2019.

[76] J. Lu, N. Li, S. Zhang, Z. Yu, H. Zheng, and B. Zheng, "Multi-scale adversarial network for underwater image restoration," *Optics & Laser Technology*, vol. 110, pp. 105–113, 2019.

[77] H. Lu, Y. Li, Y. Zhang, M. Chen, S. Serikawa, and H. Kim, "Underwater optical image processing: a comprehensive review," *Mobile networks and applications*, vol. 22, no. 6, pp. 1204–1211, 2017.

[78] M. Reyes-Sierra and C. C. Coello, "Multi-objective particle swarm optimizers: A survey of the state-of-the-art," *International journal of computational intelligence research*, vol. 2, no. 3, pp. 287–308, 2006.

[79] L. A. Zadeh, "Fuzzy sets," *Information and control*, vol. 8, no. 3, pp. 338–353, 1965.

[80] A. K. Tripathi, S. Mukhopadhyay, and A. K. Dhara, "Performance metrics for image contrast," in *Image Information Processing (ICIIP), 2011 International Conference on*. IEEE, 2011, pp. 1–4.

[81] N. M. Kwok, H. Shi, Q. P. Ha, G. Fang, S. Chen, and X. Jia, "Simultaneous image color correction and enhancement using particle swarm optimization," *Engineering Applications of Artificial Intelligence*, vol. 26, no. 10, pp. 2356–2371, 2013.

[82] N. Srinivas and K. Deb, "Muiltiobjective optimization using nondominated sorting in genetic algorithms," *Evolutionary computation*, vol. 2, no. 3, pp. 221–248, 1994.

[83] J. Knowles and D. Corne, "The pareto archived evolution strategy: A new baseline algorithm for pareto multiobjective optimisation," in *Evolutionary Computation, 1999. CEC 99. Proceedings of the 1999 Congress on*, vol. 1. IEEE, 1999, pp. 98–105.

[84] K. James and E. Russell, "Particle swarm optimization," in *Proceedings of 1995 IEEE International Conference on Neural Networks*, 1995, pp. 1942–1948.

[85] P. J. Fleming, R. C. Purshouse, and R. J. Lygoe, "Many-objective optimization: An engineering design perspective," in *Evolutionary Multi-Criterion Optimization*, C. A. Coello Coello, A. Hernández Aguirre, and E. Zitzler, Eds. Berlin, Heidelberg: Springer Berlin Heidelberg, 2005, pp. 14–32.

[86] B. Li, J. Li, K. Tang, and X. Yao, "Many-objective evolutionary algorithms: A survey," *ACM Comput. Surv.*, vol. 48, no. 1, pp. 13:1–13:35, Sep. 2015. [Online]. Available: http://doi.acm.org/10.1145/2792984

[87] C. A. C. Coello, G. T. Pulido, and M. S. Lechuga, "Handling multiple objectives with particle swarm optimization," *IEEE Transactions on evolutionary computation*, vol. 8, no. 3, pp. 256–279, 2004.

[88] K. Deb, *Multi-objective Optimisation Using Evolutionary Algorithms: An Introduction*. London: Springer London, 2011, pp. 3–34. [Online]. Available: https://doi.org/10.1007/978-0-85729-652-8_1

[89] I. C. Trelea, "The particle swarm optimization algorithm: convergence analysis and parameter selection," *Information Processing Letters*, vol. 85, no. 6, pp. 317 – 325, 2003. [Online]. Available: http://www.sciencedirect.com/science/article/pii/S0020019002004477

[90] J. E. Alvarez-Benitez, R. M. Everson, and J. E. Fieldsend, "A mopso algorithm based exclusively on pareto dominance concepts," in *Evolutionary Multi-Criterion Optimization*, C. A. Coello Coello, A. Hernández Aguirre, and E. Zitzler, Eds. Berlin, Heidelberg: Springer Berlin Heidelberg, 2005, pp. 459–473.

[91] K. Panetta, C. Gao, and S. Agaian, "Human-visual-system-inspired underwater image quality measures," *IEEE Journal of Oceanic Engineering*, vol. 41, no. 3, pp. 541–551, 2016.

[92] A. Duarte, F. Codevilla, J. D. O. Gaya, and S. S. C. Botelho, "A dataset to evaluate underwater image restoration methods," in *OCEANS 2016 - Shanghai*, April 2016, pp. 1–6.

[93] H. Singh, "WHOI color correction dataset," https://web.whoi.edu/singh/underwater-imaging/datasets/color-correction/.

[94] N. Hope, "Underwater videos and pictures," http://www.bubblevision.com/index.htm.

[95] E. Y. Lam, "Combining gray world and retinex theory for automatic white balance in digital photography," in *Proceedings of the Ninth International Symposium on Consumer Electronics, 2005. (ISCE 2005).*, June 2005, pp. 134–139.

[96] K. Iqbal, M. Odetayo, A. James, R. A. Salam, and A. Z. H. Talib, "Enhancing the low quality images using unsupervised colour correction method," in *Systems Man and Cybernetics (SMC), 2010 IEEE International Conference on*. IEEE, 2010, pp. 1703–1709.

[97] J. M. Mendel, R. I. John, and F. Liu, "Interval type-2 fuzzy logic systems made simple," *IEEE transactions on fuzzy systems*, vol. 14, no. 6, pp. 808–821, 2006.

[98] K. Zuiderveld, "Graphics gems iv," P. S. Heckbert, Ed. San Diego, CA, USA: Academic Press Professional, Inc., 1994, ch. Contrast Limited Adaptive Histogram Equalization, pp. 474–485. [Online]. Available: http://dl.acm.org/citation.cfm?id=180895.180940

[99] S. G. Mallat, "A theory for multiresolution signal decomposition: the wavelet representation," *IEEE Transactions on Pattern Analysis and Machine Intelligence*, vol. 11, no. 7, pp. 674–693, Jul 1989.

[100] L. A. Zadeh, "Fuzzy sets," in *Fuzzy Sets, Fuzzy Logic, And Fuzzy Systems: Selected Papers by Lotfi A Zadeh*. World Scientific, 1996, pp. 394–432.

[101] T. Takagi and M. Sugeno, "Fuzzy identification of systems and its applications to modeling and control," *IEEE Transactions on Systems, Man, and Cybernetics*, vol. SMC-15, no. 1, pp. 116–132, Jan 1985.

[102] N. N. Karnik and J. M. Mendel, "Centroid of a type-2 fuzzy set," *Information Sciences*, vol. 132, no. 1, pp. 195–220, 2001.

[103] A. Taskin and T. Kumbasar, "An Open Source Matlab/Simulink Toolbox for Interval Type-2 Fuzzy Logic Systems," *2015 IEEE Symposium Series on Computational Intelligence*, pp. 1561–1568, 2015. [Online]. Available: http://ieeexplore.ieee.org/document/7376796/

[104] D. J. Ketcham, "Real-time image enhancement techniques," in *Image processing*, vol. 74, 1976, pp. 120–125.

[105] A. M. Reza, "Realization of the contrast limited adaptive histogram equalization (clahe) for real-time image enhancement," *Journal of VLSI signal processing systems for signal, image and video technology*, vol. 38, no. 1, pp. 35–44, 2004.

[106] R. Eustice, O. Pizarro, H. Singh, and J. Howland, "Uwit: underwater image toolbox for optical image processing and mosaicking in matlab," in *Proceedings of the 2002 Interntional Symposium on Underwater Technology (Cat. No.02EX556)*, 2002, pp. 141–145.

[107] V. Vijayaraj, N. Younan, and C. O'Hara, "Concepts of image fusion in remote sensing applications," in *2006 IEEE International Symposium on Geoscience and Remote Sensing*, July 2006, pp. 3798–3801.

[108] M. J. Gooding, K. Rajpoot, S. Mitchell, P. Chamberlain, S. H. Kennedy, and J. A. Noble, "Investigation into the fusion of multiple 4-d fetal echocardiography images to improve image quality," *Ultrasound in medicine & biology*, vol. 36, no. 6, pp. 957–966, 2010.

[109] Z. Liu, E. Blasch, Z. Xue, J. Zhao, R. Laganiere, and W. Wu, "Objective assessment of multiresolution image fusion algorithms for context enhancement in night vision: A comparative study," *IEEE Transactions on Pattern Analysis and Machine Intelligence*, vol. 34, no. 1, pp. 94–109, Jan 2012.

[110] S. Fang, R. Deng, Y. Cao, and C. Fang, "Effective single underwater image enhancement by fusion." *JCP*, vol. 8, no. 4, pp. 904–911, 2013.

[111] Y. Wang, X. Ding, R. Wang, J. Zhang, and X. Fu, "Fusion-based underwater image enhancement by wavelet decomposition," in *Industrial Technology (ICIT), 2017 IEEE International Conference on*. IEEE, 2017, pp. 1013–1018.

[112] C. Yan, N. Sang, and T. Zhang, "Local entropy-based transition region extraction and thresholding," *Pattern Recognition Letters*, vol. 24, no. 16, pp. 2935–2941, 2003.

[113] T. Kadir and M. Brady, "Saliency, scale and image description," *International Journal of Computer Vision*, vol. 45, no. 2, pp. 83–105, Nov 2001. [Online]. Available: https://doi.org/10.1023/A:1012460413855

[114] J. Xiao, J. Hays, K. A. Ehinger, A. Oliva, and A. Torralba, "Sun database: Large-scale scene recognition from abbey to zoo," in *2010 IEEE Computer Society Conference on Computer Vision and Pattern Recognition*, June 2010, pp. 3485–3492.

[115] J. yan Huo, Y. lin Chang, J. Wang, and X. xia Wei, "Robust automatic white balance algorithm using gray color points in images," *IEEE Transactions on Consumer Electronics*, vol. 52, no. 2, pp. 541–546, May 2006.

[116] M. Yang and A. Sowmya, "An underwater color image quality evaluation metric," *IEEE Transactions on Image Processing*, vol. 24, no. 12, pp. 6062–6071, Dec 2015.

[117] H. Bay, T. Tuytelaars, and L. Van Gool, "Surf: Speeded up robust features," in *Computer Vision – ECCV 2006*, A. Leonardis, H. Bischof, and A. Pinz, Eds. Berlin, Heidelberg: Springer Berlin Heidelberg, 2006, pp. 404–417.

[118] P. J. Burt and E. H. Adelson, "The laplacian pyramid as a compact image code," in *Readings in Computer Vision*. Elsevier, 1987, pp. 671–679.

[119] K. He, J. Sun, and X. Tang, "Guided image filtering," *IEEE Transactions on Pattern Analysis and Machine Intelligence*, vol. 35, no. 6, pp. 1397–1409, June 2013.

[120] G. Buchsbaum, "A spatial processor model for object colour perception," *Journal of the Franklin Institute*, vol. 310, no. 1, pp. 1 – 26, 1980. [Online]. Available: http://www.sciencedirect.com/science/article/pii/0016003280900587

[121] R. Jain, R. Kasturi, and B. G. Schunck, *Machine vision*. McGraw-Hill New York, 1995, vol. 5.